1 2 9 0

UNIVERSIDADE Đ
COIMBRA

Margarida Conceição Moreira Sobral

Effects of Extended Passaging on the BEAS-2B Cell Line, an *In Vitro* Model of Human Lung Epithelium Established for the Study of Lung Carcinogenesis

Dezembro de 2020

Margarida Conceição Moreira Sobral

Effects of Extended Passaging on the BEAS-2B Cell Line, an *In Vitro* Model of Human Lung Epithelium Established for the Study of Lung Carcinogenesis

Trabalho realizado no âmbito da disciplina Dissertação em Bioquímica, do Mestrado em Bioquímica, sob a orientação científica da Professora Doutora Ana Margarida Malaquias Pires Urbano, do Departamento de Ciências da Vida da Faculdade de Ciências e Tecnologia da Universidade de Coimbra, e da Doutora Maria Teresa Martins da Cunha Oliveira, do Centro de Neurociências e Biologia Celular da Universidade de Coimbra, UC-Biotech.
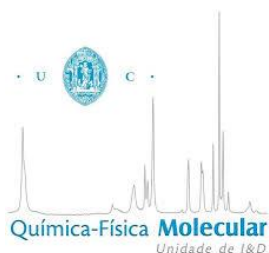
Dezembro de 2020

"O que há de mais certo é confiarmos em nós próprios, para nos tornarmos pessoas de mérito e valor."

Miguel Ângelo

Agradecimentos

Chegado o final desta etapa do meu percurso académico, gostaria de expressar os meus sinceros agradecimentos a todos que tornaram possível a realização desta dissertação.

À Professora Doutora Ana Margarida Urbano, co-orientadora desta dissertação, por me ter recebido no seu laboratório. Por toda a disponibilidade, acompanhamento e atenção dados durante todo o percurso. Por tudo o que me ensinou e, principalmente, por ter acreditado em mim.

À Doutora Teresa Oliveira, co-orientadora desta dissertação, e Professora Doutora Sónia Pinho, pela simpatia e boa disposição, por toda a ajuda na realização e planificação das experiências e pelos conhecimentos transmitidos sobre as técnicas de RT-qPCR e microscopia, que infelizmente não foram possíveis concluir devido à presente pandemia de COVID-19.

A todos os elementos da Unidade de Química-Física Molecular, pelo apoio, pela simpatia e acompanhamento ao longo deste percurso.

Aos meus colegas de laboratório, por todo o auxílio e pela companhia em todas as horas passadas na sala de cultura.

Aos meus colegas de curso e amigos, pelo apoio constante, por me conseguirem animar nos momentos mais difíceis e por todos os momentos únicos que passámos juntos. Desejo-lhes toda a sorte para o seu futuro pessoal e académico.

Por último e não menos importante, a quem sempre acreditou em mim e que sem eles nada teria sido possível. Aos meus pais e irmãos, pelo amor incondicional, pela paciência e por terem estado sempre comigo nesta longa caminhada.

Atividades realizadas durante o Mestrado em Bioquímica

ORCID ID: 0000-0002-6255-5584

Researcher ID: AAK-8570-2020

Participação em congressos e apresentação de posters:

- Apresentação de um póster intitulado "Assessment of the effects of extended passaging on the phenotype of the BEAS-2B cell line", no congresso internacional "2nd FEBS Advanced Lecture Course on Oncometabolism - From Conceptual Knowledge to Clinical Applications".

Co-autoria de artigos científicos:

- L.M.R. Ferreira, T. Cunha-Oliveira, **M.C. Sobral**, P.L. Abreu, M.C. Alpoim, A.M. Urbano, Impact of Carcinogenic Chromium on the Cellular Response to Proteotoxic Stress, Int. J. Mol. Sci. 20 (2019) 4901. https://doi.org/10.3390/ijms20194901.

- L.M.R. Ferreira, A.M. Li, T.L. Serafim, **M.C. Sobral**, M.C. Alpoim, A.M. Urbano, Intermediary metabolism: An intricate network at the crossroads of cell fate and function, Biochim. Biophys. Acta. Mol. Basis. Dis. 10 (2020) 165887. https://doi.org/10.1016/j.bbadis.2020.165887.

Index

Abbreviations and Symbols

add	Additional material of unknown origin
Ad12-SV40	Adenovirus 12-simian virus 40 hybrid virus
ADP	Adenosine diphosphate
Asc	Ascorbate
ATCC	American Type Culture Collection
ATF5	Activating transcription factor 5
ATM	Ataxia telangiectasia mutated
ATP	Adenosine triphosphate
ATR	ATM-Rad3-related
ATRIP	ATR-interacting protein
BEGM	Bronchial Epithelium Cell Growth Medium
BEP2D	Papillomavirus-immortalized human bronchial epithelial
BLM	Bloom syndrome helicase
BRCA	Breast cancer
BRIP1	BRCA1-interacting protein 1
BSA	Bovine serum albumin
CIN	Chromosomal instability
Cq	Quantification cycle
Cys	Cysteine
der	Derivative chromosome
DMSO	Dimethyl sulfoxide
DNA	Deoxyribonucleic acid
DNA-PKcs	DNA-dependent protein kinase catalytic subunit
DNP	2,4-Dinitrophenol
DPC	DNA-protein crosslink
DSB	Double-strand break
dsDNA	Double-stranded DNA
ECACC	European Collection of Authenticated Cell Cultures
EDTA	Ethylenediaminetetraacetic acid
EFSA	European Food Safety Authority
EGF	Epidermal growth factor
eHSP90	Extracellular HSP90
ELISA	Enzyme-linked immunosorbent assay
ER	Endoplasmic reticulum
ESR	Electron spin resonance
ETC	Electron transport chain
FBS	Fetal bovine serum

GH	Guanidinohydantoin
GLUT-5	Fructose transporter-5
GRP94	Glucose-regulated protein 94
GSH	Glutathione
HER2	Human epidermal growth factor receptor-2
HIF-1α	Hypoxia-inducible factor 1-alpha
HR	Homologous recombination
HRP	Horseradish peroxidase
HSE	Heat shock element
HSF	Heat shock factor
HSP	Heat shock protein
IARC	International Agency for Research on Cancer
ICL	DNA inter/intrastrand crosslink
LNCaP	Prostatic adenocarcinoma cell line
LT	Large T antigen
mar	Marker chromosome
MMLV	Moloney murine leukemia virus
MMP	Matrix metalloproteinase
MRN	Mre11-Rad50-Nbs1
MSI	Microsatellite instability
MTT	Thiazolyl blue tetrazolium bromide
NADH	Nicotinamide adenine dinucleotide, reduced form
NADPH	Nicotinamide adenine dinucleotide phosphate, reduced form
NCD	Noncommunicable disease
NEF	Nucleotide exchange factor
NHBE	Normal human bronchial epithelial
NHEJ	Non-homologous end-joining
NRT	No-reverse-transcriptase control
NSCLC	Non-small cell lung carcinoma
NTC	No-template control
NTP	National Toxicology Program
8-oxo-G	8-Oxoguanine
p	Short arm of chromosome
PBS	Phosphate-buffered saline
PDT	Population doubling time
PQC	Protein quality control
pRB	Retinoblastoma protein
q	Long arm of chromosome
RNA	Ribonucleic acid

ROS	Reactive oxygen specie
RT-qPCR	Quantitative reverse-transcription polymerase chain reaction
s.c.	Subcutaneously
SD	Standard deviation
SDH	Succinate dehydrogenase
SH	Spiroiminodihydantoin
SHE	Syrian hamster embryo
sHSP	Small HSP
SQ	Starting quantity
SSB	Single-strand break
ssDNA	Single-stranded DNA
ST	Small T antigen
Ta	Annealing temperature
TB	Trypan blue
TDT	Tumor doubling time
TMB	Tetramethylbenzidine
TRAP1	Tumor necrosis factor receptor associated protein 1
USEPA	United States Environmental Protection Agency
WRN	Werner syndrome helicase
WTHBF-6	Telomerase-immortalized human lung fibroblast

Abstract

The BEAS-2B continuous cell line, derived from normal human bronchial epithelial (NHBE) cells, has been established in 1988, by the group of Curtis C. Harris, as an *in vitro* model of normal bronchial epithelium, for the study of lung carcinogenesis.

Similar to cells from other continuous cell lines, the BEAS-2B cells are known to undergo genetic and phenotypic variations when grown *in vitro* over extended periods of time, namely at the level of gene expression and morphology. These variations might explain, at least partly, inconsistencies found in the literature in studies conducted using this cell line. Importantly, the altered cell line may no longer be a trustworthy model of the original material.

The first aim of the present study was to further characterize the effects of extended passaging on the phenotype of the BEAS-2B cell line, namely in terms of protein content, rate of lactate production, migratory capacity, stress response and resistance to mildly cytotoxic concentrations of potassium dichromate, a lung carcinogen. We found that two of these traits (stress response and rate of lactate production) changed significantly over time in culture. Altogether, our observations and those of others suggest that the degree of transformation of this cell line changes upon extensive passaging.

The second aim of the present study was to assess the impact of a prolonged exposure to mildly cytotoxic concentration Cr(VI) on several traits of the BEAS-2B cell line, namely their morphology and pattern of growth, growth rate, clonogenic potential and resistance to Cr(VI). We found that exposure to Cr(VI) for several months changed the morphology and the growth pattern of the BEAS-2B cell line and decreased its growth rates. On the other hand, no significant changes were observed in terms of clonogenic potential and resistance to Cr(VI).

Keywords: BEAS-2B cell line; extended passaging; phenotypic changes; transformation; hexavalent chromium; lung carcinogen; long-term exposure.

Sumário

A linha celular contínua BEAS-2B, derivada de células epiteliais brônquicas humanas normais, foi estabelecida em 1988, pelo grupo de Curtis C. Harris, como um modelo *in vitro* do epitélio brônquico normal, para o estudo da carcinogénese pulmonar.

De igual maneira às células de outras linhas celulares contínuas, as células BEAS-2B sofrem variações genéticas e fenotípicas quando cultivadas *in vitro* por longos períodos de tempo, nomeadamente ao nível da expressão genética e morfologia. Estas variações podem explicar, pelo menos em parte, as inconsistências encontradas na literatura em estudos que utilizaram esta linha celular. Mais importante, a linha celular alterada pode deixar de ser um modelo confiável do material original.

O primeiro objetivo de presente estudo foi caracterizar ainda mais os efeitos das passagens sucessivas no fenótipo da linha celular BEAS-2B, nomeadamente no conteúdo proteico, taxa de produção de lactato, capacidade migratória, resposta ao stress e resistência a concentrações levemente citotóxicas de dicromato de potássio, um agente carcinogénico pulmonar. Observámos que duas destas características (resposta ao stress e taxa de produção de lactato) variaram significativamente ao longo do tempo em cultura. Em conjunto, as nossas observações e as de outros sugerem que o grau de transformação desta linha celular muda com as passagens extensivas.

O segundo objetivo do presente trabalho foi avaliar o impacto da exposição prolongada a uma leve concentração citotóxica de Cr(VI) em várias características da linha celular BEAS-2B, nomeadamente na morfologia e padrão de crescimento, taxa de crescimento, potencial clonogénico e resistência a Cr(VI). Concluímos que a exposição ao Cr(VI) por vários meses afetou a morfologia e o padrão de crescimento da linha celular BEAS-2B e diminuiu as suas taxas de crescimento. Por outro lado, não foram observadas diferenças significativas no potencial clonogénico e na resistência ao Cr(VI).

Palavras-chave: Linha celular BEAS-2B; passagens sucessivas; mudanças fenotípicas; transformação; crómio hexavalente; carcinogénico pulmonar; exposição prolongada.
.

1. Introduction

1.1. The relevance of the experimental model in scientific research

The progress of science is built on the basis of the well-known scientific method, which is an empirical method. According to this method, a question leads to the formulation of a hypothesis, which consequently triggers scientific investigation, followed by the analysis and interpretation of the results obtained. Many consider Aristotle "as the inventor of scientific method because of his refined analysis of logical implications contained in demonstrative discourse, which goes well beyond natural logic and does not owe anything to the ones who philosophized before him" (phrase quoted by Riccardo Pozzo in [1]). While others consider Ibn al-Haytham the father of modern scientific method, due to his emphasis on reproducibility of its results and experimental data [2].

The planning of the experiments to be carried out is crucial for the success of the entire scientific method, since only experiments relevant to the study can create solid conclusions about the results obtained. This planning is particularly difficult when it comes to human experiments, such as epidemiological and post-mortem studies. In addition, these studies have some disadvantages, for example, post-mortem tissue samples undergo changes when compared to pre-mortem tissue samples and epidemiological studies can be difficuly to address, such as cancer. Cancer can have very long latency periods, during which individuals are often exposed to various carcinogens; thus, it is difficult to establish a cause-effect relationship [3].

The combination of all the difficulties prompted scientists to try to use tissues *in vitro*, that is, outside the body. The first attempt dates back to the 19th century, when Wilhelm Roux, a German zoologist, managed to keep living cells of the neural plate of chick embryos in saline buffer for a few days [4]. Afterwards, in 1907, Ross Granville Harrison questioned how the axon (long nerve filament) of a nerve cell is formed, whether by the linking up of short strands locally developed or by outgrowth from the cell. To answer this question, he developed a reproducible technique, which consisted on obtaining a small fragment of living tissue from the central nervous system of a young frog embryo before the axons had begun to form. Then, he placed it on a sterile coverslip with a drop of frog's fresh lymph [5]. Once lymph coagulated, he inverted the coverslip generating the hanging drop culture. Thereafter, he observed the development of axons as a result of the neural tube of the frog embryo being covered in the fluid from the lymph sac of an adult frog. With this work, he published an article for culturing nerve cells and is everywhere recognized as the originator of animal tissue culture [5,6].

In the following year, 1908, Margaret Reed explanted a small fragment of bone marrow from a guinea pig into a tube of nutrient agar, made up with physiological salt solution [6]. After a few days in the incubator, she observed that the bone marrow cells were living

and multiplying, due to the formation of a membrane on the surface of the agar and some of their nuclei exhibited mitotic figures [6]. This experiment must have been the first *in vitro* culture of mammalian cells. After this event, many others emerged that became important to the history of science, such as the discovery of a replicative senescence phase by Hayflick and Moorhead [7], the establishment of the first cell line (HeLa) [8], the production of the first hybrid mammalian cells [9] and the cloning of a mammal, the Dolly sheep [10], among many other discoveries [11–13].

The progress made in the field of cell culture to this day is enormous. The widespread use of this technique is based on the great advantage of consistency in the results. Currently, it can be said that this technique is an essential tool for the progress of science and is now a robust and reliable technology used routinely to study in different areas such as toxicology, genomics, immunology and carcinogenesis [14].

1.2. The BEAS-2B cell line as a model system for human bronchial epithelium

Bronchial carcinogenesis is a multistep pathway by which bronchial somatic cells progressively acquire the genetic changes responsible for their malignant phenotype. In addition, bronchial carcinogenesis is a long-term process that cannot be followed *in vivo*, because the human bronchus, from which most lung cancers arise, is not easily accessible for close observation and tissue biopsy. Therefore, for the study of long-term processes *in vitro*, continuous cell lines (or immortal cell lines) are useful because they can proliferate indefinitely (if a suitable fresh medium is provided continuously) and consequently do not have a finite life span, are well characterized, easier to culture than primary cell cultures and, at least theoretically, homogeneous and genetically identical, providing reproducible and consistent results [15–18].

The BEAS-2B cell line was established in 1988, by the group of Curtis C. Harris, at the National Cancer Institute, in Maryland, USA [19], in order to specifically study the multistage bronchial carcinogenesis *in vitro*. Since then, this cell line began to be used for the *in vitro* study of several other aspects of epithelial cell biology and also for investigations in other areas of research, such as immunology and toxicology [20–23].

The BEAS-2B cell line is a continuous adherent cell line derived from NHBE cells, also known as normal human tracheobronchial epithelial cells. A primary culture of NHBE cells was obtained from explants of the most distal portion of the trachea and carina collected at the autopsy specimen from a healthy person [24].

To increase the life span of the NHBE cells, Harris and his group infected them with an adenovirus 12-simian virus 40 (Ad12-SV40) hybrid virus and cloned them [19]. The SV40 genome is a covalently closed, double-stranded circular DNA molecule of 5243 bp

and encodes seven proteins: three are capsid proteins (VP1, VP2 and VP3), two are involved in the viral life cycle [large T antigen (LT) and small T antigen (ST)] and the remaining two have no known function (17 kT and agnoprotein) [25,26]. The ST is responsible for stimulating cell proliferation and facilitating the entry of LT into cells. In turn, the LT, after viral infection, triggers viral DNA synthesis by stimulating host cells to enter S phase and undergo DNA replication. Therefore, host cells lose the ability to control their own proliferation, causing an uncontrolled proliferation [25,27–29].

The immortalized clones thus obtained were named BEAS [19]. The immortalization occurred between passages 12 and 21 [30]. From the transformed colonies, three cell strains were obtained (BEAS-2A, BEAS-2B and BEAS-2C). Harris and his group determined the doubling times for the three cell strains obtained and found that, from the thirtieth duplication, there was a decrease in cell proliferation in the BEAS-2A and BEAS-2C strains. Only the BEAS-2B strain showed a continued proliferation during the period in culture [19]. In this manner, they were able to complete their goal of developing cultures with extended lifespans [19].

After completing their goal, in 1993, Harris and colleagues observed the formation of highly cystic tumors in athymic nude mice after a subcutaneous (s.c.) injection of the BEAS-2B cells in passage 32 or higher [31]. They also observed that BEAS-2B cells had a near-diploid karyotype (42 to 50 chromosomes) at least until passage 29 [19]. In 1996, Harris *et al.*, showed that the BEAS-2B cell line underwent progressive changes during extended *in vitro* passaging [30]. They observed that these cells began to show the accumulation of four abnormal chromosomes: in the chromosome 15 [(add(15)(p11.1)], 16 [add(16)(p13)], a derivative of the long arm of chromosome 8 with the long arm of the chromosome 9 [der(8;9)(q10;q10)], which decreased with the culture age, and a marker chromosome (mar). Furthermore, at passage 45, almost all cells showed all four abnormal aberrations and was observed the loss of one homolog of chromosomes 8, 15, 16, 21, and 22 [19,30,31]. These phenomena indicated that immortalization was associated with the clone selection of a mutated cell that occurred between passage 12 and passage 21. However, in 2009, in our laboratory, Rodrigues *et al.*, observed the expression of some genes involved in cell cycle control and bioenergetic metabolism in the BEAS-2B cell line, and it was concluded that this is a stable cell line capable of maintaining the integrity of the cell cycle [22].

The BEAS-2B cell line is considered nontumorigenic, but cannot be considered normal, since it was transformed by infection with viral genes to become a continuous cell line. Nonetheless, BEAS-2B cells retain fundamental characteristics of NHBE cells, such as the presence of desmosomes and tight junctions, the polygonal appearance

(characteristic of epithelial cells), nonpersistent virus, *i.e.*, they do not produce the virus with which they were immortalized, and also the ability to undergo squamous differentiation in response to serum [19,32]. Due to this latter feature, a serum-free medium should be used to culture the BEAS-2B cells, allowing the clonal growth of these cells. Thereby, when this cell line was established, Harris and collaborators used a serum-free medium, named LHC-9, which was specially formulated for the growth of NHBE cells [19,33].

1.2.1. Culture conditions for the BEAS-2B cell line

The cell bank American Type Culture Collection (ATCC), the official supplier of the BEAS-2B cell line, recommends that the initial density of BEAS-2B cells for culturing this cell line should be between 1.5 and 3 x 10^3 cells/cm^2 and the passage routine should be performed before the cultures reach high confluence. It also recommends using the bronchial epithelium cell growth medium (BEGM), a serum-free medium, and also coating the culture flasks with a mixture of fibronectin (0.01 mg/mL), collagen type I (0.03 mg/mL) and bovine serum albumin (BSA) (0.01 mg/mL) dissolved in BEGM [34]. The European Collection of Authenticated Cell Cultures (ECACC), which is also a supplier of this cell line, recommends culture conditions slightly different from ATCC, since it recommends an initial density of BEAS-2B cells between 3 and 10 x 10^3 cells/cm^2 [32].

ATCC and ECACC recommend the use of a serum-free medium due to the observations made by Harris and collaborators when they established this cell line, as already mentioned. They noted that BEAS-2B cells underwent terminal squamous differentiation in response to serum, which caused alterations in cytokine secretion in these cells [35]. In a less cited study, the authors isolated two subclones from a culture of BEAS-2B cells exposed to fetal bovine serum (FBS) and detected that only one of them was induced to undergo squamous differentiation [33]. In contrast, the other clone was mitogenically stimulated. The isolated clones were karyotypically similar and presented marker chromosomes common to those observed in the parental BEAS-2B cell line, which seemed to indicate that they originated from a common cell; but they differed in their morphology. These observations suggest that cell cultivation might induce some heterogeneity in a population with a common origin, leading to the appearance of distinct phenotypes [33]. It is important to note that the serum-free medium used by Harris and colleagues when they established the BEAS-2B cell line was the LHC-9 medium and not the BEGM, recommended by the ATCC and ECACC [19].

There are other studies that demonstrate the disadvantages of using FBS in the growth of BEAS-2B cells. For example, in 2014, Zhao and Klimecki observed that FBS

caused changes in the morphology, mRNA expression and energy metabolism of BEAS-2B cells [36]. More specifically, their study revealed that the presence of FBS in the culture medium was associated with a 1.4-fold increase the in total glycolytic capacity, a 2.0-fold increase in the oxygen consumed for adenosine triphosphate (ATP) production, a 1.9-fold increase in the basal respiration and a 2.8-fold increase in the maximal respiration, compared with BEAS-2B cultured without FBS [36]. In addition, in 2016, a previous study in our laboratory showed that the addition of FBS to the growth medium (LHC-9) induced significant changes in cell morphology [37]: cells became bigger, more flattened and had a less clearly defined border, *i.e.*, they acquired a more squamous appearance [37].

Despite the recommendations of ATCC and ECACC, there are several studies in the literature that use FBS as a supplement to the culture medium for the growth of BEAS-2B cells. FBS has become the standard medium supplement since it has a higher availability, ease of storage, high content of growth factors and low content of gamma-globulin compared to other animal sera [38]. However, the addition of animal serum in cell culture media is a potential source of contaminants, including viruses, prions and mycoplasms [39] Table 1.1 presents some studies in the literature that used different methodologies for culturing the BEAS-2B cell line compared to the methodology recommended by ATCC and ECACC.

Table 1.1. Some examples of studies that differ from the ATCC conditions in terms of both culture medium and attachment substrate for culturing BEAS-2B cells.

Culture medium	Supplement	Coating solution	Reference
DMEM	10% (v/v) FBS	Not mentioned	[40]
	10% (v/v) FBS and 1% (v/v) penicillin-streptomycin	0.5% agar	[41]
	10% (v/v) FBS, 100 U/mL penicillin and 100 µg/ml streptomycin	Not mentioned	[42]
	10% (v/v) LHC-9 medium, 10% (v/v) FBS, 100 U/mL penicillin and 100 µg/ml streptomycin	Not mentioned	[43]
	5% (v/v) FBS, 2mM L-glutamine and 100 U/mL penicillin-streptomycin	Not mentioned	[44]
BEGM	5 mg/L bovine insulin, bovine pituitary extract, 0.5 mg/L epinephrine, human EGF, 0.5 mg/L hydrocortisone, 0.1 mg/L retinoic acid, 6.5 mg/L triiodothyronine, 10 mg/L transferrin and the antibiotics amphotericin-B sulphate and gentamicin.	FNT(-) CS, Gelatin (type B) from bovine skin	[22,45]

Table 1.1. (cont.) | Some examples of studies that differ from the ATCC conditions in terms of both culture medium and attachment substrate for culturing BEAS-2B cells.

BEGM	5% (v/v) FBS	Not used	[36]
LHC-9	Not mentioned	FNT(+) CS (0.01 mg/mL), Vitrogen 100 (0.03 mg/mL) and BSA (0.01 mg/mL)	[21]
Keratinocyte SFM (serum-free medium)	EGF and pituitary extract	Not mentioned	[20]
	EGF, pituitary extract and 3% (v/v) FBS		
Ham's F12	5 µg/mL insulin, 5 µg/ml transferrin, 20 ng/ml EGF, 20 ng/ml cholera toxin, 0.1 µm dexamethasone and 30 µg/ml bovine hypothalamus extract	Not mentioned	[46]

BSA, Bovine serum albumin; DMEM, Dulbecco's modified eagle's medium; EGF, Epidermal growth factor; FBS, Fetal bovine serum; FNT(-) CS, Fibronectin-free coating solution; FNT(+) CS, Fibronectin-containing coating solution; U/mL, Concentration of enzyme activity.

Concerning the coating solution, there are several studies employing BEAS-2B cells in the literature that do not mention its use, as can be seen in Table 1.1., and one, at least, specifically mentions that BEAS-2B cultures grew in uncoated vessels [36]. Our group studied the effect of the medium on cell growth on non-coated surfaces. It was found that cells grown in BEGM were able to adhere to the substrate and form monolayers in the absence of coating. However, the cultures lost some of their homogeneity and cells did not spread as extensively as when grown in coated flasks. On the other hand, cultures completely lost their typical cobblestone growth and formed foci instead (probably reflecting a reduced adhesion to the substrate) when grown in LHC-9 medium and in the absence of coating. Altogether, these results suggested that the BEGM formulation plays a key role in the promotion of the cell attachment to the substrate [37]

Some research groups, ours included, that use the BEAS-2B cell line, do not adhere strictly to the recommendations for culturing this cell line by the ATCC and ECACC. The changes introduced in our laboratory, and probably in many other laboratories, aim to reduce the cost associated with culturing this cell line. In our laboratory, we used a culture medium and a coating solution different from those recommended by ATCC and ECACC. The serum free-medium used was the LHC-9 medium, since this medium is much cheaper than BEGM, and we removed the most expensive component from the ATCC and ECACC recommended coating solution, *i.e.*, fibronectin; thus, our coating solution consisted of a mixture of gelatin from bovine skin and BSA dissolved in phosphate-buffered saline (PBS). For convenience, we have reduced the passage frequency to just once a week. To this end, we used an initial seeding density of 2×10^3 cells/cm^2 and carried out the cell passage before the culture reached an excessive confluence, which can trigger terminal

differentiation [34]. Using the culturing conditions just described, we were able to consistently generate cultures with a healthy appearance and an apparently unlimited proliferative potential.

Altogether, these data show that, for a given cell line, different laboratories use different culture conditions. This may explain, at least in part, the different results found in the literature for similar experiments, since the culturing conditions can modulate the phenotype of cells grown *in vitro*, affecting study output and making comparisons difficult [36].

1.3. Effects of over-subculturing on cell culture

Continuous cell lines have the ability to divide indefinitely and, therefore, are used by researchers to study a wide variety of long-term processes. However, the capability of continuous cell lines to exist indefinitely opens the possibility that cell lines no longer maintains consistent morphology and key gene functions, *i.e.*, they have exceeded the safe passage number. In fact, after long-term subculturing, cells can undergo genetic and phenotypic variations, becoming even more different from the cells identified at earlier passage levels or from the primary cell culture [17]. In addition, extended passaging creates a positive selective pressure on cell cultures, leading to the formation of faster growing cells that ultimately overrun the slowest growing cells in the population [47].

Several studies have shown the divergent effects of extended passaging on morphology, growth rates, gene expression and many other features in the Caco-2 cell line, an *in vitro* model of the intestinal epithelium and is characterized by the presence of a heterogeneous mixture of subpopulations with different morphologies and biochemical characteristics, in the same culture [48]. Table 1.2 summarizes some studies that detail the effects of over-subculturing on Caco-2 cells.

Table 1.2. Some examples of studies that detail the effects of over-subculturing on Caco-2 cells.

Characteristic	Cell response after passaging	Reference
Expression of fructose transporter GLUT-5 mRNA	Increased GLUT-5 from #26 to #184	[49]
	Increased GLUT-5 from #29 to #198	[50]
TEER	Increased TEER from #35-#47 to #87-#112	[51]
	Increased TEER from #22-#33 to #72	[52]
	Increased TEER from #29 to #198	[53]
Proliferation rates	Growth rates lower in #35-#47 to #87-#112	[51]
	Growth rates lower in #22-#33 to #72	[52]

Table 1.2. (cont.) | Some examples of studies that detail the effects of over-subculturing on Caco-2 cells.

Morphology	No differences in morphology between #23-#33 and #72	[52]
	Decreased heterogeneity from #29 to #198	[53]
Cell density	Increase in cell density from #29 to #198	[53]
Paracellular permeability	No differences in permeability were observed from #35-#47 to #87-#112	[51]
	Decreased paracellular permeability from #29 to #198	[53]
Transcellular permeability	No differences in permeability were observed from #35-#47 to #87-#112	[51]
	Increased transcellular permeability from #29 to #198	[53]
Carrier-mediated transport	No differences in the permeability of ^{14}C-glycylsarcosine were observed from #35-#47 to #87-#112	[51]
	Lower permeability to ^{14}C-mannitol from #22-#33 to #72	[52]
	Decreased permeability to cephalexin, cephradine, proline and taurocholic acid from #29 to #198	[53]
AP	Higher expression of AP in #22-#33 compared with #72	[52]
	Higher expression of AP in #29 compared with #198	[53]
Drug metabolism	Higher levels of CYP3A4 (the most important drug-metabolizing enzyme) mRNA in Caco-2 cells after 28 days of culture (a considerably short period of time)	[54]

AP, Alkaline phosphatase; #, Passage number; TEER, Transepithelial electrical resistance.

Although the Caco-2 cell line has been the focus of several studies regarding the influence of passage number on various cell characteristics, the effect of extended passaging on cell culture features is not limited to the Caco-2 cell line. For example, in 1997, Chin-Mei *et al.* demonstrated that the increase of passage numbers in Syrian hamster embryo (SHE) cells decreased the doubling times and saturation (cell yield/plate), but increased the plating efficiency [55]. In the same year, Esquenet *et al.* compared cell response of prostatic adenocarcinoma cell line (LNCaP) at low and high passages to methyltrienolone (R1881), a synthetic androgen [56]. They observed that both cultures exhibited a proliferative response when exposed to increasing concentrations of R1881. However, the amplitude of this response was more pronounced in the high passages cultures than in the low passages cultures [56].

With all the studies presented here is confirmed that there is a positive selection of faster-growing subpopulations of cells in the culture with distinct phenotypic and genotypic characteristics, which results in a less heterogeneous culture. For this reason, is not recommended to use cells that have been passaged too many times [17,47]. Consequently, periodic validation of the characteristics of cultured cells is necessary and is extremely important to maintain the consistency of the culture age in order to obtain reproducible results [47].

1.3.1. Impact of extensive passaging on the BEAS-2B cell line

It is important to identify the point at which the BEAS-2B cell line undergoes significant changes caused by long-term subculturing, as these may result in different study outcomes.

Previous studies from our laboratory evaluated the effects of extensive passaging in the BEAS-2B cell line in different cellular characteristics, such as: morphology and pattern of growth, growth rate, energy metabolism (glucose consumption and lactate production rate), clonogenic potential, sensitivity of cells to FBS and chromosomal complement [22,37,57].

These cells were subcultures over 100 times (the culture was discontinued for practical reasons), which is in line with an unlimited proliferative potential. Of note, the morphological differences observed allowed the definition of three characteristic stages: the low passage stage (up to ca. passage 30), the transitional stage (from ca. passage 30 to passage 60) and the high passage stage (from ca. passage 60 onwards). Between passage 30 and passage 40 (transitional passages, cells gradually lost the typical diamond shape (polygonal shape) and cobblestone growth of epithelial cells that characterized cultures in lower passages. Furthermore, with the increase of culture age, cells became bigger and less defined in the cell border, crisscrossing became more frequent and the monolayers lost their homogeneity. In the high passages, cell size became more pronounced with increased granularity. However, cultures recovered the homogeneity of the monolayer and the crisscrossing was lost [37].

Morphological changes were accompanied by changes in other cell characteristics. Regarding growth rates, significant differences in doubling times were observed between low, transitional and high passage cultures (21.72, 18.83 and 17.46 h, respectively) (unpublished results). It was also observed that high passage cultures had a greater clonogenic potential than younger cultures (31% colony formation efficiency for low passage cultures, 19% for transitional stage cultures and 48% for high passage cultures) (unpublished results).

Concerning energy metabolism, it was found that glucose consumption and lactate production by cells in low and high passages did not differed significantly, being approximately 9 µmol glucose/4 days/10^6 cells and 18 µmol lactate/4 days/10^6 cells for both stages [57]. However, later studies revealed significant differences in lactate production at different stages of culture (1.44 µmol lactate/mg protein/hour for low passage cultures, 2.28 µmol lactate/mg protein/hour for transitional passage cultures and 1.95 µmol lactate/mg protein/hour for high passage cultures) (unpublished results).

The impact of culture age on the sensitivity of BEAS-2B cells to FBS was also assessed. Cells were exposed for five weeks to FBS, and, over this period of time, no significant differences were observed between cultures at the three different stages, with all of them exhibiting an increase in cell size, less definition of the cell border and a more flattened appearance of the cells [37]. For each culture, the proliferation rate in the presence and absence of FBS was basically the same [37].

Regarding chromosomal complement, two of the studies carried out in our laboratory observed differences in the BEAS-2B cell karyotype in low and transitional passages that accompanied the morphological changes [22,37]. Table 1.3 shows the differences in chromosomal complement that were observed in one of those studies [22].

Table 1.3. Differences in the BEAS-2B cell chromosomal complement in low and transitional passages [22]. This evaluation was made using conventional cytogenetic technique.

Culture stage	Observations
Low passage stage (#7)	Addition of material not known on chromosome 15 and chromosome 16
	isochromosome 5 [i(5)(q10)], terminal deletion of the short arm of chromosome X (Xp⁻), additional material of unidentified origin on the short arm of chromosomes 14 (14p+) and 22 (22p+) and a trisomy of chromosome 20 [tri(20)]
Transitional stage (#42)	Decrease in the percentage of cells with the alterations 14p+ and tri(20), while two new alterations emerged: a derivative of chromosome 2 [der(2)] and a terminal deletion on i(5)(q10) [i(5)(q10)del(qter)]

der, Derivative chromosome; i, Isochromosome; p, Short arm of chromosome; #, Passage number; tri, Trisomy.

Some differences found in this last study were similar to those observed by Harris and colleagues [22,30], *i.e.*, additional material on the short arms of chromosomes 15 and 16 in low passage cultures, but it is not known whether the additional material found in the study carried out in our laboratory is the same as that found in the study carried out by the Harris group. In addition, Harris *et al.* also observed that more than 25% of B39-TL cells (established by this group from tumors induced by the injection of BEAS-2B cells at passage 39 into athymic nude mice) had tri(20).

In 1994, Matturri *et al.* demonstrated that tri(20) is often found in non-small cell lung carcinomas (NSCLCs), which represent 75-80% of all lung cancers [58,59]. Consequently, the presence of this trisomy in BEAS-2B cells may be an indicator of tumorigenicity. However, this it was found in this latter study that this trisomy decreased as the culture age increased, which suggests the opposite, *i.e.*, that the tumorigenic potential of BEAS-2B cells is actually decreasing over time in culture [22].

The second (most recent) study conducted in our laboratory that evaluated the chromosomal complement of BEAS-2B cells at different stages also showed significant

differences [37]. Table 1.4 shows the differences in chromosomal complement that were observed in this study [37].

Table 1.4. Differences in the BEAS-2B cell chromosomal complement in low, transitional and high passages [37]. This evaluation was made using conventional cytogenetic technique.

Culture stage	Observations
Low passage stage (#11 and #26)	Set of chromosomal alterations reported in [22], with the addition of a derivative of the long arm of chromosome 16 with the long arm of chromosome 17 [der(16;17)]
Transitional stage (#48 to #54)	22p+, der(16;17), derivatives of the long arm of chromosome 5 with the long arm of chromosome 9 [der(5;9)] or of chromosome 15 [der(5;15)], terminal deletions of the short arm of chromosome 4 (4p-) and of the long arm of chromosome 18 (18q-), monosomy of chromosome 20 [mono(20)] and loss of chromosome Y ($-$Y)
High passage stage (#104)	All alterations observed at the transitional stage (although the incidence of the der(5;9) was much reduced) along with two new changes: additional material of unknown origin on the long arm of chromosome 9 (9q+) and a derivative of the chromosomes 2, 9 and 14 [der(2;9;14)]

der, Derivative chromosome; i, Isochromosome; mono, monosomy; p, Short arm of chromosome; q, Long arm of chromosome; #, Passage number.

Matturri *et al.* also demonstrated that chromosome Y is frequently lost in NSCLCs, which suggests that some BEAS-2B cells could be in the process of tumorigenesis [58]. It is important to note that the differences found in the transitional stage in the previously mentioned study [22] were not observed in this study [37]. This observation suggests heterogeneity of the culture when the cells are in different stages, and in turn, show different karyotypes. Overall, all of the studies mentioned showed that there is a significant chromosomal instability in BEAS-2B cells, which leads to frequent alterations of their karyotype over time in culture.

BEAS-2B cells should be an adequate model to study carcinogenesis induced by Cr(VI), which is a human lung carcinogen, since NHBE cells are the main targets of Cr(VI) carcinogenicity, an aspect discussed in the next chapter.

1.4. Chromium: general aspects

Chromium (Cr), a transition metal with an atomic weight of 52, is the 21st most abundant chemical element. In nature, this metal always occurs in combination with other elements,with the exception of meterorites, which may contain free chromium. Chromium can be found in all matter in concentrations ranging from less than 0.1 µg/m^3 in air to 4 g/kg in soils [60–62].

Chromium was discovered in 1798 by Louis Nicolas Vauquelin, a French chemist, in the mineral crocoite ($PbCrO_4$). It was, meanwhile, found in the much more abundant ore, chromite ($FeOCr_2O_3$), from which all chromium compounds are extracted [63,64]. Since its discovery, chromium's potential began to be explored and, currently, its main uses are in alloys such as stainless steel, in metal ceramics and in chrome plating [60].

As chromium applications increased, its adverse health effects on living beings began to emerge [65]. Chromium compounds were very early on recognized as skin and mucous membrane irritanting agents, causing eczema and contact dermatitis, and there were also strong suspicions that these compounds are carcinogens to humans. More recently, a link between occupational exposure to hexavalent chromium [Cr(VI)] and an increased incidence of lung cancer in workers has been firmly established [60]. The first reported case of cancer due to Cr(VI) dates back to 1890, when David Newmand reported a case of adenocarcinoma in a worker exposed to chrome pigment [66]. However, it is likely that, at the time, he may not have been aware of the importance of his observation. In 1948, Machle and Gregorius carried out the first epidemiological study, in which they demonstrated a high mortality rate (21.8%) from lung cancer in workers exposed to chromate. This value was 16 times higher than the mortality rate from lung cancer in the control population [67]. Several subsequent studies were made in order to determine concretely if there was any particular oxidation state that was responsible for this carcinogenic effect, since the identification of carcinogenic agents is essential for the prevention of riks of exposed workers [68,69].

The determination of the oxidation state of chromium responsible for the carcinogenic effect was the subject of intensive research for several decades. This heavy metal has multiple oxidation states, ranging from -II to +VI. The two oxidation states with relevance in biological systems are the trivalent state [Cr(III)] and Cr(VI), since these two forms are the only stable forms. They exhibit very different toxicities, solubilities, bioavailabilities and mobilities [68,69].

Cr(III) is the most common and stable form of chromium in the environment and in living organisms. In aqueous solutions, Cr(III) ion forms hexacoordinate complexes with a octahedral arrangement of ligands [62]. In this oxidation state, chromium showed great capacity to react with proteins, nucleic acids and other biomolecules in studies performed in acellular systems [70]. This form is regarded by many nutritionists as an unusual essential micronutrient for humans, since Cr(III) is the only known metal that forms tight kinetically inert bonds with biological ligands [71]. However, there is not sufficient information on the effects of Cr(III) deficiency in humans in order to identify a dietary

requirement. Therefore, in 2014, the European Food Safety Authority (EFSA) determined that Cr(III) is not an essential element for humans [72].

Regarding Cr(VI), this oxidation state is almost totally derived from human activities and is a toxic and strong oxidizing agent, which exists only in the oxygenated form, being the second most stable form of chromium [64]. In aqueous solutions, Cr(VI) compounds assume a tetrahedral arrangement of ligands with a negative charge [63,73]. Cr(VI) compounds exist, predominantly, as chromate anions [$(CrO_4)^{2-}$] in basic and solutions of with a physiological pH (pH > 6), dichromate [$(Cr_2O_7^{2-})$] for pH values between 2 and 6 and chromic acid (H_2CrO_4) under very acidic conditions (pH < 1) [74]. Any organic molecule with oxidizable groups can promote the reduction of Cr(VI) to Cr(III) in highly acidic environments, since Cr(VI) is a potent oxidant. Therefore, increasing pH enhances the stability of Cr(VI). In 1996, Donaldson and Barreras demonstrated that, after a 30 min incubation at pH 1.4, the human gastric juice was capable of reducing approximately 70% of Cr(VI), but was completely ineffective at pH 7.0 [75].

Due to their tetrahedral arrangement of ligands, similar to that found in sulfate (SO_4^{2-}) and phosphate (PO_4^{2-}) ions, and to their high water solubility, these complexes cross cell membranes using the general anion transport system, which is a nonselective channel. Once inside the cell, Cr(VI) is quickly reduced to Cr(III) (its major reduction product), via the tetravalent state [Cr(IV)] and to the pentavalent state [Cr(V)] [64,76]. The resulting products exert genotoxic, clastogenic (ability to induce chromosomal abnormalities) and cytotoxic effects. On the other hand, the octahedral arrangement of Cr(III) complexes, their low water solubility and the fact that they form primarily positively charged compounds, such as $Cr(H_2O)_6^{3+}$, do not allow them to use the general anion transport system, which explains their 10 to 100 times lower toxic than Cr(VI) [78,79] [64,73,77]., Cr(III) may be absorbed via pinocytosis or endocytosis. Cr(III) compounds can also accumulate around cells, inducing morphological alterations in the membrane. These changes in the membrane allow Cr(III) to penetrate the cells and be oxidized to Cr(V), but this situation is not as common as is the Cr(VI) uptake [80]. Therefore, it was concluded that Cr(VI) it is undoubtedly the carcinogenic ion. In fact, in cultured human fibroblasts, several experiments revealed that Cr(VI) compounds are approximately 1000 fold more cytotoxic and mutagenic than Cr(III) compounds [81–84].

Fortunately, there are some mammalian defense mechanisms that will inactivate a significant fraction of Cr(VI) before it enters the cells. The active extracellular conversion of Cr(VI) to Cr(III) by erythrocytes, lung epithelial fluid, alveolar macrophages, saliva, gastric juice and peripheral parenchyma cells is a very important detoxification mechanism of Cr(VI) by the organism [65,73,85], but contributes to an increase of Cr(III) in the body,

which can cause several associated diseases [86]. This reduction occurs essentially in the lungs and stomach. However, the lungs have significantly higher surface area for deposition and absorption, as compared to the stomach. When the exposure to Cr(VI) is very prolonged and/or the doses are very high, the extracellular conversion cannot completely avoid the entry of the compound into the cells. Postmortem microscopic analysis of lung tissue and biopsy samples from chromate industry workers revealed that particles containing Cr(VI) tend to accumulate in the bifurcations of the tracheobronchial tree [87]. From these bifurcations, a slow release of Cr(VI) in the close vicinity of epithelial cells occurs. In fact, most lung tumors associated with exposure to Cr(VI) are found precisely in the places where this ion accumulates, specifically in the already-mentioned bifurcations [88,89]. Cr(III) resulting from the detoxification process outside the cell binds to transferrin in plasma and distributes throughout the body and the liver and kidney quickly excrete most of it [90].

1.4.1. Cr(VI) as a lung carcinogen

Based on *in vitro, in vivo* and epidemiological studies, Cr(VI) was classified by the International Agency for Research on Cancer (IARC), the National Toxicology Program (NTP), the United States Environmental Protection Agency (USEPA) and other major international agencies as an occupational lung carcinogen [91–93].

Cr(VI) occurs, mainly in the occupational environment, including chromate production, chrome pigment production, ferrochromium and cement production, welding (stainless steel), electroplating for aerospace, tanning and aircraft manufacturing. However, nonoccupational exposures are also of concern, due to the release of Cr(VI) compounds from cigarette smoke, concrete pavement, automobile emissions, amongst other sources [73]. The toxic effects of Cr(VI) on workers are well reflected, since they are exposed to Cr(VI) by inhalation of dust, aerosols or fume and dermal contact [94]. It is of note that, although skin contact to Cr(VI) compounds can induce skin allergies, dermal necrosis, dermatitis and dermal corrosion, no significant increase in skin cancer was reported among Cr(VI)-exposed workers [95]. Table 1.5 presents selected epidemiological studies showing evidence for Cr(VI)-induced lung cancer among workers in occupational environments with significant Cr(VI) exposure.

Table 1.5. Review of selected epidemiological studies that show evidence for Cr(VI)-induced lung cancer among workers in occupational environment with significant Cr(VI) exposure.

Industry	Clear evidence of Cr(VI) induced lung cancer	Airborne exposure	References
Chromate production	Yes	20 µg/m^3	[96,97]
		≥ 1.05 µg/m^3	[98]
		720 µg/m^3	[99]
		27 µg/m^3	[100]
		Not quantified	[101]
Electroplating	Yes	Not quantified	[102]
Pigment production	Yes	Not quantified	[90]
			[103]
Aerospace	No	Not quantified	[104]
		15 µg/m^3	[105]
Welding	No	1.5 mg/m^3	[106]
Ferrochromium production	Yes	Not quantified	[107]
			[108]

An additional interesting finding was reported, in 1986, by Levy *et al.*, in rat lung [109]. They found that the most insoluble chromate (*i.e.* lead chromate) and the most soluble chromate (*i.e.* sodium dichromate) were the least carcinogenic, whereas chromates of intermediate solubility (*e.g.* strontium, calcium and zinc chromate) were the most carcinogenic. This is likely because the most soluble and insoluble chromate never reached a high enough local concentration in the immediate cellular microenvironment to cause damage. In contrast, intermediate solubility chromates can adhere to lung airway epithelial cells and slowly release high concentrations of Cr(VI) at the cell surface. Therefore, the differences in terms of water-solubility of Cr(VI) complexes may lead to different carcinogenic potencies [109].

Depending on the concentration levels of Cr(VI) compounds, all organs are susceptible to their toxic and carcinogenic effects [71]. In fact, in 2006, Iaia *et al.* confirmed that exposure to Cr(VI) increased lung, bladder and pancreatic cancer mortality among tanners [110]. In 2010, Hara *et al.* found that Cr(VI) exposure increase the risk of malignant lymphoma and brain cancer [111]. In 2015, Welling *et al.* performed a meta-analysis that suggested that Cr(VI) is a stomach carcinogen in humans [112]. In 2019, Deng *et al.* demonstrated that Cr(VI) exposure increase the risk of death by lung, larynx, kidney, bladder, testicular, bone and thyroid cancer. They also reported that Cr(VI) exposed workers are at elevated risk of respiratory system, buccal cavity, prostate, pharynx and stomach cancer [113].

There are also reported cases in human exposed to the toxic effects of Cr(VI) by ingestion. Ingestion cases are mostly acts of deliberate self-harm and they are not as common as accidental industrial exposures to fumes containing Cr(VI) compounds. The
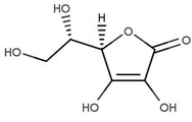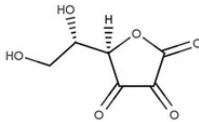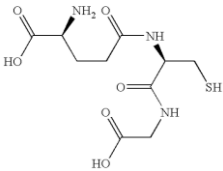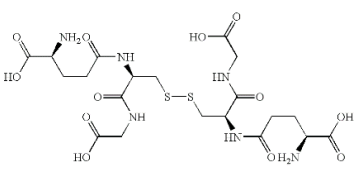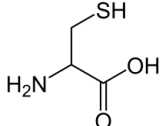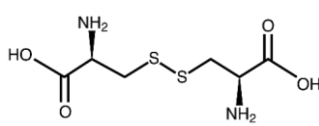
lethal oral dose is considered to be between 50 to 70 mg soluble chromates/kilogram body weight [114]. For example, in 1988, a fatal case of acute chromic acid ingestion was reported. A 44-year-old male died 1 month after the ingestion of an estimated 4,1 mg of chromic acid/kg, probably from severe gastrointestinal bleeding (an autopsy was not performed) [115]. In 1994, a 33-year-old electroplating worker consumed 125 mL of chromic acid and eventually died due to a massive gastrointestinal bleeding, hepatic injury and acute renal failure [116].

1.4.1.1. Intracellular metabolism of Cr(VI)

In vitro studies have shown that Cr(VI) by itself is not able to bind to ligands that can be found within the cell; thus, it exhibits little relevant biological activity, *i.e.*, interaction with cellular macromolecules. Once inside the reductive environment of the cell, Cr(VI) suffers a rapid and stepwise reduction to, mainly, Cr(III) [it can also form Cr(IV), Cr(V), thiol radicals, carbon-based radicals and reactive oxygen species (ROS)] as mentioned before [117]. This reduction may take place in the cytoplasm, mitochondria, nucleus or endoplasmic reticulum (ER) [117].

Several studies have identified various intracellular organelles, enzyme systems and soluble small molecules in the cytoplasm that are capable of reducing chromates that enter the cell, presumably keeping intracellular Cr(VI) concentrations low and allowing for further Cr(VI) uptake. Among these are ascorbate (Asc; vitamin C), low molecular weight thiols [glutathione (GSH) and cysteine (Cys)], nicotinamide coenzymes (NADH and NADPH), riboflavin and also some redox proteins [hemoglobin, cytochrome P450 reductase and complex I of the mitochondrial electron transport chain (ETC)] [118,119]. Hydrogen peroxide (H_2O_2) can also reduce Cr(VI) to Cr(III) thereby generating ROS [120]. Currently, it is well established that the intracellular reduction of Cr(VI) is essentially a non-enzymatic process, involving Asc and thiols (GSH and Cys), which are the main non-enzymatic reductants in physiological conditions and are kinetically favored [they are responsible for >95% of Cr(VI) reduction *in vivo*] [121]. The other reductants are also capable of reducing Cr(VI) to Cr(III) *in vitro*, but their contribution *in vivo* in not clear [119]. Table 1.6 shows the chemical structures of Asc, GSH and Cys in reduced and oxidized form.

Table 1.6. Chemical structures of reduced and oxidized forms of the three major Cr(VI)-reducing agents (Asc, GSH and Cys).

Reductant	Reduced form	Oxidized form
Ascorbate		
Glutathione		
Cysteine		

Asc is a highly efficient two-electron donor, GSH can proceed through either one- or two-electron reactions and Cys acts almost exclusively as a one-electron reducer [74]. *In vitro*, the reduction of Cr(VI) by Asc is much more rapid ($t_{1/2}$ = 1 min) than by GSH ($t_{1/2} \cong$ 13 min) and by Cys ($t_{1/2} \cong$ 60 min); thus, Asc is the primary reducer [122]. Although the rate of GSH reaction is kinetically slower than that observed for Asc, the high intracellular concentrations of GSH suggest that it is important in the reductive metabolism of Cr(VI). In contrast, Cys is the one with the lowest intracellular concentrations and is the slowest reductant; thus, the importance of Cys in Cr(VI) reduction is questionable, but might be important when there is a depletion of the other two reducers [123].

There are two possible pathways to reduce Cr(VI) using Asc, GSH and Cys, which are represented in Figure 1.1: a) the initial step involves a two electron reduction to Cr(IV) followed by one electron reduction to Cr(III) [this pathway occurs when intracellular reductant levels are present in gross excess over Cr(VI)]; or b) a series of one electron reductions may occur, producing the intermediate Cr(V) and Cr(IV) and, ultimately, Cr(III) (this pathway occurs when the levels of reductants are relatively low). Still, kinetic studies have revealed that, at physiological conditions and in the presence of physiological Cys levels, the one-electron transfer accounts for over 90% of the reduction [124].

It is important to note that, *in vivo*, the predominance of one of the pathways depends not only on the proportion of reducer to Cr(VI), but also on the specific coordinated ligands, the presence of other oxidants (*e.g.*, carbohydrates) and catalytic metals, such as iron (Fe) [73].
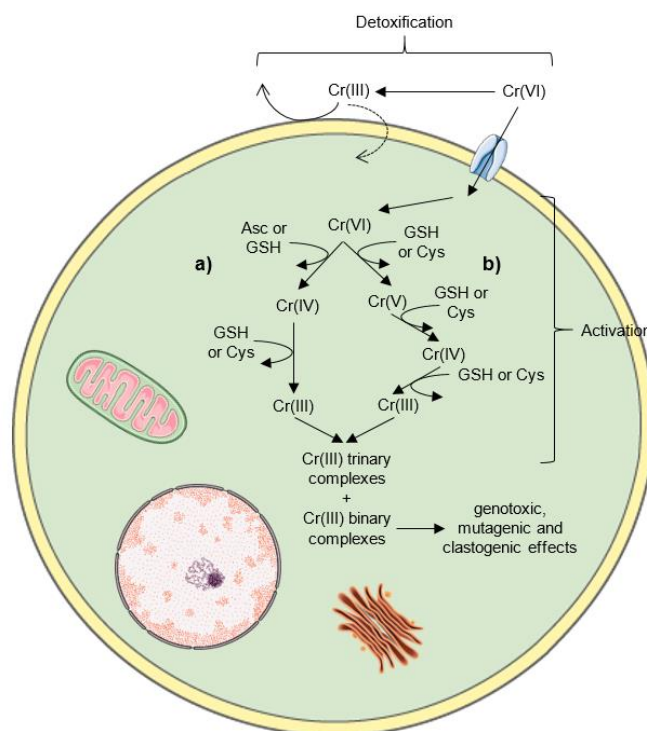
Figure 1.1. Schematic representation of the two pathways for Cr(VI) reduction. The Cr(VI) that escapes the process of extracellular detoxification is absorbed by cells. Inside the cell, Cr(VI) can be reduced in two different ways, one *via* one-electron transfers, sequentially generating Cr(V), Cr(IV) and Cr(III) by GSH or Cys, while the other one is initiated by a two-electron transfer, by Asc or GSH, directly generating Cr(IV) followed by one electron reduction to Cr(III). Figure based on information available in [121].

1.4.1.2. Molecular basis of Cr(VI)-induced carcinogenesis

The reduction of Cr(VI) inside the cell can cause both oxidative (ROS, carbon radicals) and nonoxidative (chromium-DNA interactions) forms of DNA damage, which include damage to the DNA bases and the sugar-phosphate backbone, altering gene expression of the exposed cells. These damages culminate in biological effects such as tissue lesions or cancer [125]. In fact, when the intracellular levels of ROS are not properly controlled, they react extensively and indiscriminately with biomolecules, generating additional reactive species, culminating in the propagation of radical chain reactions [126].

Several electron spin resonance (ESR) studies by Shi and collaborators have revealed that the reduction of Cr(VI), in the presence of H_2O_2, generates not only Cr(III), but also the intermediate Cr(V) and very reactive hydroxyl radicals (OH•), which are the most potent form of ROS being able to oxidize most biomolecules [127–129]. Based on these studies, two theories emerged proposing a dominant role for oxidative DNA damage in Cr(VI)-carcinogenesis: a) a central role for ROS in Cr(VI)-carcinogenesis [130,131] and b) a central role for tetraperoxochromate(V) (CrO_8^{3-}) ion in Cr(VI)-carcinogenesis [132].

However, high concentrations of Cr(VI) and H_2O_2 were necessary to detect OH• and CrO_8^{3-} by the ESR technique, which compromises the validity of these theories. Nevertheless, *in vivo* studies demonstrate that the formation of ROS and the oxidizing abilities of Cr(V) contribute to the induction of stress in Cr(VI)-treated cells. An association was observed between ROS and liver and kidney injuries in rodents exposed to soluble Cr(VI) compounds [133] and increased ROS levels upon Cr(VI) exposure have been frequently reported [134]. Also, it was reported that the presence of peroxidases and other ROS scavengers can have protective effects against Cr(VI)-induced damage [135]. In 2001, Sugden *et al.* showed that a high-valent Cr(V) complex, Cr(V)-Salen complex, can directly oxidize DNA bases, resulting in the formation of a large number of modified base products with one of the most noteworthy being 8-oxoguanine (8-oxo-G) (also known as 7,8-dihydro-8-oxoguanine) [136]. Further oxidation of 8-oxo-G can produce several base products, such as imidazolone, oxazalone, guanidinohydantoin (GH) and spiroiminodihydantoin (SH), which interact with cytosine and adenine nucleotides with the same affinity and eventually causing the transversion mutation from G:C to T:A when present on template DNA during replication [136,137].

Inflammation has also been suggested as a possible mechanism for lung tumor development in rodents exposed to Cr(VI). In 2004, Kim *et al.* showed that the inhalation by rats of chromium trioxide resulted in very little toxicity and in an increased inflammatory response due to the presence of macrophages [138]. In addition, in 2009, Beaver *et al.* exposed mice to zinc chromate and observed an alveolar and interstitial inflammation [139].

Other authors consider that the formation of chromium-DNA binding (adducts) has a fundamental role in the Cr(VI)-carcinogenesis, because, unlike oxidative damage to DNA, this type of lesion can be observed even under relatively mild exposure conditions to Cr(VI) [122,140]. In chromium-DNA adducts, which are the most abundant and specific type of DNA damage by Cr(VI), Cr(III) can coordinate DNA either directly or *via* the intermediate Cr(IV) and Cr(V), through both covalent binding or electrostatic/ionic interactions. Cr(III) contains six coordinate sites, forming hexacoordinate complexes with many ligands such as single amino acids, proteins, ribonucleic acid (RNA) and deoxyribonucleic acid (DNA) [121]. Cr(III)-DNA adducts includes binary [Cr(III)-DNA] and several ternary [ligand-Cr(III)-DNA] adducts and this last form of adducts are the most common in mammalian cells. In fact, Cr(III) tends to establish coordinated bonds with its intracellular reducers: Cys-Cr(III)-DNA, GSH-Cr(III)-DNA and Asc-Cr(III)-DNA. Cys-Cr(III)-DNA, GSH-Cr(III)-DNA are the most abundant ternary complexes detected under conditions of Asc deficiency [141], whereas Asc-Cr(III)-DNA predominates in the presence of biological levels of Asc [142]. In addition, direct Cr(III)-DNA interaction can induce many other types of DNA damage, such

as DNA-protein crosslinks (DPCs); chromium-DNA inter/intrastrand crosslinks (DNA ICLs) and single and double-strand breaks (DNA SSBs and DNA DSBs, respectively) [70,121]. Figure 1.2 represents the major pathways involved in the formation of genetic lesions by chromium.
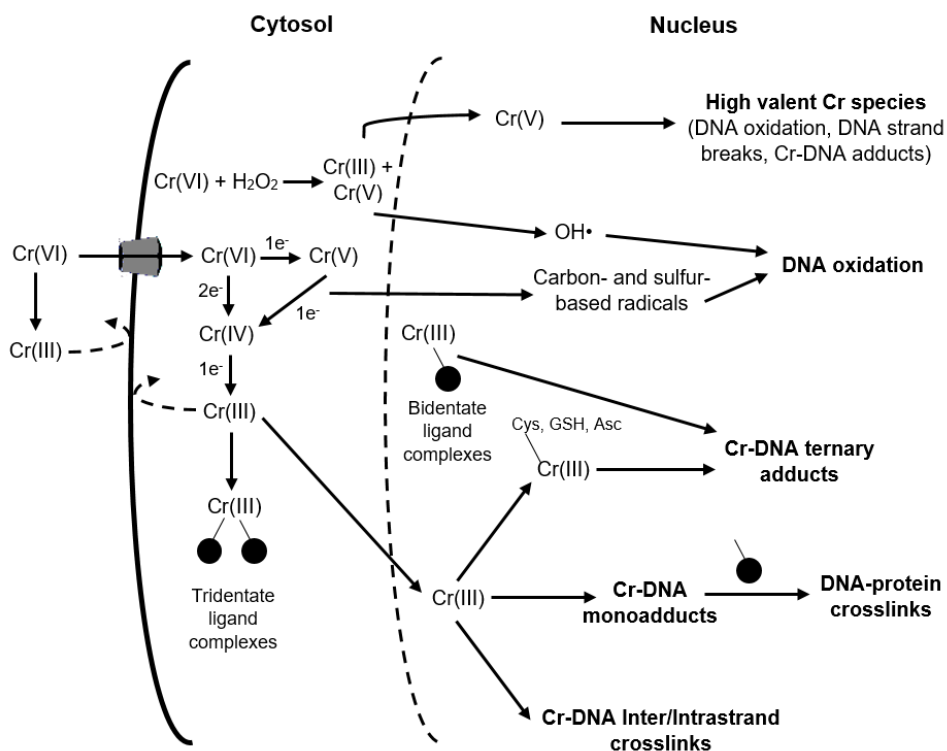

Figure 1.2. Schematic representation of the interrelationships between chromium metabolism and genotoxicity. Cr(VI) enters the cell *via* anionic transporters and is rapidly reduced, by a one or two electron mechanism, to Cr(III) [the reduction can produce the high valent Cr species Cr(IV) and Cr(V)]. Cr(III), the ultimate DNA reactive species, Cr(IV) and Cr(V) display an appreciable affinity for both DNA bases and the phosphate backbone leading to the formation of Cr-DNA monoadducts, DPCs, Cr-DNA ICLs and ternary adducts. Cr(V) can directly oxidize DNA bases (8-oxo-G) and produce DNA SSBs and DNA DSBs. Cr(VI) can also be reduced by H_2O_2 (at high levels, mM), generating Cr(III), Cr(V) and the hydroxyl radical (OH•), which lead to oxidative DNA damage. It is important to note that the location of some species or reactions represented in the scheme is not intended to imply that these occur exclusively within that intracellular compartment. Figure based on the information available in [121].

DPCs are stable ternary DNA adducts and constitute about 50% of all chromium-DNA binding events [141]. Concerning DNA ICLs, they are a highly toxic form of DNA damage because the two strands of DNA become covalently bound together, causing a problem in replication and, consequently, preventing transcription and translation [137,143]. Concerning to DNA SSBs and DNA DSBs, they are the most dangerous type of DNA lesions and one of the most commonly reported lesions arising from Cr(VI) treatment. In fact, DNA DSBs are deleterious forms of DNA damage and, if not properly repaired, induce a strong apoptotic response. Furthermore, when two DNA SSBs are close to each

other, or when the DNA-replication apparatus encounters a DNA SSB, DNA DSBs are formed. In this turn, these types of lesions can be the result of oxygen/carbon radical generation or of replication forks encountering DNA lesions. The repair process of DNA SSBs and DNA DSBs can lead to mutations and chromosome rearrangements, which result in cell death or cancer [144]. All of these types of DNA damage reported do not occur in cell-free systems in the absence of reducing agents, which confirms that Cr(III), Cr(IV) and Cr(V) formed during intracellular Cr(VI) reduction are primarily responsible for the observed genotoxicity [114].

1.5. Cancer and genomic instability

Nowadays, noncommunicable diseases (NCDs), also known as chronic diseases, are responsible for the majority of global deaths, in which cancer is considered the main cause of death and the greatest impediment to an increase in life expectancy in all countries [145]. Therefore, one of the major goals of scientists is to discover the molecular basis of the neoplastic transformation in order to better understand this process and create possible therapies.

Tumorigenesis is a multistep process based on genetic alterations that lead to the progressive transformation of normal human cells into highly malignant derivatives. In 2000, Douglas Hanahan and Robert A. Weinberg identified, for the first time, six essential alterations in cell physiology that all cells acquire when undergoing neoplastic transformation, called the hallmarks of cancer. The characteristics then defined were as follows: insensitivity to growth suppressors, ability to sustain proliferative signaling, limitless replicative potential, resistance to cell death, induction of angiogenesis and activation of tissue invasion and metastasis [146]. More recently, in 2011, the same investigators added two new hallmarks to the set already defined in 2000, namely: ability to avoid destruction by the immune system and to deregulate cellular energetics (Figure 1.3) [147]. The acquisition of these skills allows the uncontrolled proliferation, survival and spread to other tissues, characteristics that identify all cancer cells. In 2009, Luo *et al*. proposed five additional hallmarks of cancer relating to the presence of stress in cancer, namely: DNA damage and DNA replication stress, oxidative stress, mitotic stress, proteotoxic stress and metabolic stress. These five hallmarks of cancer describe the state of cancer cells (characterized by the presence of various stresses), but do not describe functional capabilities of cancer like the original hallmarks [148].
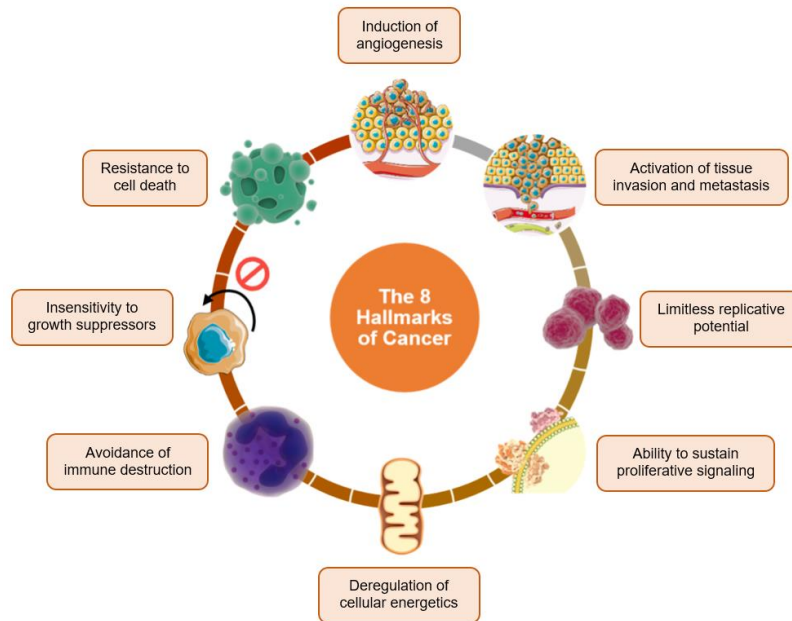
Figure 1.3. The 8 Hallmarks of Cancer. The investigators Douglas Hanahan and Robert A. Weinberg identified eight essential alterations in cell physiology that all cells acquire when undergoing neoplastic transformation: insensitivity to growth suppressors, ability to sustain proliferative signaling, limitless replicative potential, resistance to cell death, induction of angiogenesis, activation of tissue invasion and metastasis, ability to avoid destruction by the immune system and to deregulate cellular energetics. Figure based on the information available in [146,147].

The progression of malignancy also depends on other factors, such as genomic instability, mutations and inflammation (characteristics identified by Hanahan and Weinberg) [147]. In fact, the success of the acquisition of the eight hallmarks depends largely on changes in genomes of cancer cells. According to the dominant paradigm, carcinogenesis involves the successive acquisition of genetic alterations, resulting in genomic instability, that confer certain growth advantages [149]. Genomic instability is characterized at two distinct levels: in a smaller group of tumors, genomic instability is observed at the nucleotide level and results from base substitutions, deletions or insertions, called microsatellite instability (MSI; also known as MIN), and in most cancers, genomic instability is observed at the level of chromosomes, resulting in losses and gains of whole chromosomes or in large portions of them, called chromosomal instability (CIN) [150].

In hereditary cancers, the presence of mutations in caretaker genes, *i.e.*, genes that primarily function is to maintain genomic stability (DNA repair genes and mitotic checkpoint genes), has been correlated to the appearance of MSI and CIN. For example, germline mutations in breast cancer susceptibility 1 and 2 (*BRCA1* and *BRCA2*), BRCA1-interacting protein 1 (*BRIP1*), Werner syndrome helicase (*WRN*) and Bloom syndrome helicase (*BLM*), which are caretaker genes, have been linked to the repair of DNA damage, such as DNA DSBs and DNA ICLs, resulting in the development of several cancers, including breast and ovarian cancer [151]. The tumor suppressor gene *TP53*, which encodes p53, and the ataxia

telangiectasia mutated (*ATM*) gene, despite having a role in the DNA damage response, are not considered caretaker genes [151].

The molecular basis of genomic instability in sporadic cancers remains uncertain. Initially it was considered the hypothesis that the most frequently mutated genes in human cancer are the ones responsible for the presence of genomic instability [151]. However, several studies suggested that very few tumor suppressor genes, DNA damage checkpoint genes and genes that regulate cell growth are mutated, deleted and/or amplified in sporadic human cancers [152–154]. Some authors hypothesized that the activation of oncogenes, such as *RAS*, and growth signalling pathways might induce genomic instability; thus, they proposed an "oncogene-induced DNA replication stress model" [151,155]. According to this model, DNA damage results from the oncogene-induced collapse of DNA replication forks, *i.e.*, oncogene activation is capable to directly interfere with normal DNA replication, leading to DNA replication stress, which is characterized by the stalling or slowing of replication fork progression during DNA synthesis and, if not resolved by replication checkpoint mechanisms, to mutations and CIN, which characterizes almost all sporadic human cancers [151]. Several studies carried out in mammalian cells cultured *in vitro*, human xenografts, mouse models and even in yeast confirmed this model and they showed that genomic instability preferentially affects specific genomic sites, called common fragile sites, which are particularly sensitive to DNA replication stress [151].

DNA damage activates DNA-damage-response pathways in hereditary and sporadic cancers, which includes: cell-cycle arrest by checkpoints, transcription of a group of genes associated with DNA repair and apoptosis, if the damage cannot be repaired. For example, the presence of DNA DSBs, the most harmful and most common form of DNA damage, is recognized by sensor proteins (proteins that are rapidly activated in response to DNA damage), which transmits the signal to a series of down-stream effector molecules (Figure 1.4) [156].
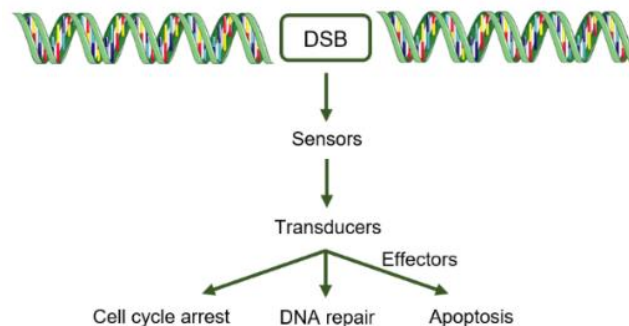

Figure 1.4. Signaling of DNA DSBs. The presence of DNA DSBs is recognized by a protein sensor, which transmits the signal to a series of down-stream effector molecules to activate cell cycle arrest or DNA repair or cell death if the damage is irreparable. Figure based on the information available in [156].

One of the earliest events occurring following DNA damage is the appearance of DNA damage-response kinases (sensor proteins), which are responsible for the activation of the major DNA DSBs and single-stranded DNA (ssDNA) repair pathways and checkpoint responses, namely: ATM, ATM-Rad3-related (ATR) and DNA-dependent protein kinase catalytic subunit (DNA-PKcs). ATM and DNA-PKcs respond mainly to DNA DSBs (mostly ATM), whereas ATR is activated by ssDNA [157]. The recruitment of these proteins to DNA lesions is facilitated by specific partner proteins, specifically: ATR-interacting protein (ATRIP), which facilitates the recruitment of ATR to ssDNA; Ku70/Ku80 heterodimer, which facilitates the recruitment of DNA-PKcs to DNA DSBs [known as non-homologous end-joining (NHEJ) repair] and the Mre11-Rad50-Nbs1 (MRN) complex, which has a helicase and exonuclease activities and facilitates the recruitment of ATM to DNA DSBs [known as homologous recombination (HR) repair]. This last recruitment also requires Rad52, which is a DNA-end-binding protein, and Rad51, which forms filaments along the unwound DNA strand to facilitate strand invasion [156].

ATR, ATM and DNA-PKcs induce the production of Ser139-phosphorylated histone H2AX, which is also known as γH2AX, at the site of DNA damage [158]. H2AX constitutes approximately 25% of total histone H2A and contains the preserved amino acid motif for phosphorylation by ATR, ATM and DNA-PKcs. The importance of γH2AX goes beyond its utility as a biochemical marker of, mainly, DNA DSBs, as it eventually spreads over large chromatin regions, stimulating other histone modifications, large-scale chromatin remodelling and recruitment of numerous DNA repair factors [153].

The protein product of *TP53*, p53, is a DNA damage checkpoint protein that responds to oncogene-induced DNA damage and is phosphorylated by the sensor proteins ATM, ATR and DNA-PKcs when the DNA damage is not repaired, which can result in the amplification or loss of chromosomal material of one or more regions encoding a tumor suppressor gene and the translocation of chromosome segments in a reciprocal or non-reciprocal fashion [159]. Therefore, these events activate the p53 protein and, consequently, induce the proliferation arrest, apoptosis or senescence. However, if the *TP53* gene is mutated (this gene is highly mutated in human cancers in response to oncogene-induced DNA damage), there is a defective checkpoint with the loss of the p53 protein and thus the cell may develop cancer (Figure 1.5).
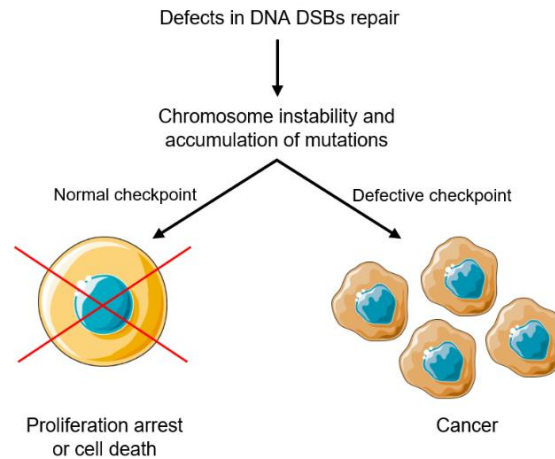
Figure 1.5. Schematic representation of the two possible pathways that can happen when DNA DSBs cannot be repaired. When cells fail to repair the DNA DSBs correctly, genetic instability, chromosomal rearrangements and accumulation of mutations can occur. These events then trigger cell-cycle checkpoints resulting in growth arrest or cell death, or, if the checkpoints are inactivated by mutations, this leads to tumorigenesis. Figure based on the information available in [156].

1.5.1. Genomic instability in Cr(VI)-induced carcinogenesis

All cells that underwent neoplastic transformation shared the eight hallmarks of cancer. Therefore, since Cr(VI) is a well-established human lung carcinogen, through the intracellular reduction of Cr(VI) to Cr(III), it is not surprising that cells exposed to this compound exhibit several of those capacities, such as resistance to cell death [160], activation of invasion and metastasis [161], ability to sustain proliferative signaling [162], induction of angiogenesis [40] and deregulation of cellular energetics [134]. In addition, there are also studies that demonstrate that cells exposed to Cr(VI) induce genomic instability and mutations [70,139,163].

Concerning genomic instability, MSI is mostly observed in Cr(VI)-induced lung cancers [164]. Nevertheless, as Cr(VI)-induced carcinogenicity is characterized by several DNA damage, mostly DNA DSBs, some Cr(VI)-induced lung carcinomas result from aneuploidy and, consequently, CIN [163]. Aneuploidy creates positive feedback, since it destabilizes the structure of chromosomes, resulting in even more genomic instability [165]. In fact, lung cancers exhibit a high incidence of chromosomal instability, specifically 70% to 80% of malignant lung tumors exhibit severe aneuploidy [166]. For example, in 2010, Holmes *et al.* observed that chronic exposure to particulate Cr(VI) compounds, specifically zinc chromate (one of the most potent carcinogens), in telomerase-immortalized human lung fibroblasts (WTHBF-6) cells, induce aneuploidy, in the form of hypodiploidy, hyperdiploidy and tetraploidy. In addition, they also observed that zinc chromate also induced centrosome amplification (the presence of more than two centrosomes), which is a common event in lung cancer, producing cells with centriolar defects and prolonged G2 arrest [167]. In 2007, Xie *et*

al. observed that lead chromate exposure in papillomavirus-immortalized human bronchial epithelial (BEP2D) cells induced aneuploid metaphases and centrosome amplification after 120 h [168].

A recent study carried out by DeLoughery *et al.*, in 2015, demonstrated that Cr(VI)-induced DNA DSBs caused extensive γH2AX phosphorylation but it was mediated by ATR in Asc-restored human H460 lung epithelial cells [158]. The authors provided a possible explanation for a selective ATR activation instead of ATM, based on the structure of DNA DSB ends: the model HR repair consists of the bounding of blunt-ended DNA DSB with the MRN complex for recruitment and activation of ATM, which operates by excising a DNA strand, resulting in ssDNA. Therefore, most Cr(VI)-induced DNA DSBs are likely to contain single-stranded tails, which are potent activators of ATR [158].

During HR repair, the Rad51 protein plays a key role. This protein is loaded into the ssDNA, creating a helical nucleoprotein filament responsible for identifying a homologous sequence and strand invasion. After the strand successfully invades the donor duplex, repair synthesis occurs using the donor duplex as a template and Holliday junctions are resolved, resulting in high fidelity repair [169]. Therefore, Rad51 is the defining biochemical step of HR. Furthermore, coimmunoprecipitation experiments indicate that BRCA1, BRCA2 and Rad51 are physically associated [170]. In addition, cells containing mutations in either *BRCA1* or *BRCA2* are exquisitely sensitive to DNA DSBs, showing severely impaired HR repair [171]. Altogether, these studies indicate that BRCA1 and BRCA2, along with Rad51, are crucial component of HR repair in cells.

In 2016, Browning *et al.*, showed that chronic exposure to Cr(VI) inhibits the HR repair in WTHBF-6 cells [169]. They observed that, while HR repair response is activated after 24 h Cr(VI) exposure, this repair pathway and Rad51 nucleofilament formation are inhibited by prolonged (120 h) Cr(VI) exposure [169]. They concluded that Cr(VI) inhibits HR repair through the misregulation of Rad51 and its proper localization to the nucleus. The inhibition of this repair pathway is an important component in the carcinogenetic mechanism of Cr(VI), since this process is correlated with an increase of structural chromosome damage [169]. In 2017, the same group identified the system of carcinogenesis in lung carcinoma caused by Cr(VI) particulate [172]. They investigated the effects of prolonged Cr(VI) exposure on the Rad51 nuclear import mediator proteins, Rad51C and BRCA2, in WTHBF-6 cells, since nuclear import of Rad51 is crucial to its function. They observed that 24 h Cr(VI) exposure induced proper localization of Rad51C and BRCA2, but 120 h Cr(VI) exposure increased the cytoplasmic localization of both proteins. Therefore, the authors concluded that Cr(VI)-exposure inhibits the nuclear import of Rad51C and BRCA2, resulting in the cytoplasmic accumulation of Rad51 [172].

Despite the progress made in recent years, a great deal of research is still needed to elucidate the role that the observed genomic instability has in the development and progression of Cr(VI)-induced carcinogenesis. Several studies have reported extensive numerical chromosomal aberrations, but have not identified which chromosomes were affected by these changes. Therefore, it is not possible to know which tumor suppressor genes, oncogenes or other cancer-related genes have their expression altered.

1.6. The importance of the stress response in biological systems

The stress response is a highly conserved mechanism used by all organisms (prokaryotic and eukaryotic) in order to maintain cellular homeostasis under proteotoxic stress, *i.e.*, stresses that impose conformational alterations to proteins and eventually lead to their denaturation and/or aggregation, such as a nonlethal temperature (40-43 ºC) and heavy metals [*e.g.* Cr(VI)]. When cells are exposed to one or more stresses, the synthesis of most proteins is suppressed, but a small number of proteins are rapidly synthesized, called "stress proteins" or "heat shock proteins (HSPs)" [173]. HSPs are essential molecular chaperones conserved through cell evolution (*e.g.*, some domains of HSP70 are 96% similar between *E. coli* and human) necessary for cell survival against the stresses found in the environment, preventing the onset of programmed cell death and allowing the resumption of normal metabolism through proteome repair (HSPs are also needed in basal conditions) [174].

The stress response was initially discovered by Ritossa, in 1962 [175]. Ritossa demonstrated that elevated temperature induces well-defined variations in the puffing pattern in salivary gland chromosomes of a fruit fly, *Drosophila busckii*, and this variation always showed the same bands [175]. In addition, she observed that 2,4-dinitrophenol (DNP), an uncoupler of oxidative phosphorylation, produced the same effects as thermal shock in the induction of the new puffing pattern, suggesting that heat shock and metabolic stress could be upregulating the transcription of the same set of genes [175].

At the time when Ritossa discovered the stress response, HSPs were not yet known. In fact, HSPs were discovered by Tissières *et al.*, in 1974. They observed that the variations observed by Ritossa in fruit fly chromosomes coincided with the synthesis of a small number of new proteins after subjecting the cells to a heat shock [176]. Later, in 1988, Riabowol *et al.*, in order to demonstrate that HSPs play a crucial role in survival during and after stress in mammalian cells, they observed that the addition of antibodies against a specific type of HSP (HSP70) to cultured rat fibroblasts and incubated at 45 ºC for 30 min, caused cell death, concluding that the loss of the HSPs is lethal to cells [177].

Mammals express many types of HSPs, which are commonly classified according to their molecular weights in 6 families, since their function was unknown at the time of their

discovery: small HSPs (sHSP) (they have a molecular weight between 15 and 40 kDa and are ATP-independent), HSP60, 70, 90, 100 and 110 (these 5 families are ATP-dependent) [178,179]. As chaperones, all HSP families are mediators of protein folding (they recognize exposed hydrophobic patches on a protein's surface and help the protein to refold into its proper conformation) with subtly different properties and functions between the families [178]. In addition, they also play a critical role in the translocation of proteins to their final subcellular locations and in the regulation of proteins degradation [180]. Different members of the HSP family collaborate with each other in a signaling network to regulate cellular functions [181]. Interestingly, each compartment of the eukaryotic cells has a protein quality control (PQC) system that functions to monitor and repair damage to the proteome, since different compartments of the cell have their own characteristic proteome [179]. It is important to note that HSPs are no enzymes, therefore their interacting partners in the proteome are known as clients and not substrate [182].

In eukaryotic cells and in a stressful situation, the rapid synthesis of HSPs is primarily a result of heat shock factor (HSF) (in mammals, the main regulator of the stress response is HSF1), a transcription factor that is activated with a proteotoxic stress. In unstressed cells, HSF is a monomer present in both the cytoplasm and nucleus, so does not have DNA binding activity [183]. When the cell responds to any stress, HSF assembles into a homotrimer and accumulates within the nucleus, attaching itself to the heat shock elements (HSE), a specific DNA recognition sequence. This transcriptional activation leads to increased levels of HSP and the formation of an HSF-HSP complex, which is important to the conversion of the active HSF trimer to the monomer, dissociating from the DNA (Figure 1.6) [183].

Once the importance of the stress response in the maintenance of cellular homeostasis has been demonstrated, it is not surprising that its deregulation has been associated with several pathologies (*e.g.* cancer and neurodegenerative diseases) and aging [180].
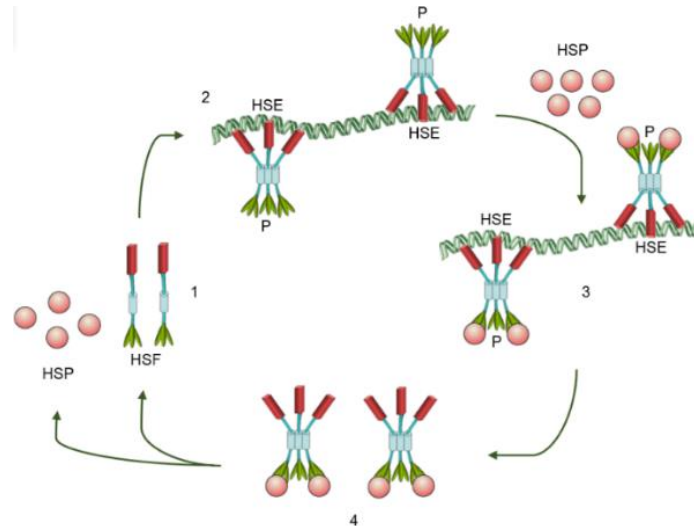
Figure 1.6. A model of HSF regulation. In the unstressed cell, HSF is maintained in a monomeric (non-DNA binding) form (1). Upon heat shock or other forms of stress, HSF assembles into a trimer, binds to HSE and becomes phosphorylated (2). Transcriptional activation of the heat shock genes leads to increased levels of HSP and to formation of an HSP-HSF complex (3). Finally, HSF dissociates from the DNA and is eventually converted to non-DNA binding monomers (4). Figure based on the information available in [183].

1.6.1. The involvement of the stress response in carcinogenesis

HSPs participate in many events related to cancer and are now well-established oncoproteins, mainly because these chaperones play, in cancer cells, an essential role in the suppression of apoptosis, in the regulation of angiogenesis, in cell migration, invasion and metastasis, allowing for tumor progression [181,184]. In fact, cancer cells rely more on HSPs than normal cells for proliferation and survival, becoming dependent on a constant supply of large concentrations of HSPs, since this type of cells have many misfolded proteins that need chaperone activity for correction due to the inhospitable environment that is found in the tumor microenvironment, *e.g.* fluctuations of oxygen supply, a scarcity of nutrients and acidic environment. The increased levels of HSPs are mainly due to an increase in HSF1 activity. Nevertheless, promoters of the HSP gene can also be activated by the loss of the tumor suppressor protein p53, as well as by the activation of the oncogenic transcription factor c-MYC (encoded by *c-MYC*), which regulates gene expression pleiotropically (when one gene influences two or more unrelated phenotypic traits), serving as an integrator of cell cycle regulation and cellular metabolism [87,185]. Altogether, HSPs have two distinct main functions: they are involved in maintaining cellular homeostasis and are part of the resilience behind cancer cells [87,178].

Once demonstrated that HSPs are overexpressed in cancer cells, the development of various HSPs inhibitors has demonstrated progress in the treatment of cancer, such as antibodies, natural compounds, peptides, and vaccines [184]. Furthermore, the combination of different HSP inhibitors can improve the anticancer efficacy [181].

As mentioned before, intracellular HSPs, most notably HSP90s (the most prominent family of HSPs participating in nearly every cellular process under normal conditions), have been shown to accumulate to high levels in many types of cancer [87,186].

1.6.1.1. HSP90 and cancer

HSP90 family consists of 4 members and is highly conserved by all organisms, exhibiting a sequence similarity of 50% between *Escherichia coli* HSP90 and human HSP90 [187]. The family members are: HSP90α and HSP90β (encoded by, respectively, the *HSP90AA1* and *HSP90AB1* genes), which are both cytoplasmic members and the most prevalent of all family members (together they constitute 2% of total cellular protein content); tumor necrosis factor receptor associated protein 1 (TRAP1) (encoded by the *TRAP1* gene), which is found in mitochondria, and the glucose-regulated protein 94 (GRP94) (encoded by the *GRP94* gene), which is found in the lumen of the ER [188].

HSP90s are essential proteins under normal growth conditions and stress conditions in all eukaryotes, since they participate in the folding, maturation and degradation of structurally and sequentially unrelated client proteins and in many cellular functions, such as protein trafficking, receptor maturation and signal transduction [189]. In stress situations, HSP90α is the most induced family member, while HSP90β acts more as a "housekeeping chaperone" [179]. Typically, HSP90s act downstream of HSP70 in the later stages of protein folding, refining the structures of client proteins into functional conformations and, unlike HSP70 that recognizes short, hydrophobic patches, HSP90s usually bind partially folded, less hydrophobic intermediates [189]. Therefore, the main role of HSP90s is to stabilize meta-stable proteins [87,186].

Regarding its structure, HSP90s are flexible phosphorylated homodimers and dimerization is essential for their function *in vivo* [188]. Each protomer consists of three highly conserved domains: a ≈ 25 kDa N-terminal nucleotide-binding domain that exhibits ATPase activity; a ≈ 40 kDa middle domain, which binds the client and, together with the amino-terminal domain is important for ATP hydrolysis; and a ≈ 12 kDa C-terminal domain, which mediates HSP90 dimerization [179]. During the ATPase cycle, HSP90s suffer large conformational changes, which are essential to properly chaperone their client proteins. In the absence of ATP, HSP90s adopt mainly a V-shaped open conformation. Then, when the ATP binds to HSP90s, they suffer a structural rearrangement that leads to an N-terminally closed state via intermediate steps [188].

As mentioned before, cancer cells are "addicted" to HSP90s (mostly the HSP90α isoform) since, in order to allow increasingly more mutated oncoproteins and tumor suppressor proteins to work, it is necessary to avoid their degradation [87]. Therefore, many

of the HSP90s clients are oncoproteins, such as several receptor tyrosine kinases and steroid hormone receptors, like telomerase (an enzyme required for immortalization); the human epidermal growth factor receptor-2 (HER-2), associated with uncontrolled proliferation; AKT, involved in the deregulation of the apoptosis; matrix metalloproteinases (MMPs), involved in tissue invasion and metastasis and hypoxia-inducible factor 1-alpha (HIF-1α), crucial for angiogenesis [87].

Curiously, HSP90 is considered the main negative regulator of HSF1, since it appears to be active despite the high levels of HSP90. This phenomenon can occur in two ways: post-translational changes in HSP90s, which can influence its intracellular properties, or changes in HSF1 itself, which explains its hyperactivation during oncogenesis, with a consequent increase in HSP90 levels [178].

Several groups [190–192] identified a new role for HSP90 outside of cancer cells. Extracellular HSP90 (eHSP90) (HSP90 present on the cell surface and secreted HSP90 pool) has been shown to be critical for the regulation of tumor invasiveness and metastasis (central processes associated with cancer lethality). For example, Eustace et al., in 2004, showed that eHSP90α activated MMP2 and mediated cancer cell invasion [193]. In 2008, Sidera et al. showed that eHSP90 activated MMP9 and additional extracellular clients, such as the extracellular domain of the receptor tyrosine kinase HER-2, generating cytoskeletal rearrangements required for cell motility and invasion [194]. It is important to note that it is currently unclear which eHSP90 population is responsible for changes in cell behaviour and phenotype.

1.7. Impact of a long-term exposure to Cr(VI) on the BEAS-2B cell line

In order to establish malignantly transformed subclonal cell lines, previous studies conducted in our laboratory continuously exposed BEAS-2B cells to slightly cytotoxic Cr(VI)-doses, since high doses of Cr(VI) cause cell cycle arrest and apoptosis, and evaluated several cellular characteristics, such as their morphology, pattern of growth, clonogenic potential, chromosomal complement and glucose consumption [22,37,45,195]. In fact, in 1991, Snow and Xu demonstrated that to occur the tumorigenesis process is necessary low doses of Cr(VI), since high levels of Cr-DNA binding resulted in inhibition of polymerase activity, which leads to apoptosis and, consequently, prevents carcinogenesis and, on the contrary, low levels of Cr-DNA binding increased polymerase activity and processivity, which were associated with a decrease in DNA replication fidelity. Therefore, mild doses of Cr(VI) doses are preferred for the study of the impact of long-term exposure to Cr(VI) [196].

One of the studies conducted in our laboratory observed that BEAS-2B cells after prolonged exposure (12 passages) to 1 µM Cr(VI) underwent morphological changes

(cultures became heterogeneous, exhibiting areas where apparently normal diamond-shaped epithelial cells and morphologically altered cells coexisted) and became increasingly less resistant to trypsinization, revealing a reduced adhesiveness to the substratum [22]. It is generally accepted that alterations in cell morphology and pattern of growth are indicative of cell transformation. They also assessed the clonogenic survival of Cr(VI)-exposed BEAS-2B cells and observed that these cultures had the clonogenic survival only slightly lower (by less that 10%) than that of the control cultures. This decreased clonogenic efficiency was consistent with the result of the reported higher duplication time exhibited by BEAS-2B cells exposed to 1 µM Cr(VI), since prolonged exposure to this Cr(VI) dose did not result in significant cell death (confirming the low cytotoxicity of the Cr(VI) dose used). Concerning cells' ploidy, they also observed some changes: early stages of exposure to Cr(VI) had an increase in the number of hyperdiploid cells compared to the control and later stages of exposure to Cr(VI) had an increase in hypodiploid cells compared to the control. Finally, they observed that BEAS-2B cells exposed to Cr(VI) overexpressed some genes commonly involved in malignant transformation, such as *c-MYC*, *EGFR*, *HIF-1α* and *LDH-A* [22].

Changes in morphology and pattern of growth were also observed in a later study in which cultures were chronically exposed to 1 and 2 µM Cr(VI) for 15 passages [45]. They observed that cultures became heterogeneous with a completely disorganized appearance showing areas where cells grew with no formal pattern, frequent criss-crossing, with an increase in the number of round and refractile cells, of multinucleated enlarged cells and in the granularity, suggesting a premature senescence status (feature observed in cultures exposed to DNA-damaging agents). Therefore, they concluded that, although immortalized, BEAS-2B cells are still capable of undergoing senescence in response to potentially oncogenic events, possibly being a protective response to potential carcinogenic stimuli. They also observed that chronic Cr(VI) exposure could give rise to a population of cells able to proliferate in anchorage-free conditions, an important step in the establishment of metastases. In terms of proliferation time, it was found that the doubling time of cultures chronically exposed to mildly cytotoxic Cr(VI) doses (28 h and 36 h to 1 and 2 µM Cr(VI), respectively) were higher than those compared to control (22 h). These results were explained by the fact that Cr(VI) interferes with cell adhesion to the substratum, which causes a significant cell-cycle delay and, consequently, results in an extended "lag phase" [45].

In 2010, another study carried out in our laboratory demonstrated that chronic exposure of BEAS-2B cells to subcytotoxic and mildly cytotoxic concentrations of Cr(VI) (over six passages) induced a stimulatory effect on energy metabolism, such as glucose uptake and lactate production [195].

In contrast to the studies mentioned, a more recent study did not observed morphological differences after 10 months of exposure of the BEAS-2B cells to 1 μM Cr(VI) [37], which might be due to the fact that the exposure regimens employed in the first two studies are different from this study. This is another example that demonstrates the importance of maintaining the same conditions in order to obtain reproducible results. In this study, cells were seeded with an cell density of 2000 cells/cm^2 and cultured in LHC-9, while in the first two previously mentioned studies, the seeding density was 4000 cells/cm^2 and the culture medium was BEGM [22,45]. Once the culture media seems to play a role in cell adhesion to the substrate, the use of different culture media might be particularly relevant. Another parameter assessed was the chromosomal complement of BEAS-2B cells. Using conventional cytogenetics, no Cr(VI)-induced chromosomal alterations were detected. In fact, all chromosomal alterations observed in Cr(VI)-exposed cells were also present in the non-exposed cells, which were always maintained in parallel. Taken together all the results, it seemed that the exposure regimen used might not have been sufficient to induce the early stages of neoplastic transformation [37].

1.8. Objectives

The first aim of the present study was to further characterize the effects of extended passaging on the phenotype of the BEAS-2B cell line, namely in terms of protein content, rate of lactate production, migratory capacity, stress response and resistance to mildly cytotoxic concentrations of potassium dichromate, a lung carcinogen.

The second aim of the present study was to assess the impact of a prolonged exposure to mildly cytotoxic concentration Cr(VI) on several traits of the BEAS-2B cell line, namely their morphology and pattern of growth, growth rate, clonogenic potential and resistance to Cr(VI).

2. Materials and Methods

2.1. Materials

All the materials used in the experimental work described in this dissertation are listed in Table 2.1.

Table 2.1. List of materials used in the experimental work described in this dissertation.

Material	Manufacture	Reference	Supplier
General materials			
Bovine serum albumin (BSA, ≥ 96%)	Sigma-Aldrich®	A9647	Sigma-Aldrich® Química S.A., Sintra, Portugal
Crystal violet ($C_{25}N_3H_{30}Cl$, 0.5%)	Sigma-Aldrich®	548629	Sigma-Aldrich® Química S.A., Sintra, Portugal
Dimethyl sulfoxide (DMSO, C_2H_6OS, ≥ 99.9%)	Sigma-Aldrich®	472301	Sigma-Aldrich® Química S.A., Sintra, Portugal
Ethylenediaminetetraacetic acid (EDTA, $C_{10}H_{16}N_2O_8$, > 99%)	Sigma-Aldrich®	E5134	Sigma-Aldrich® Química S.A., Sintra, Portugal
Fetal bovine serum (FBS)	Life Technologies™	10270-106	Alfagene®, Carcavelos, Portugal
Gelatin, from bovine skin	Sigma-Aldrich®	G9391	Sigma-Aldrich® Química S.A., Sintra, Portugal
Gibco® LHC-9 medium	Life Technologies™	12680-013	Alfagene®, Carcavelos, Portugal
Glutaraldehyde ($C_5H_8O_2$, 6.0%)	Sigma-Aldrich®	111308	Sigma-Aldrich® Química S.A., Sintra, Portugal
Hydrochloric acid (HCl, 37%)	Sigma-Aldrich®	320331	Sigma-Aldrich® Química S.A., Sintra, Portugal
Potassium chloride (KCl, ≥ 99 %)	Sigma-Aldrich®	P5405	Sigma-Aldrich® Química S.A., Sintra, Portugal
Potassium dichromate ($K_2Cr_2O_7$, ≥ 99.5%)	Sigma-Aldrich®	P2588	Sigma-Aldrich® Química S.A., Sintra, Portugal
Potassium phosphate monobasic (KH_2PO_4, ≥ 99.0%)	Sigma-Aldrich®	P5379	Sigma-Aldrich® Química S.A., Sintra, Portugal
Sodium chloride (NaCl, 99.0-101.5%)	VWR Chemicals	27810.295	VWR International, Alfragide, Portugal
Sodium hydroxide (NaOH, ≥ 98.0%)	Sigma-Aldrich®	71689	Sigma-Aldrich® Química S.A., Sintra, Portugal
Sodium phosphate dibasic (Na_2HPO_4, ≥ 99%)	Sigma-Aldrich®	S0876	Sigma-Aldrich® Química S.A., Sintra, Portugal
Thiazolyl blue tetrazolium bromide (MTT, $C_{18}H_{16}BrN_5S$, 98%)	Sigma-Aldrich®	M2128	Sigma-Aldrich® Química S.A., Sintra, Portugal

Table 2.1. (cont.) | List of materials used in the experimental work described in this dissertation.

TritonTM X-100, 0.1% (v/v) ($C_{14}H_{22}O(C_2H_4O)_n$)	Sigma-Aldrich®	T8787	Sigma-Aldrich® Química S.A., Sintra, Portugal
Trypan Blue 0.4% (w/v) (TB, $C_{34}H_{28}N_6O_{14}S_4$)	Sigma-Aldrich®	T8154	Sigma-Aldrich® Química S.A., Sintra, Portugal
Trypsin solution from porcine pancreas, 2.5% (w/v)	Sigma-Aldrich®	T4549	Sigma-Aldrich® Química S.A., Sintra, Portugal
Material for the quantification of total protein content			
Bio-Rad Protein Assay Dye Reagent Concentrate	Bio-Rad Laboratories Lda.	5000006	Bio-Rad Laboratories Lda, Amadora, Portugal
Material for the quantification of lactate			
Kit L-Lactate (LAC)	Randox	LC2389	Irlandox Laboratories Lda., Porto, Portugal
Material for the quantification of HSP90α levels			
HSP90α ELISA Kit	Enzo Life Sciences® Inc.	ADI-EKS-895	Grupo Taper S.A., Sintra, Portugal
Protease inhibitor cocktail	Sigma-Aldrich®	P8340	Sigma-Aldrich® Química S.A., Sintra, Portugal
Material for cell culture			
Disposable plastic material routinely used in cell culture (culture flasks, multi-well plates, centrifuge tubes and serological pipettes)	Orange Scientific	*	Frilabo, Maia, Portugal
6-well cell culture plates	Corning Incorporated	3516	Sigma-Aldrich® Química S.A., Sintra, Portugal

*References for each material can be found in the manufacturer's website (http://www.frilabo.pt/pt/consumiveis-1/cultura-celular).

2.2. Biological material

The BEAS-2B cell line was used in all the experiments described in this dissertation. This cell line was purchased from ECACC (Salisbury, UK; ECACC no. 95102433), as a cryopreserved cellular suspension. In our laboratory, passage 1 was assigned to the culture initiated from the frozen aliquot supplied by ECACC.

2.3. Equipment

All the equipment used in the experimental work described in this dissertation is listed in Table 2.2.

Table 2.2. List of equipment used in the experimental work described in this dissertation.

Equipment	Manufacturer	Model	Distributor
Balance (analytical)	Acculab	ALC-810.2	Sartorius, S.A., Lisboa, Portugal
Balance (precision)	Acculab	ALC-210.4	Sartorius, S.A., Lisboa, Portugal
Bench autoclave	Prestige Medical	220140 Omega Media	Ezequiel Panão Jorge, Electromédica, Coimbra, Portugal
Bench centrifuge	MPW Medical Instruments®	MPW-350R	Not known
Bench microcentrifuge	Eppendorf	Minispin	VWR International Lda., Carnaxide, Portugal
Camera	Olympus	DP20	Not known
Camera monitor	SyncMaster 151s	00124110	Samsung, Lisboa, Portugal
CO_2 incubator	Sanyo	COM-19AIC(UV)	Not known
Dry bath	Biogen Científica	AccuBlock Digital Dry Bath Model D1100	Not known
Liquid nitrogen container	Cryo Diffusion S.A.S.	B2048	Not known
Microplate reader	BioTek	µQuant	IZASA Portugal, Carnaxide, Portugal
Mr. Frosty™ freezing container	Thermo Scientific	5001-001	VWR International Lda., Carnaxide, Portugal
Optical microscope	Olympus	CKX41	Not known
pH meter	SevenCompact	S220	Mettler Toledo, Porto, Portugal
Real-time Thermal Cycler	Bio-Rad Laboratories Lda	CFX96™ Optics Module	Bio-Rad Laboratories Lda, Amadora, Portugal
UV-visible spectrophotometer	Thermo Scientific	Nanodrop T042	VWR International Lda., Carnaxide, Portugal
Vertical laminar flux cabinet	Kojair®	020236 BW-100	Frilabo, Lda., Porto, Portugal
Visible spectrophotometer	Thermo Scientific	Genesys 20 4001/4	VWR International Lda., Carnaxide, Portugal
Water bath	Clifton®	NEI-14 79004	Frilabo, Lda., Porto, Portugal
Water purification system	Millipore S.A.	Slimplicity® SIMS50000	Interface, Equipamento e Técnica Lda., Amadora, Portugal

2.4. Culture of BEAS-2B cells

2.4.1. Composition of the solutions used

Ultrapure water was used in the preparation of all solutions used in cell culture. DMSO, the 2% (w/v) BSA aqueous solution and the 100 µM potassium dichromate solution, were sterilized by filtration using a 0.22 µm pore size syringe filter. All filtrations were carried out in a laminar flow cabinet. All other solutions were autoclaved at 121 ºC and 1.39 atm, for around 15-20 min, depending on the size of the load and the contents.

- **Phosphate Buffered Saline (PBS), 10_x solution**

  - 1.37 M NaCl
  - 27 mM KCl
  - 81 mM Na_2HPO_4
  - 15 mM KH_2PO_4

  After complete dissolution of the salts in water, the pH of the solution was adjusted to 7.4 by dropwise addition of diluted HCl and/or NaOH solutions. The working solution, PBS 1_x, was prepared by diluting the PBS 10_x solution with water.

- **Trypsin-EDTA solution**

  - 90 mL PBS 1_x
  - 20 mg Na_2EDTA
  - 10 mL pancreatic porcine trypsin at 2.5% (w/v)

  To prepare this solution, the specified volume of pancreatic porcine trypsin solution was added, under aseptic conditions, to sterilized, Na_2EDTA-containing PBS.

- **Bovine skin gelatin, 2% (w/v)**

  - 2 g gelatin from bovine skin
  - 100 mL ultrapure water

  The 2 g of gelatin from bovine skin were added very slowly to 100 mL of ultrapure water with magnetic stirring. After complete dissolution, the solution obtained was autoclaved and then allowed to cool at room temperature.

- **BSA solution, 2% (w/v)**

  - 1 g BSA
  - 50 mL ultrapure water

  The gram of BSA was added to 50 ml of ultrapure water and mixed with the help of a vortex mixer. Then it was filtered according to the instructions mentioned above.

- **Coating solution**

  - 45 mL PBS 1_x
  - 50 mL bovine skin gelatin aqueous solution at 2% (w/v)
  - 5 mL BSA aqueous solution at 2% (w/v)

  This solution was processed in the culture room under aseptic conditions, in a laminar flow chamber.

- **Potassium dichromate ($K_2Cr_2O_7$), 50 µM solution**

  - 1.5 mg $K_2Cr_2O_7$
  - 50 mL ultrapure water

  The potassium dichromate was added to 50 ml of ultrapure water and mixed with the help of a vortex mixer. Then it was filtered according to the instructions mentioned above.

2.4.2. Cell culture routine

BEAS-2B cells, grown as adherent monolayers, were cultured in 25 cm^2 filter-vented flask (except when otherwise stated) using a serum-free medium containing retinoic acid, epinephrine, gentamicin (antibiotic), bovine insulin, hydrocortisone, human epidermal growth factor (EGF), transferrin, bovine pituitary extract and triiodothyronine [197] and maintained at 37 ºC in a humidified atmosphere of 95% (v/v) air/5% (v/v) CO_2. The medium employed was in LHC-9, a serum-free medium.

Filter-vented culture flasks were coated with coating solution (see section 2.4.1 for more details) (about 0.04 mL/cm^2 of growth surface) 2 h before their use. Immediately before seeding the cells, the excess of coating solution was removed, the flask was washed twice with PBS 1_x and fresh cultured medium was added (about 0.2 mL/cm^2 of growth surface).

Cells were seeded at a density of 2000 cells/cm^2 and cultures were passaged once a week, when cultures reached 80% confluence (to have never reached the stationary phase of growth). All procedures of the cell passage were always handled under aseptic conditions, in a laminar flow cabinet. The passage procedure, shown in Figure 2.1, was as follows. First, the culture medium was discarded and the cell monolayer was washed twice with 2 mL of PBS 1$_x$. Then, 1 mL of trypsin-EDTA solution was added and spread over the entire growth surface. The excess of trypsin was removed and trypsinization was observed upon examination using an optical microscope in order to detect, in a timely manner, the moment when cells were released from the flask, to avoid damaging the cells. Detached cells were easily detected, since they became smaller, brighter and round. Thereafter, to dilute trypsin, 8 mL of PBS 1$_x$ were added to the flask and the cellular suspension was centrifuged at 590 *g* for 7 min at room temperature. The resulting pellet was resuspended in an appropriate volume of culture medium (usually 4 mL). Then, a small volume of the suspension was collected and used for cell counting (section 2.5). Finally, the desired volume to prepare a new culture with the desired seeding was calculated and added to the vessel after homogenization of the cellular suspension.
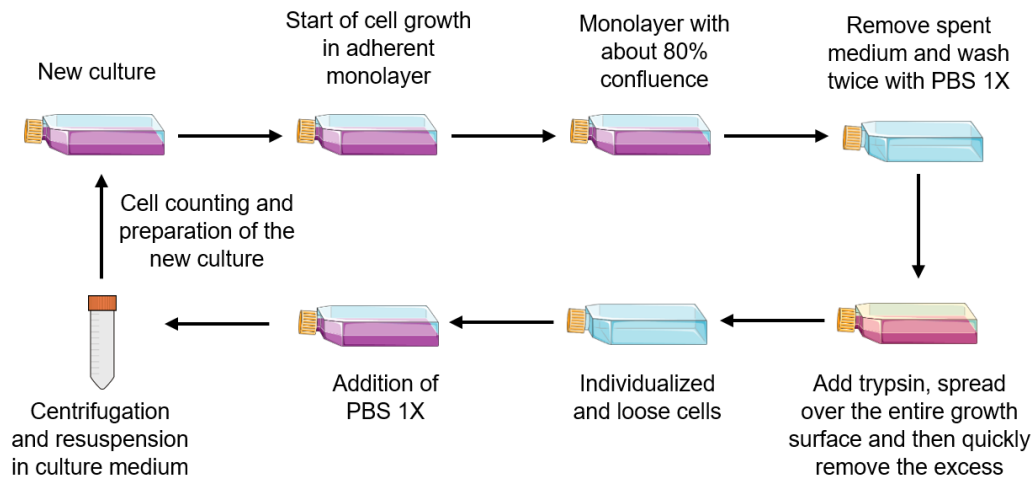

Figure 2.1. Schematic representation of the fundamental steps required for cell subculturing. Before an excessive confluence was reached, cell subculturing was performed. The culture medium was removed from the flask and the cell monolayer was washed twice with PBS 1$_x$. Then, cells were trypsinized and the cellular suspension was resuspended in PBS 1$_x$. Next, the cell suspension was centrifuged and the resulting pellet was resuspended in fresh culture medium. Finally, after cell counting (section 2.5), an appropriate volume of cellular suspension was transferred to a new flask.

For cultures chronically exposed 1 µM Cr(VI), 50 µL of a filter-sterilized 50 µM potassium dichromate solution were added, 24 h after passage. The corresponding control cultures, which were maintained in parallel, received an equal volume of ultrapure water.

2.4.3. Culture initiation and cryopreservation

In order to start a new cell culture, an aliquot of cryopreserved cells was rapidly thawed and transferred to a new pre-coated culture flask with 75 cm^2 of growth area, containing 15 mL of culture medium. After a 24 h incubation, the culture medium was discarded in order to remove dead cells and DMSO, which are constituents of the freezing medium (section 2.4.4), and replaced with fresh medium. Cells were then incubated again until the culture was ready for subculturing.

To prepare cells for cryopreservation in our laboratory, 1 mL cell aliquots containing between 1 and 4 million cells were normally prepared (Figure 2.2). To freeze three cell aliquots, flask with 75 cm^2 of growth area were prepared and, before excessive confluence was reached, the culture medium was removed and the cell monolayer was washed twice with PBS 1$_x$. Then, cells were trypsinized, resuspended in PBS 1$_x$ and centrifuged at 590 g for 7 min (section 2.4.2). The pellet obtained was resuspended in a solution containing culture medium (LHC-9), FBS and DMSO in a 7:2:1 ratio. Then, cell aliquots were transferred to a Mr. Frosty^{TM} freezing container, which was filled with isopropanol to allow cells to be cooled at a slow and constant rate (usually 1 ºC min^{-1}) [198], and kept at -80 ºC for at least 5 h. Finally, aliquots were stored in a liquid nitrogen container, at -196 ºC, where they remained until necessary.
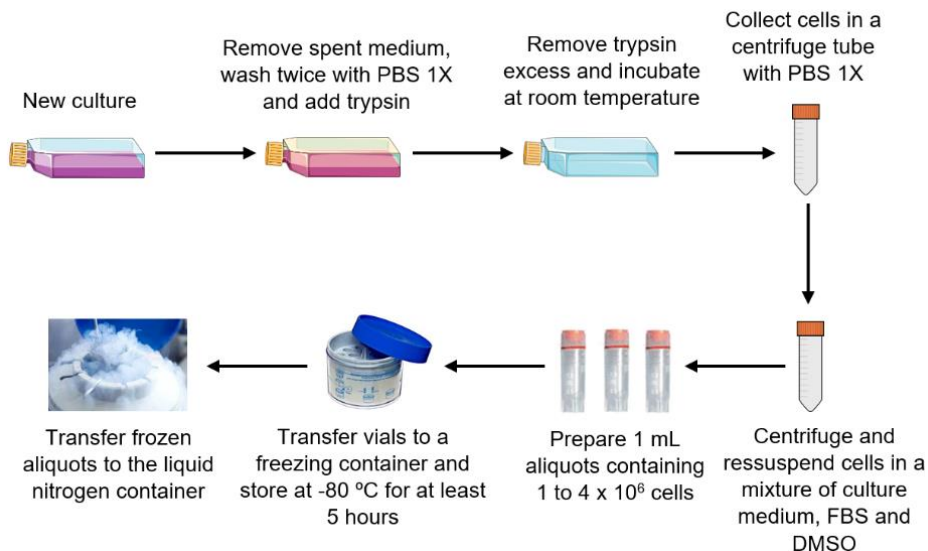

Figure 2.2. Schematic representation of the main steps required for cell freezing. Until centrifugation, the steps are those of routine sub-culturing. After centrifugation, the cell pellet was resuspended in a mixture of culture medium (LHC-9), FBS and DMSO in a 7:2:1 ratio. Aliquots of 1 mL, containing 1 to 4 million cells, were transferred to a Mr. Frosty^{TM} freezing container that was stored at -80 ºC for at least 5 h. After this time, the aliquots were transferred to a liquid nitrogen container.

2.5. Cell counting using the Trypan Blue dye exclusion method

The Trypan Blue (TB) dye exclusion method was used in routine cell culture as well as in the preparation of cultures for experiments.

The TB dye exclusion method is a simple and rapid technique to measure cell viability in a cell suspension. This method takes advantage of the fact that live cells have an intact cell membrane and, consequently, TB does not enter the cell interior, while the dead cells let this dye enter the cell interior because they have damaged membranes. As a result, a viable cell will have a clear cytoplasm whereas a dead cell will have a blue cytoplasm, allowing easy identification under an inverted microscope. However, this method has the disadvantage of not being able to differentiate a non-viable cell from a cell that has an abnormal cell membrane but might be able to repair it and become fully viable [199].

Samples for cell counting were prepared by mixing small volumes of the cellular suspension and 0.4% (w/v) solution of TB in appropriate proportions, normally 20 μL of TB and 100 μL of cellular suspension. After thorough homogenization, this mixture was used to fill the two chambers of a hemocytometer. Upon examination under an inverted microscope, the cells in each corner square of the two counting areas were counted and averaged, following the rules depicted in Figure 2.3.
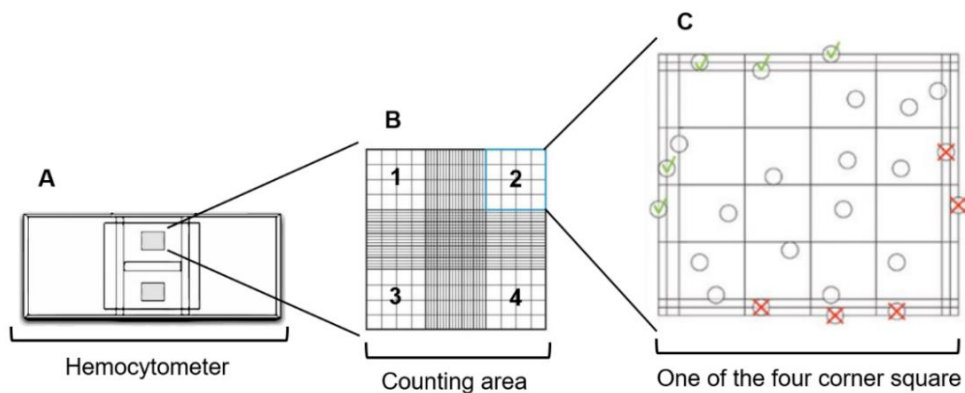

Figure 2.3. Schematic representation of (A) hemocytometer and of (B) one of its counting areas and (C) one of the four corner squares. Before cell counting, a coverslip was placed over the hemocytometer and the cellular suspension with TB was added to both counting areas of the hemocytometer. Only the cells present in the numbered corner squares were counted according to the rule depicted in panel (C), *i.e.* the circles with green checkmark and the empty circles indicate the counted cells (inside the grid and overlapping with the top and left edges), while the circles with red cross indicate the cells that were excluded of the counting.

For each cellular suspension at least two counts were carried out, and if those counts differed by more than 10%, a third count was done. Using the count number for each counting area, the volume of each corner square (1 x 10^{-4} mL) and taking into account the

dilution factor, the total number of cells per mL of cellular suspension was determined, using equation 1.

$$\text{Cells}/\text{mL} = x \times \frac{\text{dilution factor}}{1 \times 10^{-4} \text{ mL}} \qquad (1)$$

x – mean number of cells counted in the eight corner squares of the two counting areas.

2.6. Morphological studies

The cell morphology and pattern of growth of BEAS-2B cells were monitored by phase-contrast microscopy with an Olympus CKX41 microscope equipped with an Olympus OD-20 camera.

2.7. Cellular treatment with Cr(VI)

Treatment with Cr(VI) was performed at least 5 h (normally 24 h) after the establishment of the cultures to allow the adhesion of cells to the substrate and the recovery of cells from the stress caused by the subculturing. In all experiments, all cultures, including controls [0 μM Cr(VI)], were established and processed in parallel and all received the same volume of the addition vehicle (ultrapure water) as the treated cultured did.

2.8. Evaluation of bioenergetic parameters

There is a range of methods for the evaluation of bioenergetic parameters, each with its advantages and limitations. To quantify the same parameter, there may be methods with more advantages than others, for example, in terms of sensitivity and time consumed, but less advantageous with regard, for example, to the costs and necessary equipment. The following sections describe the methods selected for quantifying the rate of lactate production by cells in the culture medium and the total protein content in the cell culture.
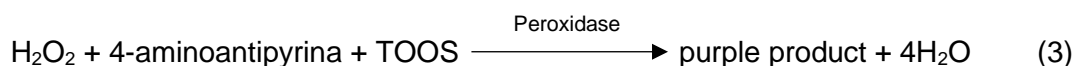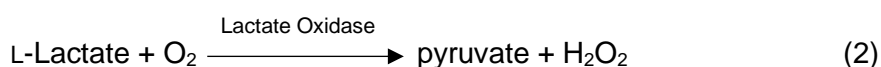
In this dissertation, the quantifications of total protein and lactate were performed at room temperature with commercial kits based on enzymatic reactions. This type of assays is very specific and has a relatively low cost. The protocols used were those recommended by the manufacturer.

2.8.1. Lactate quantification

For the quantification of lactate, BEAS-2B cell cultures from different passage stages were prepared in 6-well cell culture plates (Corning Incorporated) with a seeding density of 2000 cells/cm^2. After a week, the culture medium was removed and 1.5 mL of fresh medium

was added. Then, after 2.5 h, 100 µL of medium samples were collected for analysis and were placed for 15 min in a dry bath at 80 ºC in order to inactivate certain enzymes that maintain activity outside the cellular environment. When the samples were not immediately analyzed, they were stored at -20 ºC until their analysis.

For the enzymatic determination of L-Lactate present in the culture medium, the commercial kit L-Lactate (LAC), from Randox, was used. Increased concentration of lactate in the sample is an indicator of increased rates of lactic acid fermentation. This method is based on the quantification of a colored product that is formed according to the following reactions (equations 2 and 3):

$$\text{L-Lactate} + O_2 \xrightarrow{\text{Lactate Oxidase}} \text{pyruvate} + H_2O_2 \qquad (2)$$

$$H_2O_2 + \text{4-aminoantipyrina} + \text{TOOS} \xrightarrow{\text{Peroxidase}} \text{purple product} + 4H_2O \qquad (3)$$

TOOS: N-ethyl-N-(2 hydroxy-3-sulphopropyl)m-toluidine

The absorbance at 550 nm of the generated colored product is directly proportional to the concentration of lactate present in the samples. This commercial kit provides the enzyme reagent, consisting of the enzymes 4-aminoantipyrine, lactate oxidase, peroxidase and ascorbate oxidase, all in lyophilized form, the buffer substance TOOS and the standard L-Lactate for the standard curve.

The protocol provided by the supplier indicates that the enzyme reagent must be added with 6 mL of the buffer TOOS. However, for an economical reason, we added 6 mL of ultrapure water to the mixture, making sure that the results were not affected by this process.

In order to construct a standard curve (A_{550} vs lactate concentration), four lactate solutions with concentrations between 0 and 4,38 mM were prepared by diluting with ultrapure water the standard lactate provided by the kit. For the quantification of lactate, the procedure described in Table 2.3 was followed. After reading the absorbances at 550 nm, on a visible spectrophotometer, the concentration of the lactate in each sample was calculated using the standard curve.

Table 2.3. Procedure for quantifying L-Lactate, using the Randox L-Lactate kit.

	Blank	Sample/Standard lactate
Ultrapure water (µL)	20	-
Sample or standard lactate (µL)	-	20
Enzyme reagent diluted with ultrapure water and TOOS (1:2) (µL)	800	
Mix and read the absorbance at 550 nm after 15 min of incubation at room temperature		

2.8.2. Protein content quantification

For the quantification of the total cellular protein content, BEAS-2B cell cultures from different passage stages were prepared in 6-well cell culture plates (Corning Incorporated) with a seeding density of 2000 cells/cm^2. After a week, the culture medium was removed from each well and the cell monolayer was washed twice with 1 mL of PBS 1_x. Then, after removing all residual PBS 1_x with a micropipette, 400 µL of Triton^{TM} X-100 0.1% (v/v) was added per well and allowed to act overnight at 4 ºC. Triton^{TM} X-100 is a common non-ionic surfactant, non-denaturing and emulsifier which is used to solubilize proteins [200,201].

The next day, a cell scraper was used to put the protein content in suspension. Then, using a micropipette, the protein suspension was resuspended and 500 µL of sample was collected. When the samples were not immediately analyzed, they were stored at -20 ºC until their analysis.

For the quantification of the total protein levels in the cell lysates, the Bradford method was chosen, using the Bio-Rad Protein Assay Dye Reagent Concentrate. The Bradford or Comassie Blue dye method relies on the binding of the dye Coomassie Brilliant Blue G-250 to proteins and is a rapid, sensitive, inexpensive and specific method [202]. This dye can exist in three different ionic forms: cationic, neutral and anionic. Under acidic conditions, the red cationic form of the dye, which have an absorbance maximum at 465 nm, changes to the anionic blue form, which have an absorbance maximum at 595 nm, when the dye binds to protein. Coomassie dye binds to protein molecules by two means: the triphenylmethane group [-C(C$_6$H$_5$)$_3$] binds to nonpolar structures in proteins and the anion sulfonate groups (-SO$_3^-$) interact with protein cationic side chains (*e.g.*, arginine, lysine) [203]. Therefore, the quantity of protein can be estimated by determining the amount of dye in the blue ionic form at 595 nm [204,205]. In the Dye Reagent concentrate, the Comassie Blue dye is in a double protonated form that has a reddish-brown color.

BSA was used as standard, as it is one of the most commonly used calibration proteins for its ready availability and low cost [203]. In order to construct a standard curve

(A_{550} vs protein concentration), solutions with concentrations between 0 to 10 µg/mL were prepared from a 1 mg/mL BSA stock solution. For protein quantification, the procedure described in Table 2.4 was followed. After reading the absorbances at 595 nm, on a visible spectrophotometer, the concentration of the protein content in each sample was calculated using the standard curve.

Table 2.4. Procedure for the quantification of total protein content, using the Bio-Rad Protein Assay Dye Reagent Concentrate.

	Blank	Sample/Standards
Ultrapure water (µL)	800	780
Sample or standard BSA (µL)	-	20
Reagent (µL)	200	
Mix and read the absorbance at 595 nm after 15 min of incubation at room temperature		

2.9. Quantification of intracellular HSP90α levels

The intracellular levels of HSP90α (no reactivity with HSP90β and GRP94) were determined using the commercially available Enzyme-linked immunosorbent assay (ELISA) kit (Table 2.1). The use of this kit ensures a rapid, reliable and sensitive (limit of detection is 50 pg/mL) quantification of the protein of interest. The precise quantification is possible due to a standard curve prepared for each assay from serial dilutions of HSP90α standard provided with the kit.

Cell lysates used in the assay were prepared from BEAS-2B cultures from different passage stages. Cells were seeded at 4000 cells/cm^2 in 25 cm^2 flasks (one flask per lysate). Then, the cultures were allowed to grow for three days until cell lysate preparations (Figure 2.4). Preparation of the cell lysates was done according to the manufacturer's instructions. After being collected in a centrifuge tube with PBS 1_x, cells were centrifuged at 590 *g* for 7 min at 21 ºC. Then, the pellets obtained were resuspended in an appropriate volume of extraction reagent 1_x (500 µL), supplemented with a protease inhibitor cocktail (1 µL) in order to avoid degradation of the proteins, since proteases are capable of degrading proteins in the extracts. Cells suspensions were incubated on ice for 30 min with occasional mixing. After, these cells suspensions were centrifuged at 20925 *g* for 10 min at 4 ºC. Cell lysates were the supernatants of this centrifugation.
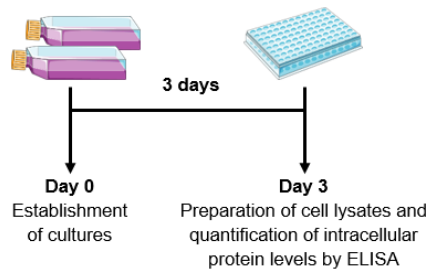
Figure 2.4. Protocol used in the determination of the effects of extensive passaging on the intracellular levels of HSP90α. Three days after the establishment of the cultures, cell lysates were prepared and intracellular HSP90α levels were quantified by ELISA.

A portion of the cell lysate was used in the assay (if it was not used on the same day as the extraction, the lysates were kept at -80 ºC), and another portion was stored at 4 ºC to be used in the quantification of total protein levels (section 2.12.2) (when the quantification of the total protein content was not carried out on the same day, the samples were kept at -20 ºC).

The assay plates provided in the kits were pre-coated with a specific mouse monoclonal antibody that binds to HSP90α in the samples or in the standards. The captured protein was then detected using an HSP90α antibody conjugated to the enzyme horseradish peroxidase (HRP). 3,3',5,5'-Tetramethylbenzidine (TMB) was the substrate of HRP used, being converted in a blue product through oxidation and in proportion to the amount of captured HSP90α. An acidic solution is used to stop the color development, and convert the blue color to yellow. The intensity of the yellow color was read at 450 nm using a microplate reader. The detailed protocol is schematically represented in Figure 2.5.
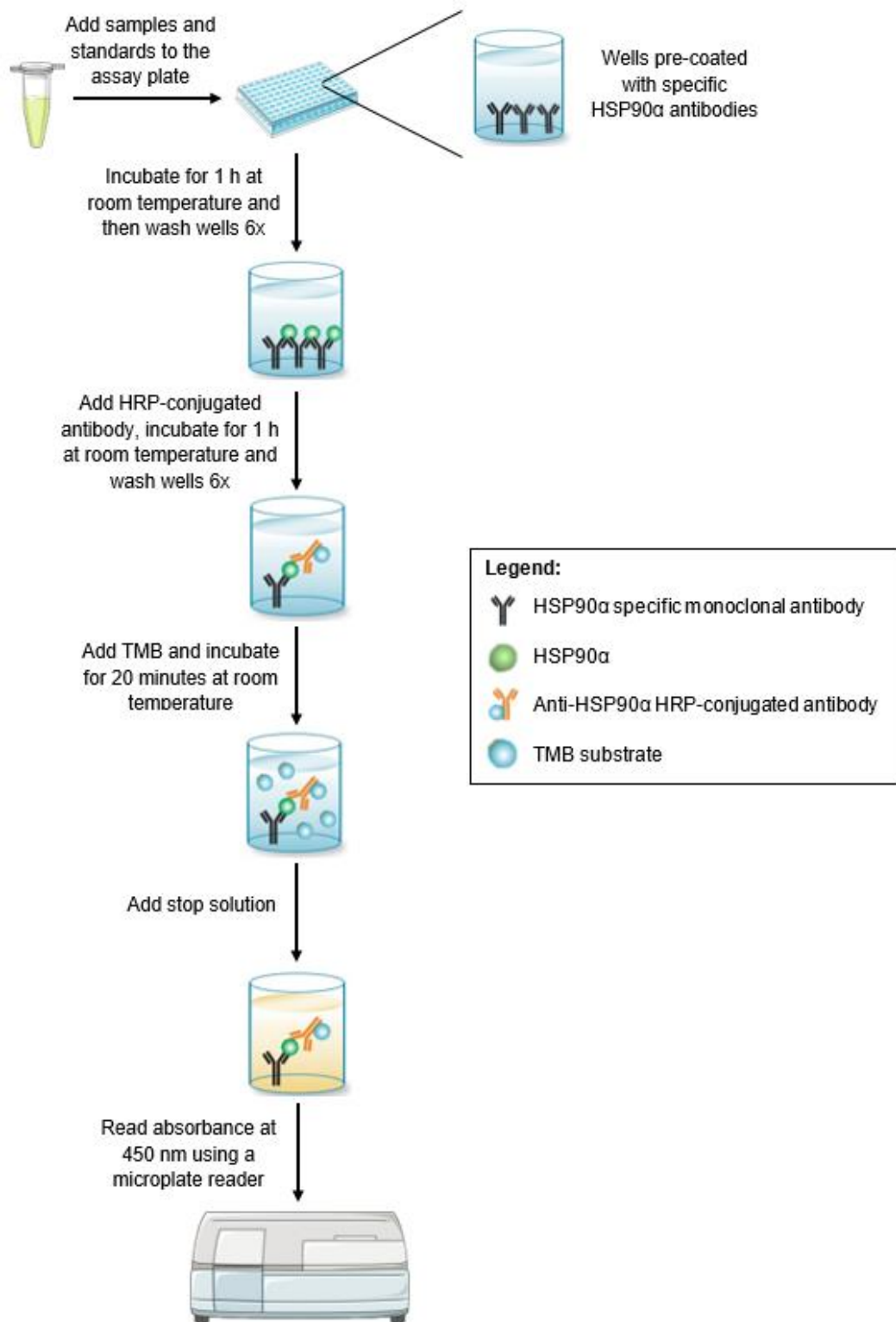
Figure 2.5. Schematic representation of the protocol followed for the quantification of Hsp90α in cell lysates, using a commercially available ELISA kit.

HRP, horseradish peroxidase; TMB, 3,3',5,5'-Tetramethylbenzidine.

2.10. Cytotoxicity assay

2.10.1. Based on clonogenic assay

The cytotoxicity assay based on clonogenic assay was carried out with the objective of evaluating the resistance of BEAS-2B cells from different passages to Cr(VI).

When the BEAS-2B cultures had grown to approximately 80% confluence, the cells were seeded at 800 cells/well in 6-well cell culture plates (Corning Incorporated) (instead of T25 flaks as mentioned in the previous section to save material) and treated with 1 μM Cr(VI) for 9 days (ultrapure water as the solvent control).

Both Cr(VI) and ultrapure water (for the controls) were added 24 h after the establishment of cultures (Figure 2.6). Nine days later, colony counting was performed in the same way for the clonogenic assays (section 2.9).
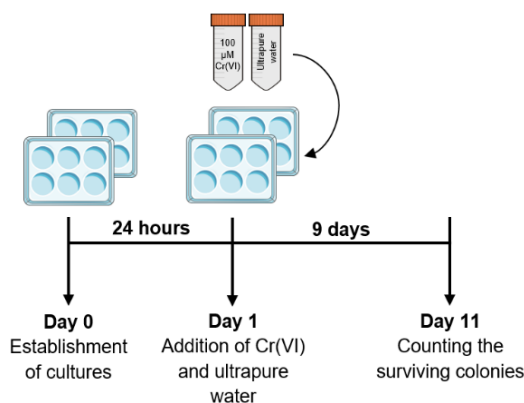

Figure 2.6. Protocol used for the analysis of cell viability based on the clonogenic potential. Cr(VI) and ultrapure water were added 24 h after the establishment of cultures. The colonies counting was performed as described in section 2.9.

2.10.2. Based on colorimetric assay

This experiment was carried out with the objective of evaluating the resistance of BEAS-2B cells to Cr(VI).

Cell viability was also determined using the yellow tetrazolium salt (MTT) colorimetric assay. This assay is designed for the spectrophotometric quantification of cell growth and viability and is based on the cleavage of the MTT molecule to purple formazan crystals by metabolic active cells. The enzymatic reduction of MTT to formazan is catalysed by mitochondrial succinate dehydrogenase (SDH), which involves the pyridine nucleotide cofactors NADH or NADPH. Since SDH is an important enzyme complex that participates in both the tricarboxylic acid cycle and the electron transport chain, the MTT assay is dependent on mitochondrial respiration and is directly related to cell viability [206].

The formazan crystals formed are insoluble in water. Upon solubilisation using an organic solvent, they give rise to a colored solution and can be quantified by spectrophotometry at 570 nm. The absorbances of the colored solutions are read at a wavelength of 570 nm (the greater the formazan concentration, the higher the absorbance) and 690 nm, which absorbs the MTT. Therefore, the subtraction of these two values corresponds to the absorbance value of formazan. This assay allows the rapid and convenient handling of a high number of samples and ensures a high degree of accuracy [206].

For this experiment, cells were seeded at 8000 cells/cm^2 in 24-well cell culture plates (Orange Scientific REF 4430300) and treated with different concentrations of Cr(VI) (1, 2 and 4 µM) for 48 h, with ultrapure water as the solvent control. After a 72 h incubation, cells were treated with 50 µL of a 5 mg/mL MTT, for 3 h at 37 ºC in the incubator [the volume of MTT used corresponds to 10% (v/v) of the total volume of the well]. After incubation, the medium was removed, with care to not destroy the formazan crystals, and 300 µL DMSO were added to each well in order to completely dissolve the formazan crystals, resulting in a homogeneous solution of violet color. Finally, the culture plate was read by a scanning multiwell visible spectrophotometer at 570 and 690 nm, using the Biotek Gen5^{TM} version 1.11 data analysis software (Figure 2.7).
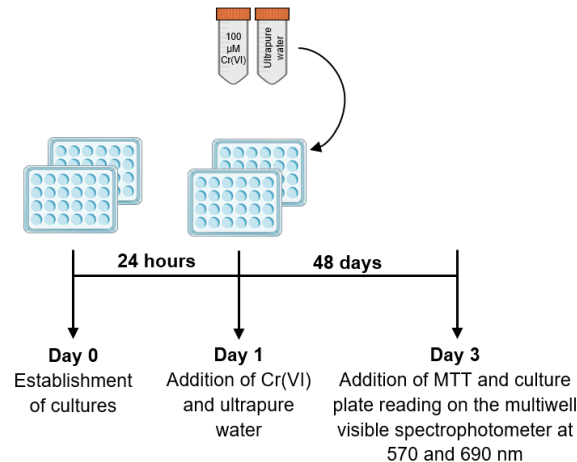

Figure 2.7. Protocol used for the analysis of cell viability based on the MTT metabolization. Cr(VI) and ultrapure water were added 24 h after the establishment of cultures. 3 days after the cultures were established, MTT was added to the wells, the formazan crystals were resuspended in DMSO and the culture plate was read by a scanning multiwell visible spectrophotometer at 570 and 690 nm.

2.11. Wound healing assay

The wound healing assay is a standard *in vitro* technique for studying cell migration and cell-cell interaction in two dimensions (2D). In this assay, also called a scratch assay, a cell-free area is created in a confluent monolayer by, commonly, physical exclusion (can

also be created through mechanical, thermal or chemical damage). The area without cells induces the cells to migrate into the gap.

One limitation of this assay is that there may be inconsistencies with the size and depth of the scratch, since when the scratch is done manually, it is common that the edge limits are irregular, which makes analysing data more difficult. In addition, the damage can physically damage the cells surrounding the wound. This limitation is less common with automated technologies.

For this experiment, cells were seeded at 36000 cells/cm^2 in 6-well cell culture plates (Corning Incorporated) and cultured in LHC-9 medium. Cultures were allowed to grow for three days. On the third day, the confluent monolayer was scratched with a 200-µL pipette tip and the medium was renewed to remove damaged cells. Then, digital photos were taken of known locations at 0, 9 and 24 h after injury using a phase-contrast microscope equipped with an Olympus OD-20 camera (Figure 2.8). Wound repair (WR) was expressed as a percentage of the initial wound distance between each wound edge measured at the start of the experiment and was calculated using the following formula:

%WR = ((initial distance between each wound edge – 9 or 24 h wound distance between cells that migrated more on each side) / initial distance between each wound edge) x 100.

In each experiment, three photos on each location were analysed and the mean was calculated. The distance between each edge of the wound over time was measured using the ImageJ bundled with 64-bit Java 1.8.0_172 program.
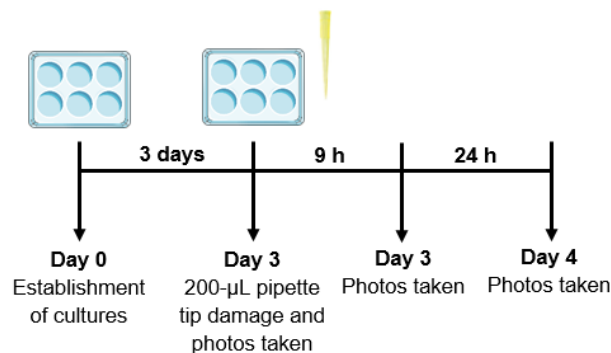

Figure 2.8. Protocol used for the wound healing assay. The 200-µL pipette tip damage was caused three days after the establishment of the cultures. In each experiment 3 photos were taken of places known per well at 0, 9 and 24 h after injury.

2.12. Determination of doubling times

The population doubling time (PDT) is the time required for a cell culture to double in number. Normally, the PDT does not take into account any cells that were lost due to death from apoptosis or necrosis [207].

Cells that grow in culture have different rates in each of the different phases of the growth cycle (lag, exponential and stationary phases). For the determinations of doubling times, cultures were in exponential phase, which allowed to obtain more constant and reproducible results in comparison with the other phases [207].

Doubling times were determined using BEAS-2B cell cultures, which were monitored for three days, with two time points each day (in the morning and in the evening). For each condition tested, triplicate cultures per time point were established in 6-well cell culture plates (Corning Incorporated), at a seeding density of 2000 cells/cm^2. At the desired time points, the medium of the corresponding cultures was removed and the cell monolayer was washed twice with 1 mL of PBS 1_x. All residual PBS was removed using a micropipette. Then, 300 µL of trypsin-EDTA solution were added to each well and, after a brief incubation at room temperature, 200 µL of PBS 1_x was added to dilute the trypsin solution and facilitate cell suspension. After resuspension, cells were immediately transferred to microcentrifuge tubes and sat on ice until cell counting, to inhibit trypsin activity.

Doubling times were determined by dividing the natural logarithm of 2 by the slope of the line, that relates the natural logarithm of the total number of cells and the time elapsed since the preparation of the cultures.

2.13. Clonogenic assay

The clonogenic assay, also known as colony formation assay, was used to assess cell proliferation. This *in vitro* assay evaluates the ability of a single cell to grow into a colony. Therefore, this assay tests every cell in the population for its ability to undergo "unlimited" division. Only a fraction of seeded cells have the capacity to produce colonies [208].

For this assay, cultures were seeded in 25 cm^2 filter-vented flask at a cell density of 400 cells/flask. Cultures were then allowed to grow for 11 days. After 11 days, the surviving colonies were scored to assess cloning efficiency. To this end, colonies were washed twice with 2 mL of PBS 1_x and then fixed and stained by addition of 1 mL of glutaraldehyde 6.0% (v/v)/crystal violet 0.5% (w/v). Approximately 40 min later, the growth surface of the flasks was washed with water.

2.14. Statistical analysis

For statistical analysis of the experimental data obtained, the GraphPad Prism 8.0.2 software for Windows (GraphPad Software Inc, California, USA) was used. The statistical relevance of differences between groups was examined using the paired *t* test and, in experiments in which more than two conditions were simultaneously tested, the one-way

ANOVA method was used. In experiments that used the one-way *ANOVA* method were followed by a multiple comparison test (*Tukey*). The results were presented as mean ± standard deviation (S.D.). Differences with $p < 0.05$ were considered statistically significant.

3. Results and Discussion

3.1. Impact of extensive passaging on the BEAS-2B cell line

As mentioned in the Introduction, the authors that established the BEAS-2B cell line reported genetic and phenotypic changes upon extensive passaging. Some of these changes were in line with an increased degree of transformation, namely the acquisition of weak tumorigenicity [22,37,57].

Aiming at establishing the safe passage number for this cell line, *i.e.*, the passage number beyond which it can no longer be regarded as a relevant model of human lung epithelium, our research group cultured this cell line up to passage 105 [37]. Microscopic inspection of the cultures showed that cells maintained their morphology and pattern of growth up to ca. passage 30. Between passage 30 and passage 40, cells started losing their typical polygonal shape and the typical cobblestone growth of epithelial cells. From ca. passage 40, cells appeared slightly bigger and their shape became less defined. Significantly, between ca. passage 30 and passage 60, crisscrossing became more frequent and the monolayers lost their homogeneity. From ca. passage 60, the increase in cell size became more pronounced and cells exhibited an increased granularity. On the other hand, monolayer homogeneity was recovered and crisscrossing was mostly lost, *i.e.*, cells reacquired the typical shape and growth pattern of epithelial cells, which may indicate the existence of a positive selection. Based on these observations, three passage stages were defined: the low passage stage (up to ca. passage 30), the transitional stage (from ca. passage 30 to passage 60) and the high passage stage (from ca. passage 60 onwards) [37].

Other changes observed upon extended passage included changes in the karyotype [22,37], rates of glucose consumption and lactate production [57], doubling times (unpublished results), clonogenic potential (unpublished results) and sensitivity to FBS [37]. Interestingly, similar passage stages could have been defined based on each of these cell characteristics.

The first aim of the present study was to further characterize the effects of extended passaging on the phenotype of the BEAS-2B cell line, namely at the level of protein content, stress response, rate of lactate production, migratory capacity and resistance to mildly cytotoxic concentrations of potassium dichromate, a human lung carcinogen. Cultures with different culture ages were kept and analysed in parallel. The results obtained in this part of the study are presented and discussed in the sections that follow.

3.1.1. Impact on cell morphology and pattern of growth

In the present study, similar changes in morphology and pattern of growth were observed (Figure 3.1) and, as such, the same passage stages were adopted and used when discussing the impact of extensive passaging on the properties of the cells.
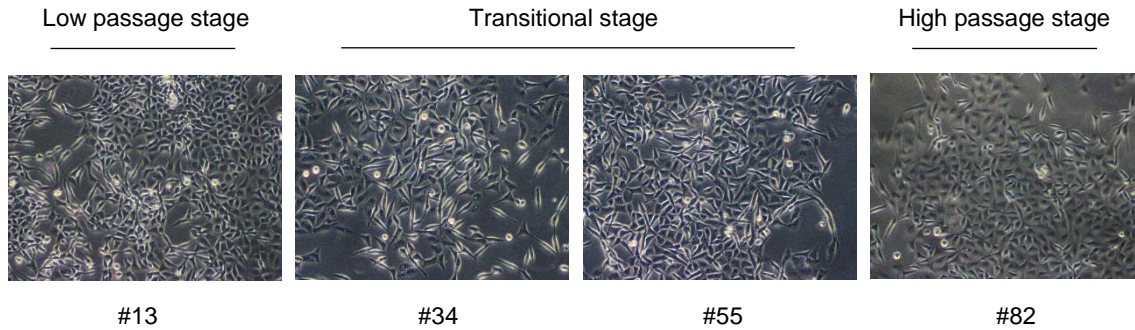
Low passage stage	Transitional stage		High passage stage

#13	#34	#55	#82

Figure 3.1. Impact of culture age on the morphology and pattern of growth of BEAS-2B cells. Representative micrographs (100x magnification) of BEAS-2B cells, at the passages indicated at the bottom of each micrograph. Changes in cell morphology and pattern of growth became noticeable from #30: cells started losing their typical diamond shape (polygonal shape) and the typical cobblestone growth of epithelial cells. From ca. #40, cells became apparently slightly bigger and their shape became less defined. Significantly, crisscrossing became more frequent and the monolayers lost their homogeneity. From ca. #60, the apparent increase in cell size became more pronounced and cells exhibited an increased granularity. On the other hand, monolayer homogeneity was recovered and crisscrossing was mostly lost. Cells were cultured in coated flasks, in LHC-9 medium. # - passage number

3.1.2. Impact on the cellular protein content

In order to assess whether the increases in cell size suggested by microscopic observation were apparent or real, the protein contents of cells at the three passage stages were determined.

Contrary to our expectations, BEAS-2B cells in the low passage stage and in the intermediary stage shared a similar protein content. Regarding cells in the high passage stage, their protein content was slightly higher (by about 9%), but the difference was not statistically significant (Figure 3.2).
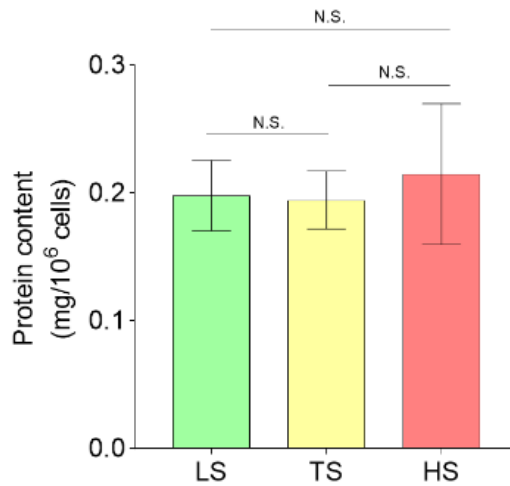
Figure 3.2. Impact of extended passaging on the protein content of BEAS-2B cells. LS: Low passage stage (#14 to #16); TS: Transitional stage (#51 to #53); HS: High passage stage (#83 to #85). For the quantification of the protein content, the Bio-Rad Protein Assay Dye Reagent Concentrate was used (section 2.12.2 for more information). Results are presented as mean ± SD of four independent experiments (n = 4), using in all of them triplicates of cultures for each condition analyzed. Experimental data were analyzed with the software GraphPad Prism 8.0.2, using the *one-way ANOVA* method followed by the *Tukey's* multiple comparison test. No statistically significant differences were observed (p > 0,05). # - passage number; N.S., not significant.

3.1.3. Impact on the HSP90α levels, a key component of the stress response

Taking into consideration the report by Harris and colleagues that BEAS-2B cells developed weak tumorigenicity when they were extensively passaged [31], it seemed interesting to check the effect of extended passaging on cellular parameters indicative of transformation status, such as the intracellular levels of HSP90α. In fact, it is known that tumor cells have increased levels of this protein [87,186].

Of note, no studies could be found in the literature regarding the impact of extensive passaging on intracellular HSP90α protein levels.

Inspection of Figure 3.3 shows that the intracellular HSP90α protein levels in transitional stage cultures were significant higher (by over 25%) than those in low passage stage and high passage stage cultures. It must be stressed, though, that these results are from a single independent experiment.

The results obtained suggest that the levels of intracellular stress to which cultures in the transitional stage are exposed are significantly higher that those experienced by low passage stage cells and high passage stage cells. Altogether, these results suggest that BEAS-2B cells undergo a crisis between passages 30 and 60, after which they recover, at least partially, their initial characteristics.
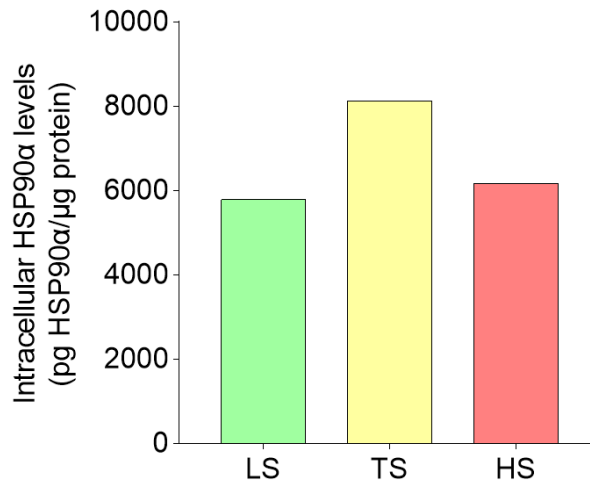
Figure 3.3. Effects of extensive passaging in the BEAS-2B cell line on the levels of Hsp90α, a key component of the stress response. LS: Low passage stage (#12); TS: Transitional stage (#50); HS: High passage stage (#73). HSP90α levels were determined using a commercially available ELISA kit, as described in section 2.13. The results were normalized to total protein levels, which were determined by the Bradford method (section 2.12.2). Results are presented as mean ± SD of one independent experiment, using in all of them duplicates of cultures for each condition analyzed. Experimental data were analyzed with the software GraphPad Prism 8.0.2, using the *one-way ANOVA* method followed by the *Tukey's* multiple comparison test: **, p < 0.01 for TS in comparison with HS and ***, p < 0.001 for LS in comparison with TS. # - passage number.

3.1.4. Impact on the resistance to mildly cytotoxic concentrations of Cr(VI)

Another parameter evaluated was resistance to Cr(VI)-induced cell death. In fact, resistance to cell death is one of the eight hallmarks of cancer defined by Hanahan and Weinberg [146] and the investigation of the mechanisms underlying Cr(VI) toxicity are one of the main lines of research of our laboratory [22,37,45,76,195,209,210].

The cellular response to DNA damaging agents typically involves cell cycle arrest followed by a cellular fate that is determined by the extent of DNA damage. When damage is irreparable, these cells remove themselves from the proliferating population by undergoing either apoptosis or cellular senescence, apparently to avoid the propagation of damaged DNA.

As mentioned before (section 1.4), Cr(VI), a human lung carcinogen, is a strong oxidizing agent and a potent DNA damaging agent, via Cr(III), the final product of its intracellular reduction, which forms complexes with small molecules to RNA, DNA and proteins [64,76]. Consequently, Cr(III) produces genotoxic, clastogenic and mutagenic effects, interfering with the normal functions of cells, thus compromising cell viability. Some studies show that at high Cr(VI) exposure levels, a very small fraction of cells survive and present replicative potential. These cells managed to escape death even with extensive DNA damage. It has been shown that cells exposed to Cr(VI) have, mostly, the *TP53* gene

mutated, creating a deficient checkpoint with the loss of the p53 protein and, therefore, they are capable to continue to proliferate [160].

In the present study, the impact of extensive passaging on the resistance to mildly cytotoxic concentration of Cr(VI) was evaluated by two different techniques: the MTT and the clonogenic assays.

The increased HSP90α levels exhibited by cells in the transitional stage suggested that they might be more resistant to Cr(VI), which is an inducer of proteotoxic stress [87,186]. However, no significant differences were observed (Figure 3.4), indicating that increased HSP90α protein levels alone do not confer increased resistance to this carcinogen.,
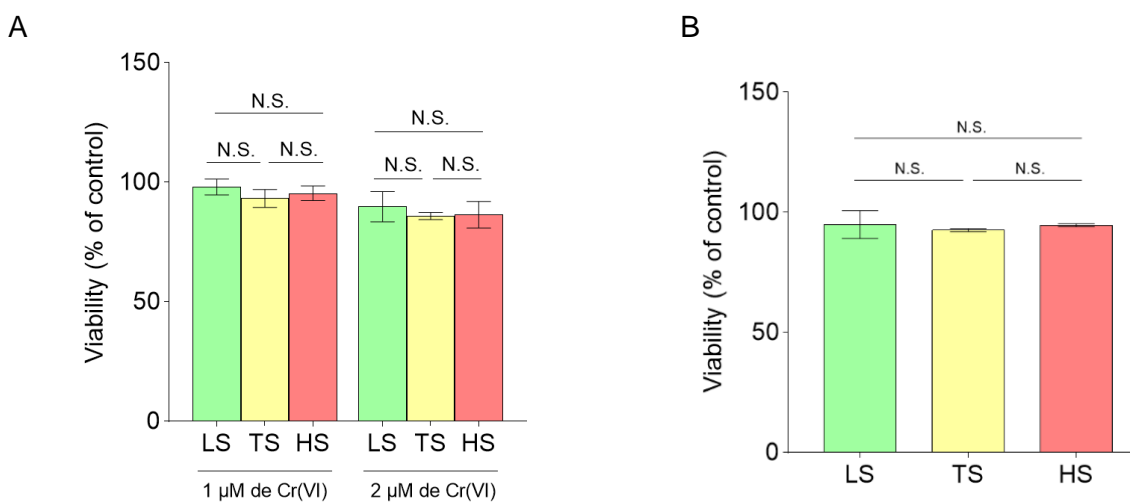

Figure 3.4. Impact of extended passaging on resistance to mildly cytotoxic concentration of Cr(VI) in BEAS-2B cells, as assessed by the MTT colorimetric assay (exposure for 48 hours) (A) and the clonogenic assay (exposure for 9 days) (B). LS: Low passage stage (#8 to #10 for the MTT assay and #10, #12 and #13 for the clonogenic assay); TS: Transitional stage (#37 to #39 for the MTT assay and #52, #54 and #55 for the clonogenic assay); HS: High passage stage (#69 to #71 for the MTT assay and #79, #81 and #82 for the clonogenic assay). In the MTT assay was evaluated two concentrations of Cr(VI) (1 and 2 μM), while in the clonogenic assay only 1 μM Cr(VI) was evaluated. Colony counting in the clonogenic assay was performed as described in section 2.9. Results are presented as mean ± SD of three independent experiments (n = 3), using in all of them triplicates of cultures for each condition analyzed. Experimental data were analyzed with the software GraphPad Prism 8.0.2, using the *one-way ANOVA* method followed by the *Tukey's* multiple comparison test. There were no statistically significant differences (p > 0,05). # - passage number; N.S., not significant.

3.1.5. Impact on the lactate production rate

For almost a century, lactate was viewed as a waste product of anaerobic metabolism and cause of muscle fatigue, but now is known to be, *via* the Lactate Shuttle, one of the most important energy fuels, which circulates throughout the body and is used by almost all tissues. In fact, circulating lactate is the mechanism by which whole body metabolism is coordinated [211–214].

It has been known for decades, since the seminal studies carried out by Otto Warburg in the 1920s, that most solid tumors exhibit a specific metabolic pattern,

characterized by a strong reliance on lactic fermentation, even under fully oxygenated conditions [215]. This particular metabolic reprogramming, known as the Warburg effect, provides the background for several therapeutic approaches and diagnosis, such as the design of inhibitors of glycolytic enzymes and positron emission tomography, respectively [216]. Nevertheless, the exact role of the Warburg effect in carcinogenesis and, in particular, in the changes produced by extensive passaging, remains unknown [215].

In the present study, the production of lactate rate was evaluated in well-aerated cultures in different passage stages. The results obtained are summarized in Figure 3.5.
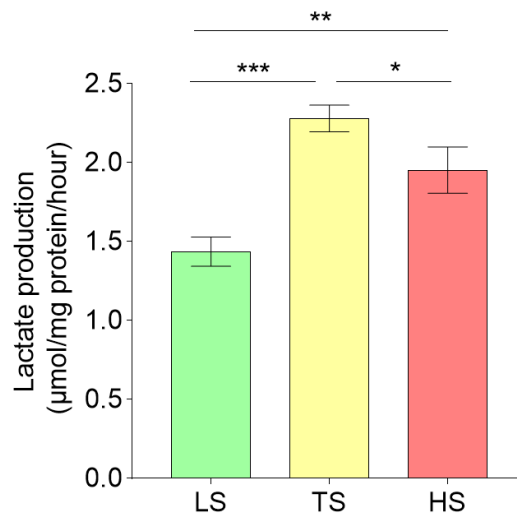

Figure 3.5. Impact of extended passaging on lactate production by BEAS-2B cells. LS: Low passage stage (#14, #15 and #17); TS: Transitional stage (#51, #52 and #54); HS: High passage stage (#83, #84 and #86). Media samples were collected 2.5 h after changing the culture medium. For the quantification of lactate in the culture medium, the kit L-Lactate (LAC), from Randox, was used (see section 2.12.1 for more information). Results are presented as mean ± SD of three independent experiments (n = 3), using in all of them triplicates of cultures for each condition analyzed. Experimental data were analyzed with the software GraphPad Prism 8.0.2, using the *one-way ANOVA* method followed by the *Tukey's* multiple comparison test: *, $p < 0.05$ for TS in comparison with HS; **, $p < 0.01$ for LS in comparison with HS and ***, $p < 0.001$ for LS in comparison with TS. # - passage number.

It is possible to observe that low passage cultures were those with lower rates of lactate production (1,437 µmol lactate/mg protein/hour), which is in agreement with a lower transformation status. Once again, the changes observed in the transitional stage cultures, in this case a significantly increased lactate production (2,281 µmol lactate/mg protein/hour) were less pronounced in the high passage cultures (1,954 µmol lactate/mg protein/hour), but still significantly different from those of the cells in the low passage stage.

3.1.6. Impact on the migratory capacity

In multicellular organisms, cell migration is a key process involved in many physiological events, such as embryological development, morphogenesis, neurogenesis,

angiogenesis, wound healing, immune defense and inflammation. In addition, cell migration is also implicated in non-physiological events, such as the transformation of cells [217]. Thus, another parameter assessed in this study was the migratory capacity of the BEAS-2B cells in the different passage stages.

Many of the characteristics associated with transformation *in vitro* are the result of cell surface modifications, *e.g.*, changes in the cell surface glycoproteins and in cell adhesion molecules, which can be related with the development of metastasis and invasion *in vivo*. Hynes et al. observed that fibronectin is lost from the surface of transformed fibroblasts due to alteration in integrins [218]. This loss may contribute to a decrease in cell-substrate and cell-cell adhesion and to a decreased requirement for attachment for the cells to proliferate, promoting cell migration [219].

Migration begins when a cell responds to an external signal that leads to the polarization, followed by a coordinated cycle of actin polymerization-dependent protrusion, integrin/actin-mediated focal adhesion and cell body translocation, which leads to the cell movement [217].

There is an obvious analogy between altered cell adhesion in culture and detachment from the tissue in which a tumor arises and the subsequent formation of metastases in distant sites, but the molecular mechanisms behind this analogy are not clear.

Most studies on cell motility have been performed in two-dimensional (2D) culture systems instead of three-dimensional (3D) culture systems, which limits our understanding of the mechanisms of cell migration, since cells use different cell migration strategies in 3D. Nevertheless, 2D cell culture still provides important insights into the molecular basis of cell protrusions and cell polarity.

In the present study, the migratory capacity was evaluated using the wound healing assay. The results can be observed in Figure 3.6 and 3.7. Wound repair (WR) was expressed as a percentage of the initial wound distance between each wound edge measured at the start of the experiment and was calculated using the following formula:

%WR = ((initial distance between each wound edge – 9 or 24 h wound distance between cells that migrated more on each side) / initial distance between each wound edge) x 100.
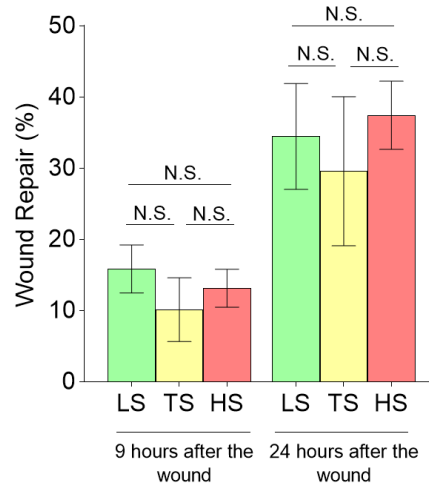
Figure 3.6. Impact of extended passaging on migratory capacity of BEAS-2B cells. LS: Low passage stage (#11 and #12); TS: Transitional stage (#40 and #41); HS: High passage stage (#72 and #73). The wound healing assay was performed as described in section 2.11. Results are presented as mean ± SD of three independent experiments (n = 3), using in all of them triplicates of cultures for each condition analyzed. Experimental data were analyzed with the software GraphPad Prism 8.0.2, using the *one-way ANOVA* method followed by the *Tukey's* multiple comparison test. There were no statistically significant differences ($p > 0,05$). # - passage number; N.S., not significant.
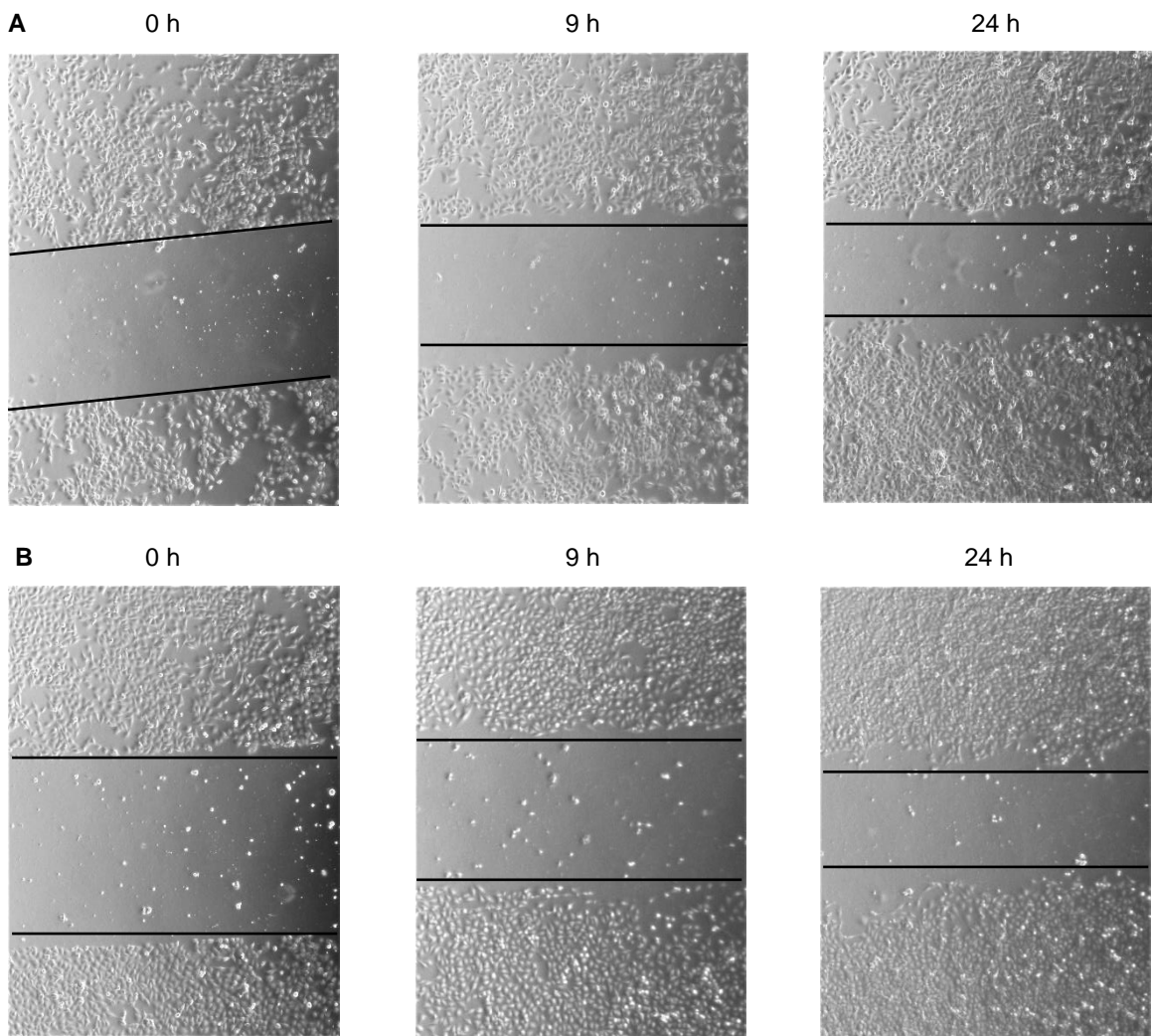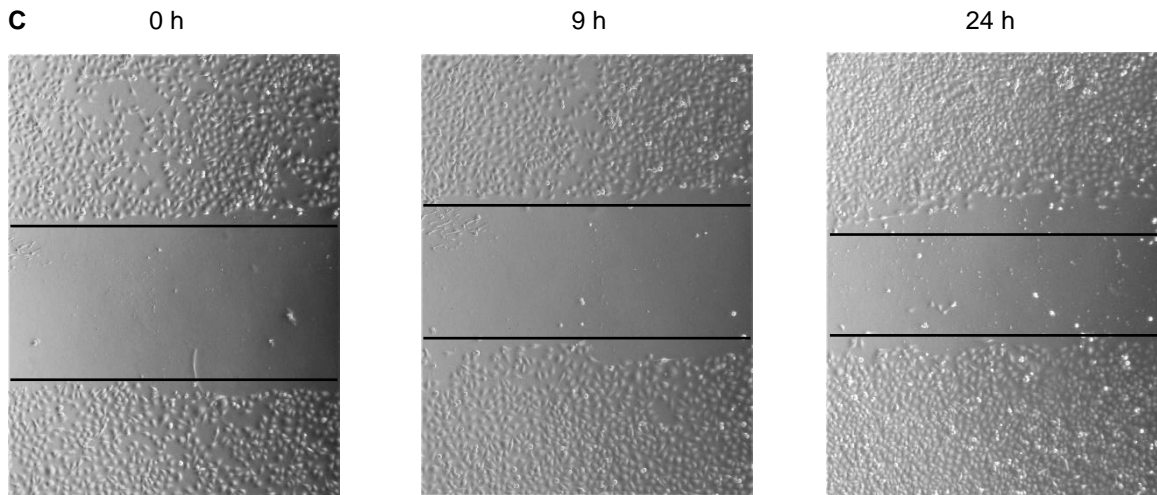
Figure 3.7. Representative micrographs (40x magnification) of BEAS-2B cultures in the low passage stage (#11) (A), in the transitional stage (#41) (B) and in the high passage stage (#72) (C) at the moment immediately after making the wound (0 h), 9 h and 24 h after the wound (all photos correspond to the same location in the well). Photos were taken using a phase-contrast microscope equipped with an Olympus OD-20 camera. The two lines delimit the edges of the wound taking into account the cells that migrated the most. It is noticeable that there is a repair of the wound over time in culture in all passage stages.

Through the results represented in Figure 3.6 it was possible to conclude that the cultures in low passage stage were those that demonstrated a greater cell migration (15.8% of WR) after 9 h after the wound compared to cultures in the transitional stage (10.1% of WR) and to cultures in the high passage stage (13.1% of WR), although the differences were not significant. On the other hand, 24 h after the wound, the cultures in the high passage stage were those that exhibited a greater cell migration (37.4% of WR), compared to cultures in the transitional stage (29.6% of WR) and to cultures in the low passage stage (34.5% of WR), although again the differences were not significant.

3.2. Impact of a long-term exposure to Cr(VI) on the BEAS-2B cell line

As discussed in section 1.4.1.2, cells exposed to Cr(VI) experience several oxidative and nonoxidative DNA damages [161]. Cr(VI) is considered a DNA damaging agent and, therefore an apoptosis-inducing agent at levels that overcome intracellular DNA repair mechanisms.

The use of inadequate exposure regimes and inadequate cell lines in studies investigating Cr(VI)-induced carcinogenesis have compromised the elucidation of the molecular basis of this process. In this study, to overcome this limitation, we used the BEAS-2B cell line, a cellular model representative of the human bronchial epithelium, which is the main target of Cr(VI) carcinogenity *in vivo*, and an exposure regimen of mild cytotoxicity [weekly addition of 1 µM Cr(VI) to the culture medium], since results obtained in studies

involving concentrations of Cr(VI) that are too cytotoxic should be interpreted with caution, as these will not mimic real exposures.

In previous studies from our laboratory, it was observed that BEAS-2B cells that resisted to mild concentrations of Cr(VI) [1 and 2 µM Cr(VI)] exhibited increased proliferation rates, alterations in cell morphology and pattern of growth [45] and a stimulatory effect on glucose uptake and lactate production [194]. This suggested that, somehow, those cells were able to not only resist the several damages induced by Cr(VI) exposure, but also gain a proliferative advantage over their non-exposed counterparts. Thus, Cr(VI) might protect transformed cells from the additional stresses they will encounter during neoplastic transformation.

In the present study, we assessed the impact of a prolonged exposure to a sub-lethal concentration Cr(VI) on several traits of the BEAS-2B cell line, namely their morphology and pattern of growth, growth rate, clonogenic potential and resistance to cytotoxic and subcytotoxic concentrations of potassium dichromate. The BEAS-2B cells used to assess the impact of long-term exposure to Cr(VI) on various cellular characteristics had already been exposed to Cr(VI) for ca. 4 by another members of our laboratory.

3.2.1. Impact on cell morphology and pattern of growth

In studies previously carried out in our laboratory, changes in terms of both morphology and pattern of growth were observed with long-term exposure to mild cytotoxic exposure to Cr(VI): cultures became heterogeneous, exhibiting areas where apparently normal diamond-shaped epithelial cells and morphologically altered cells coexisted and frequent criss-crossing (with an increase in the number of round and refractile cells, multinucleated enlarged cells and in the granularity) [22,45].

In the present study, similar changes in morphology and pattern of growth were observed (Figure 3.8). However, was not observed an increase in in the number of round and refractile cells.

These results indicate that cells exposed for more than 12 months to 1 µM Cr(VI) underwent possibly transformation, which resulted in morphological changes and growth pattern.
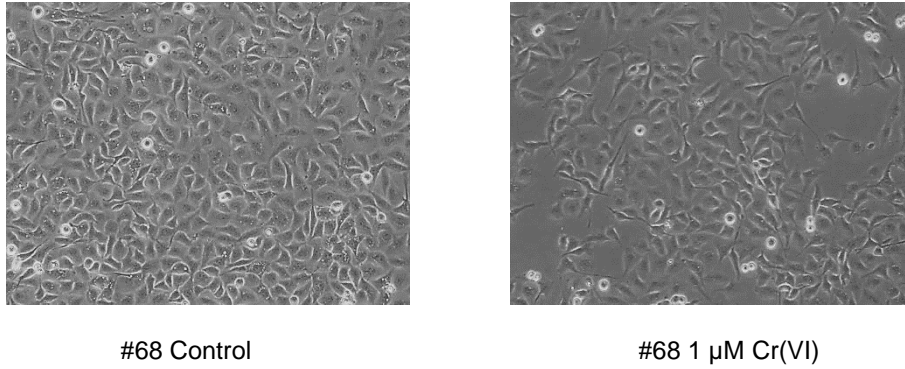
<div align="center">#68 Control   #68 1 µM Cr(VI)</div>

Figure 3.8. Impact of a long-term exposure to 1 µM Cr(VI) on the morphology and pattern of growth of BEAS-2B cells. Representative micrographs (100x magnification) of BEAS-2B cells, at the passages indicated at the bottom of each micrograph (#, passage number). Cells were cultured in coated flasks, in LHC-9 medium. It was observed that cultures exposed to 1 µM Cr(VI) for more than 12 months had a heterogeneous monolayer (with areas where normal cells coexisted with cells that had an abnormal morphology) and a higher frequency of criss-crossing. # - passage number

3.2.2. Impact on the doubling time

In order to continue investigating the effects of long-term exposure to 1 µM Cr(VI) on cellular parameters indicative of transformation status, it was evaluated the doubling time.

Recently, several studies have appeared focusing on the tumor doubling time (TDT) of lung cancer [220,221]. These studies demonstrated a relationship between TDT and lung cancer prognosis: a longer TDT is associated with a better prognosis. This association is not limited to lung cancer, other studies have investigated TDT in different cancers with imaging modalities and concluded that shorter TDTs are correlated with tumor malignancy and poor prognoses [222,223]. Therefore, TDT has been shown to be a good prognostic marker for the disease progression and survival of various cancers.

As it is well-understood, both local spreading and cell division are responsible for cancer expansion and progress. Thus, it is in the interest of tumor cells to have rapid cell division in order to reach different sites more quickly. Therefore, it is possible that transformed cells chronically exposed to Cr(VI) exhibit a decrease in the doubling time. The results are shown in Figure 3.9.

As expected, we observed a decrease in the doubling times of the cultures exposed to 1 µM Cr(VI) (18.30 h) compared to the control cultures (19.61 h). These results demonstrate that cultures exposed to 1 µM Cr(VI) for a long time have probably undergone transformation, which resulted in a decrease in cell division time.
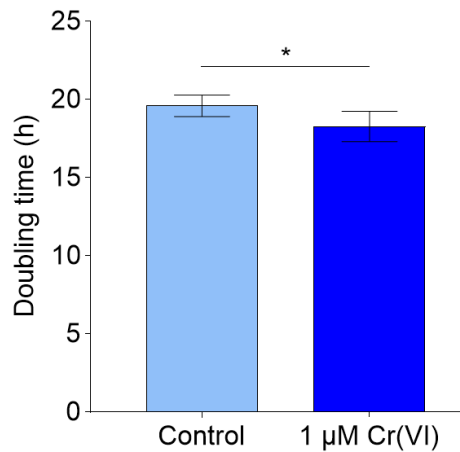
Figure 3.9. Impact of a long-term exposure to 1 μM Cr(VI) on the doubling time of BEAS-2B cells. Duplication times were determined according to the protocol described in the section 2.7. Results are presented as mean ± SD of three independent experiments (n = 3), using in all of them triplicates of cultures for each condition analyzed. Experimental data were analyzed with the software GraphPad Prism 8.0.2, using the *t-student paired* test, *, $p < 0.05$.

3.2.3. Impact on the clonogenic potential

In order to continue investigating the effects of long-term exposure to 1 μM Cr(VI) on cellular parameters indicative of transformation status, it was also evaluated cell proliferation by clonogenic potential.

The cancer cell acquires characteristics that allow survival beyond its normal life span and to proliferate abnormally. In fact, one of the eleven hallmarks of cancer described by Hanahan and Weinberg is the ability of tumor cells to have a limitless replicative potential.

Normal cells and transformed cells behave differently in relation to proliferation in culture. The main distinction between transformed cells and normal cells in culture is that normal cells exhibit density-dependent inhibition of cell proliferation. Normal cells proliferate until they reach a finite cell density (determined by the availability of growth factors added to the culture medium). Then, they cease proliferation and become quiescent (arrested in the G_0 stage of the cell cycle). On the contrary, the proliferation of transformed cells is not sensitive to density-dependent inhibition, since this type of cells do not cease proliferation and enter G0, continuing to grow until high cell densities in culture, mimicking their uncontrolled proliferation *in vivo* [224].

It is expected that cells exposed to Cr(VI) for a long time have a greater proliferation capacity than control cells, indicating a higher level of transformation. The results are shown in Figure 3.10.
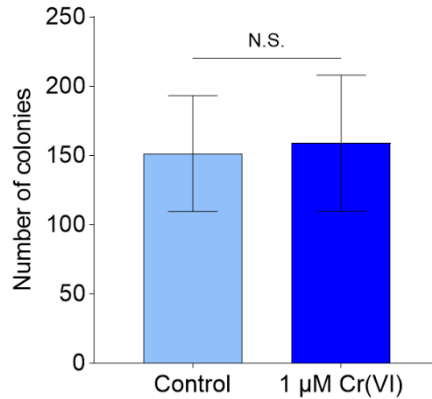
Figure 3.10. Impact of a long-term exposure to Cr(VI) on clonogenic potential of the BEAS-2B cell line. Colony counting was performed as described in section 2.9. Results are presented as mean ± SD of seven independent experiments (n = 7), using in all of them duplicates of cultures for each condition analyzed. Experimental data were analyzed with the software GraphPad Prism 8.0.2, using the *t-student paired* test. No statistically significant differences were observed (p > 0,05). N.S., not significant.

The results obtained do not indicate that the cultures exposed for long periods of time to 1 µM Cr(VI) acquired cellular transformation, at least with regard to the proliferative capacity. There was a slight increase in the number of colonies exposed to Cr(VI) but this increase was not significant. Thus, although the cultures were exposed for more than 12 months to 1 µM Cr(VI), it may not have been sufficient to induce transformation at the level of cell proliferation. It should be noted that our exposure regime included only a weekly addition of soluble Cr(VI), which is rapidly absorbed by the cells. In addition, only the effects of up to 12 months of exposure were evaluated, while chromate workers are subjected to daily exposure for consecutive years. Therefore, it may be necessary to increase the number of cell treatments per week and/or to prolong the exposure period, in order to more closely mimic the conditions that lead to the development of Cr(VI)-induced carcinogenesis *in vivo*.

3.2.4. Impact on the resistance to cytotoxic and subcytotoxic concentrations of Cr(VI)

As mentioned before, Cr(VI) is a human lung carcinogen, a strong oxidizing agent and a potent DNA damaging agent with the ability to interfere with the normal functions of cells, thus compromising cell viability. In addition, some cells exposed to Cr(VI) have the ability to escape cell death induced by this compound, even with extensive DNA damage. Thus, Cr(VI) seems to have the ability to induce cellular transformation, conferring resistance to cells against external or intracellular stresses.

In order to investigate whether cultures exposed for a long period of time to 1 µM Cr(VI) acquired an additional resistance to death caused by Cr(VI), one of the initiating events

of Cr(VI)-induced cellular transformation, we opted for evaluating the effects of a short-term exposure of 48 h to subcytotoxic (1 and 2 µM) and cytotoxic (4 µM) concentrations of Cr(VI). The results are shown in Figure 3.11.
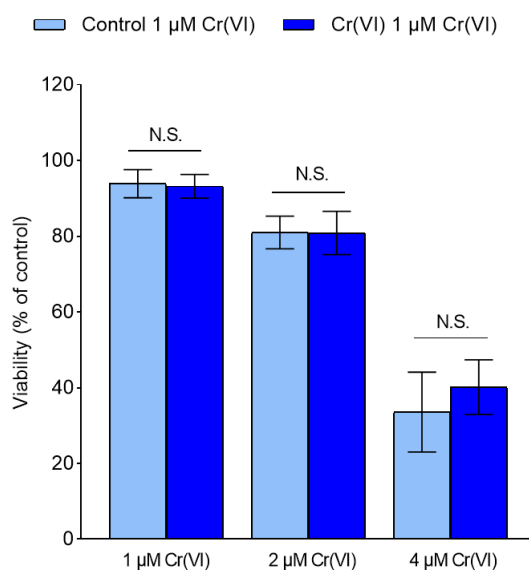

Figure 3.11. Impact of a long-term exposure to 1 µM Cr(VI) on the resistance to subcytotoxic (1 and 2 µM) and cytotoxic (4 µM) concentrations of Cr(VI) by the colorimetric assay (MTT). These experiments were determined according to the protocol described in the section 2.10.2. Results are presented as mean ± SD of three independent experiments (n = 6), using in all of them triplicates of cultures for each condition analyzed. Experimental data were analyzed with the software GraphPad Prism 8.0.2, using the *t-student paired* test. N.S., not significant.

Treatment of BEAS-2B cell cultures for 48 h with 1, 2 and 4 µM of Cr(VI) caused a 6.10% (not significant result), 18.95% and 66.41% reduction of live cells in control cultures, respectively and a 6.78% (not significant result), 19.11% and 59.86% reduction of live cells in 1 µM Cr(VI) cultures, respectively (Figure 3.11). Only concentration of 2 and 4 µM showed statistically significant decreases, with the results being clearly concentration-dependent. Overall, no significant resistance to cell death was observed in long-term exposed cultures to 1 µM Cr(VI). However, a slight increase in cell viability was observed in the 4 µM condition in long-term exposed cultures to 1 µM Cr(VI) compared to the control, although this increase was not significant. In future experiments, it may be necessary to increase the concentration of Cr(VI) in order to understand whether the slight increase seen in cell viability in cultures chronically exposed to 1 µM Cr(VI) and exposed to 4 µM Cr(VI) also occurs with concentrations higher.

4. Conclusions and Future Perspectives

The BEAS-2B cell line was used in all experiments performed in this study. It is a cell line established from normal cells of the human bronchial epithelium that, although transformed with a hybrid virus, retains most of the characteristics of NHBE cells [19,32].

Genomic instability, upregulation of the stress response, changes in morphology and other cellular characteristics have been frequently observed in transformed cells and were proposed to play important roles in cancer development and progression, thus suggesting novel avenues for the development of new cancer therapies.

Little is known regarding the molecular mechanisms behind cell transformation over time in culture. In order to complement, even partially, the information already gathered for the BEAS-2B cell line, we studied the effect of extensive passaging in several traits of this cell line.

When cultures were grown for extended periods, we could confirm the observation previously made by members of our group that cells with different culture ages have different morphological aspects and growth patterns. This led us to adopt the three culture stages (low, transitional and high passage stage) previously defined in our laboratory [37]. The microscopical suggestion of increased sizes over time in culture was not confirmed by the values obtained for the protein content of the cells in the three passage stages, as no significant differences were detected. One possibility is that cells do not become larger and only look so due their increased spacing in the monolayers that form. The impact of extensive passaging was also assessed in response to stress, through the intracellular levels of HSP90α, and in the rate of lactate production, as these characteristics might be used as indicators of cellular transformation stage. In both cases, significant increases could be observed between cells in the low passage stage and those in the transitional stage. Interestingly, differences between cells in the low passage stage and those in the high passage stage were much less pronounces, similar to what had been previously observed in terms of the changes in morphology and pattern of growth. Resistance to mild concentrations of Cr(VI) (1 and 2 μM), a human lung carcinogen, and migratory capacity were also evaluated. It was hypothesized that older cultures had a greater resistance to cell death induced by Cr(VI) and a greater migratory capacity, but no significant differences were observed.

Further studies will be needed in order to understand the pronounced molecular alterations that cells undergo during the transitional stage and that are reverted, at least partially, during the high passage stage. The impact of extensive passaging on the mRNA levels of some components of cancer-related pathways, using the quantitative polymerase chain reaction technique, and on the morphology and growth pattern, using higher resolution microscopy, were initiated but could not be completed due to the current COVID-19 pandemic.

The impact of long-term exposure to a mild concentration of Cr(VI) (1 µM) was also assessed in the BEAS-2B cell line. One of the parameters evaluated was cell morphology and growth pattern. It was observed that cultures became quite heterogeneous when exposed for long periods of time to Cr(VI), in line with observations previously made in our laboratory with a different exposure regimen and culture conditions [22,45]. These morphological changes were accompanied by changes in the proliferative capacity, since it was observed that cultures exposed to a long-term exposure to 1 µM Cr(VI) had a shorter doubling time than the control cultures, a common feature in transformed cells. Clonogenic potential and resistance to subcytotoxic and cytotoxic concentrations to Cr(VI) were also evaluated, but no significant differences were observed between cultures exposed to long periods to Cr(VI) and control cultures.

The assessment of the impact of Cr(VI) exposure on the mRNA levels of some components of cancer-related pathways were also initiated, but, once again, could not be completed due to the current COVID-19 pandemic. This and other future studies will certainly contribute to a better understanding of the cellular and molecular changes that accompany long-term exposures to Cr(VI). Among the parameters to be analyzed in the future are the energy metabolism of the cells, submicroscopic structural chromosomal alterations (using molecular cytogenetic techniques) and stress response.

5. References

[1]   R. Pozzo, The impact of aristotelianism on modern philosophy, 1st ed., The Catholic University of America Press, 2003.

[2]   J. Al-Khalili, The "first true scientist," BBC NEWS. (2009). http://news.bbc.co.uk/2/hi/science/nature/7810846.stm (accessed October 11, 2020).

[3]   J.B. Watkins, C.D. Klaassen, Casarett & Doull's essentials of toxicology, 3th ed., The McGraw-Hill Companies, Inc, 2015.

[4]   C. Rodríguez-Hernandez, S. Torres-García, C. Olvera, F. Ramírez Castillo, A. Loera Muro, F. González, A. Guerrero-Barrera, Cell culture: history, development and prospects, Int. J. Curr. Res. Acad. Rev. 2 (2014) 188–200. https://www.researchgate.net/publication/269932638.

[5]   R.G. Harrison, M.J. Greenman, F.P. Mall, C.M. Jackson, Observations of the living developing nerve fiber, Anat. Rec. Adv. Integr. Anat. Evol. Biol. 1 (1907) 116–128. https://doi.org/10.1002/ar.1090010503.

[6]   G.W. Corner, Warren Harmon Lewis 1870-1964, Biogr. Mem. Natl. Acad. Sci. (1967) 39:323-358. http://www.nasonline.org/publications/biographical-memoirs/memoir-pdfs/lewis-warren-h.pdf (accessed April 17, 2020).

[7]   L. Hayflick, P.S. Moorhead, The serial cultivation of human diploid cell strains, Exp. Cell Res. 25 (1961) 585–621. https://doi.org/10.1016/0014-4827(61)90192-6.

[8]   S. Bhatia, T. Naved, S. Sardana, Introduction to animal tissue culture science, in: Introd. to Pharm. Biotechnol. Vol. 3, 1st ed., IOP Publishing, 2019: pp. 1–30. https://doi.org/10.1088/2053-2563/aafac0ch1.

[9]   H. Harris, J.F. Watkins, G.L. Campbell, E.P. Evans, C.E. Ford, Mitosis in hybrid cells derived from mouse and man, Nature. 207 (1965) 606–608. https://doi.org/10.1038/207606a0.

[10]   I. Wilmut, A.E. Schnieke, J. McWhir, A.J. Kind, K.H. Campbell, Viable offspring derived from fetal and adult mammalian cells, Nature. 385 (1997) 810–813. https://doi.org/10.1038/385810a0.

[11]   T.J. Wiktor, M. V Fernandes, H. Koprowshi, Cultivation of rabies virus in human diploid cell strain wi-38, J. Immunol. 93 (1964) 353–366. https://pubmed.ncbi.nlm.nih.gov/14218592/.

[12]   G. Augusti-Tocco, G. Sato, Establishment of functional clonal lines of neurons from mouse neuroblastoma, Proc. Natl. Acad. Sci. 64 (1969) 311 LP – 315. https://doi.org/10.1073/pnas.64.1.311.

[13]   F.L. Graham, A.J. van der Eb, A new technique for the assay of infectivity of human adenovirus 5 DNA, Virology. 52 (1973) 456–467. https://doi.org/10.1016/0042-6822(73)90341-3.

[14]   F. Li, N. Vijayasankaran, A.Y. Shen, R. Kiss, A. Amanullah, Cell culture processes for monoclonal antibody production, MAbs. 2 (2010) 466–479. https://doi.org/10.4161/mabs.2.5.12720.

[15]   G. Kaur, J.M. Dufour, Cell lines: valuable tools or useless artifacts, Spermatogenesis. 2 (2012) 1–5. https://doi.org/10.4161/spmg.19885.

[16]   R. Jain, H. Savla, I. Naik, J. Maniar, K. Punjabi, S. Vaidya, M. Menon, Novel nanotechnology based delivery systems for chemotherapy and prophylaxis of tuberculosis, in: C.M. Hussain (Ed.), Handb. Nanomater. Ind. Appl., 1st ed., Elsevier, 2018: pp. 587–620. https://doi.org/10.1016/B978-0-12-813351-4.00034-1.

[17]   M. Carter, J. Shieh, Cell Culture Techniques, in: Guid. to Res. Tech. Neurosci., 2nd

ed., Academic Press, 2015: pp. 295–310. https://doi.org/10.1016/B978-0-12-800511-8.00014-9.

[18]   C.C. Harris, Human tissues and cells in carcinogenesis research, Cancer Res. 47 (1987) 1–10. https://cancerres.aacrjournals.org/content/47/1/1.full-text.pdf.

[19]   R.R. Reddel, Y. Ke, B.I. Gerwin, M.G. McMenamin, J.F. Lechner, R.T. Su, D.E. Brash, J.B. Park, J.S. Rhim, C.C. Harris, Transformation of human bronchial epithelial cells by infection with SV40 or adenovirus-12 SV40 hybrid virus, or transfection via strontium phosphate coprecipitation with a plasmid containing SV40 early region genes, Cancer Res. 48 (1988) 1904–1909. https://cancerres.aacrjournals.org/content/48/7/1904.long.

[20]   J.E. Kim, K.H. Koo, Y.H. Kim, J. Sohn, Y.G. Park, Identification of potential lung cancer biomarkers using an in vitro carcinogenesis model, Exp. Mol. Med. 40 (2008) 709–720. https://doi.org/10.3858/emm.2008.40.6.709.

[21]   A.S. Andrew, A.J. Warren, A. Barchowsky, K.A. Temple, L. Klei, N. V Soucy, K.A. O'Hara, J.W. Hamilton, Genomic and proteomic profiling of responses to toxic metals in human lung cells, Environ. Health Perspect. 111 (2003) 825–835. https://doi.org/10.1289/ehp.111-1241504.

[22]   C.F.D. Rodrigues, A.M. Urbano, E. Matoso, I. Carreira, A. Almeida, P. Santos, F. Botelho, L. Carvalho, M. Alves, C. Monteiro, A.N. Costa, V. Moreno, M.C. Alpoim, Human bronchial epithelial cells malignantly transformed by hexavalent chromium exhibit an aneuploid phenotype but no microsatellite instability, Mutat. Res. 670 (2009) 42–52. https://doi.org/10.1016/j.mrfmmm.2009.07.004.

[23]   J.M. Veranth, C.A. Reilly, M.M. Veranth, T.A. Moss, C.R. Langelier, D.L. Lanza, G.S. Yost, Inflammatory cytokines and cell death in BEAS-2B lung cells treated with soil dust, lipopolysaccharide, and surface-modified particles, Toxicol. Sci. 82 (2004) 88–96. https://doi.org/10.1093/toxsci/kfh248.

[24]   A.S. Davis, D.S. Chertow, J.E. Moyer, J. Suzich, A. Sandouk, D.W. Dorward, C. Logun, J.H. Shelhamer, J.K. Taubenberger, Validation of normal human bronchial epithelial cells as a model for influenza A infections in human distal trachea, J. Histochem. Cytochem. 63 (2015) 312–328. https://doi.org/10.1369/0022155415570968.

[25]   R.A. Vilchez, J.S. Butel, Emergent human pathogen simian virus 40 and its role in cancer, Clin. Microbiol. Rev. 17 (2004) 495–508. https://doi.org/10.1128/CMR.17.3.495-508.2004.

[26]   C. MacDonald, Development of new cell lines for animal cell biotechnology, Crit. Rev. Biotechnol. 10 (1990) 155–178. https://doi.org/10.3109/07388559009068265.

[27]   K.K. Jha, S. Banga, V. Palejwala, H.L. Ozer, SV40-Mediated immortalization, Exp. Cell Res. 245 (1998) 1–7. https://doi.org/10.1006/excr.1998.4272.

[28]   D.P. Lane, p53, guardian of the genome, Nature. 358 (1992) 15–16. https://doi.org/10.1038/358015a0.

[29]   R.A. Weinberg, The retinoblastoma protein and cell cycle control, Cell. 81 (1995) 323–330. https://doi.org/10.1016/0092-8674(95)90385-2.

[30]   Y. Ohnuki, R.R. Reddel, S.E. Bates, T.A. Lehman, J.F. Lechner, C.C. Harris, Chromosomal changes and progressive tumorigenesis of human bronchial epithelial cell lines, Cancer Genet. Cytogenet. 92 (1996) 99–110. https://doi.org/10.1016/s0165-4608(96)00156-2.

[31]   R.R. Reddel, S.E. Salghetti, J.C. Willey, Y. Ohnuki, Y. Ke, B.I. Gerwin, J.F. Lechner,

C.C. Harris, Development of tumorigenicity in simian virus 40-immortalized human bronchial epithelial cell lines, Cancer Res. 53 (1993) 985–991. https://cancerres.aacrjournals.org/content/53/5/985.full-text.pdf.

[32]   Culture Collections, Eur. Collect. Authenticated Cell Cult. (n.d.). https://www.phe-culturecollections.org.uk/products/celllines/generalcell/detail.jsp?refId=95102433&collection=ecacc_gc (accessed April 1, 2020).

[33]   Y. Ke, R.R. Reddel, B.I. Gerwin, M. Miyashita, M. McMenamin, J.F. Lechner, C.C. Harris, Human bronchial epithelial cells with integrated SV40 virus T antigen genes retain the ability to undergo squamous differentiation, Differentiation. 38 (1988) 60–66. https://doi.org/10.1111/j.1432-0436.1988.tb00592.x.

[34]   BEAS-2B (ATCC® CRL-9609™), (n.d.). https://atcc.org/products/all/CRL-9609.aspx#culturemethod (accessed May 20, 2020).

[35]   J.F. Lechner, A. Haugen, I.A. McClendon, A.M. Shamsuddin, Induction of squamous differentiation of normal human bronchial epithelial cells by small amounts of serum, Differentiation. 25 (1984) 229–237. https://doi.org/10.1111/j.1432-0436.1984.tb01361.x.

[36]   F. Zhao, W.T. Klimecki, Culture conditions profoundly impact phenotype in BEAS-2B, a human pulmonary epithelial model, J. Appl. Toxicol. 35 (2015) 945–951. https://doi.org/10.1002/jat.3094.

[37]   P.A.L. Abreu, Mechanisms of hexavalent chromium carcinogenicity: effects on the stress response and on the genomic stability of the BEAS-2B cell line, Diss. Mestr. Em Bioquímica - Univ. Coimbra. (2016). https://estudogeral.sib.uc.pt/handle/10316/34194 (accessed April 2, 2020).

[38]   D. Barnes, G. Sato, Serum-free cell culture: a unifying approach, Cell. 22 (1980) 649–655. https://doi.org/10.1016/0092-8674(80)90540-1.

[39]   M.S. Even, C.B. Sandusky, N.D. Barnard, Serum-free hybridoma culture: ethical, scientific and safety considerations, Trends Biotechnol. 24 (2006) 105–108. https://doi.org/10.1016/j.tibtech.2006.01.001.

[40]   J. He, X. Qian, R. Carpenter, Q. Xu, L. Wang, Y. Qi, Z.-X. Wang, L.-Z. Liu, B.-H. Jiang, Repression of miR-143 mediates Cr (VI)-induced tumor angiogenesis via IGF-IR/IRS1/ERK/IL-8 pathway, Toxicol. Sci. 134 (2013) 26–38. https://doi.org/10.1093/toxsci/kft101.

[41]   Y.-H. Park, D. Kim, J. Dai, Z. Zhang, Human bronchial epithelial BEAS-2B cells, an appropriate in vitro model to study heavy metals induced carcinogenesis, Toxicol. Appl. Pharmacol. 287 (2015) 240–245. https://doi.org/10.1016/j.taap.2015.06.008.

[42]   H. Sun, H.A. Clancy, T. Kluz, J. Zavadil, M. Costa, Comparison of gene expression profiles in chromate transformed BEAS-2B cells, PLoS One. 6 (2011) e17982. https://doi.org/10.1371/journal.pone.0017982.

[43]   J.M. Myers, W.E. Antholine, C.R. Myers, The intracellular redox stress caused by hexavalent chromium is selective for proteins that have key roles in cell survival and thiol redox control, Toxicology. 281 (2011) 37–47. https://doi.org/10.1016/j.tox.2011.01.001.

[44]   T.A. Stueckle, Y. Lu, M.E. Davis, L. Wang, B.-H. Jiang, I. Holaskova, R. Schafer, J.B. Barnett, Y. Rojanasakul, Chronic occupational exposure to arsenic induces carcinogenic gene signaling networks and neoplastic transformation in human lung epithelial cells, Toxicol. Appl. Pharmacol. 261 (2012) 204–216. https://doi.org/10.1016/j.taap.2012.04.003.

[45] A.N. Costa, V. Moreno, M.J. Prieto, A.M. Urbano, M.C. Alpoim, Induction of morphological changes in BEAS-2B human bronchial epithelial cells following chronic sub-cytotoxic and mildly cytotoxic hexavalent chromium exposures, Mol. Carcinog. 49 (2010) 582–591. https://doi.org/10.1002/mc.20624.

[46] D. Lau, L. Xue, R. Hu, T. Liaw, R. Wu, S. Reddy, Expression and regulation of a molecular marker, SPR1, in multistep bronchial carcinogenesis, Am. J. Respir. Cell Mol. Biol. 22 (2000) 92–96. https://doi.org/10.1165/ajrcmb.22.1.3637.

[47] P. Hughes, D. Marshall, Y. Reid, H. Parkes, C. Gelber, The costs of using unauthenticated, over-passaged cell lines: how much more data do we need?, Biotechniques. 43 (2007) 575–586. https://doi.org/10.2144/000112598.

[48] M.D. Peterson, M.S. Mooseker, Characterization of the enterocyte-like brush border cytoskeleton of the C2BBe clones of the human intestinal cell line, Caco-2, J. Cell Sci. 102 (1992) 581–600. https://jcs.biologists.org/content/joces/102/3/581.full.pdf.

[49] L. Mahraoui, M. Rousset, E. Dussaulx, D. Darmoul, A. Zweibaum, E. Brot-Laroche, Expression and localization of GLUT-5 in Caco-2 cells, human small intestine, and colon, Am. J. Physiol. 263 (1992) G312-8. https://doi.org/10.1152/ajpgi.1992.263.3.G312.

[50] I. Chantret, A. Rodolosse, A. Barbat, E. Dussaulx, E. Brot-Laroche, A. Zweibaum, M. Rousset, Differential expression of sucrase-isomaltase in clones isolated from early and late passages of the cell line Caco-2: evidence for glucose-dependent negative regulation, J. Cell Sci. 107 (Pt 1) (1994) 213–225. https://www.ncbi.nlm.nih.gov/pubmed/8175910.

[51] S. Lu, A.W. Gough, W.F. Bobrowski, B.H. Stewart, Transport properties are not altered across Caco-2 cells with heightened TEER despite underlying physiological and ultrastructural changes, J. Pharm. Sci. 85 (1996) 270–273. https://doi.org/10.1021/js950269u.

[52] M.J. Briske-Anderson, J.W. Finley, S.M. Newman, The influence of culture time and passage number on the morphological and physiological development of Caco-2 cells, Proc. Soc. Exp. Biol. Med. 214 (1997) 248–257. https://doi.org/10.3181/00379727-214-44093.

[53] H. Yu, T.J. Cook, P.J. Sinko, Evidence for diminished functional expression of intestinal transporters in Caco-2 cell monolayers at high passages, Pharm. Res. 14 (1997) 757–762. https://doi.org/10.1023/a:1012150405949.

[54] T. Nakumura, T. Sakaeda, N. Ohmoto, Y. Moriya, C. Komoto, T. Shirakawa, A. Gotoh, M. Matsuo, K. Okmura, Gene expression profiles of ABC transporters and cytochrome P450 3A in Caco-2 and human colorectal cancer cell lines, Pharm. Res. 20 (2003) 324–327. https://doi.org/10.1023/a:1022251910820.

[55] C.M. Chang-Liu, G.E. Woloschak, Effect of passage number on cellular response to DNA-damaging agents: cell survival and gene expression, Cancer Lett. 113 (1997) 77–86. https://doi.org/10.1016/s0304-3835(97)04599-0.

[56] M. Esquenet, J. V Swinnen, W. Heyns, G. Verhoeven, LNCaP prostatic adenocarcinoma cells derived from low and high passage numbers display divergent responses not only to androgens but also to retinoids, J. Steroid Biochem. Mol. Biol. 62 (1997) 391–399. https://doi.org/10.1016/s0960-0760(97)00054-x.

[57] D.C. Ferreira, Efeitos do crómio hexavalente no metabolismo energético de uma linha celular do epitélio brônquico humano, Diss. Mestr. Em Bioquímica - Univ. Coimbra. (2015). https://estudogeral.sib.uc.pt/handle/10316/32123 (accessed April 2, 2020).

[58] L. Matturri, A.M. Lavezzi, Recurrent chromosome alterations in non-small cell lung cancer, Eur. J. Histochem. 38 (1994) 53–58. https://www.ncbi.nlm.nih.gov/pubmed/7517731.

[59] J.R. Testa, J.M. Siegfried, Z. Liu, J.D. Hunt, M.M. Feder, S. Litwin, J.Y. Zhou, T. Taguchi, S.M. Keller, Cytogenetic analysis of 63 non-small cell lung carcinomas: recurrent chromosome alterations amid frequent and widespread genomic upheaval, Genes. Chromosomes Cancer. 11 (1994) 178–194. https://doi.org/10.1002/gcc.2870110307.

[60] D.G. Barceloux, Chromium, J. Toxicol. Clin. Toxicol. 37 (1999) 173–194. https://doi.org/10.1081/clt-100102418.

[61] T.F.E. Wikipedia, Chromium, (n.d.). https://en.wikipedia.org/wiki/Chromium (accessed May 8, 2020).

[62] S. Mishra, R.N. Bharagava, Toxic and genotoxic effects of hexavalent chromium in environment and its bioremediation strategies, J. Environ. Sci. Health. C. Environ. Carcinog. Ecotoxicol. Rev. 34 (2016) 1–32. https://doi.org/10.1080/10590501.2015.1096883.

[63] M. Costa, C.B. Klein, Toxicity and carcinogenicity of chromium compounds in humans, Crit. Rev. Toxicol. 36 (2006) 155–163. https://doi.org/10.1080/10408440500534032.

[64] M.D. Cohen, B. Kargacin, C.B. Klein, M. Costa, Mechanisms of chromium carcinogenicity and toxicity, Crit. Rev. Toxicol. 23 (1993) 255–281. https://doi.org/10.3109/10408449309105012.

[65] F. Baruthio, Toxic effects of chromium and its compounds, Biol. Trace Elem. Res. 32 (1992) 145–153. https://doi.org/10.1007/BF02784599.

[66] D. Newman, A case of adeno-carcinoma of the left inferior turbinated body, and perforation of the nasal septum, in the person of a worker in chrome pigments, Glasgow Med. J. 33 (1890) 469–470.

[67] W. Machle, F. Gregorius, Cancer of the respiratory system in the United States chromate producing industry, Public Heal. Reports (Washington, D.C. 1896). 63 (1948) 1114–1127.

[68] S. Langard, Role of chemical species and exposure characteristics in cancer among persons occupationally exposed to chromium compounds, Scand. J. Work. Environ. Health. 19 Suppl 1 (1993) 81–89.

[69] S. Langard, One hundred years of chromium and cancer: a review of epidemiological evidence and selected case reports, Am. J. Ind. Med. 17 (1990) 189–215. https://doi.org/10.1002/ajim.4700170205.

[70] A.M. Urbano, C.F.D. Rodrigues, M.C. Alpoim, Hexavalent chromium exposure, genomic instability and lung cancer, Gene Ther. Mol. Biol. 12B (2008) 219–238.

[71] M. Costa, Toxicity and carcinogenicity of Cr(VI) in animal models and humans, Crit. Rev. Toxicol. 27 (1997) 431–442. https://doi.org/10.3109/10408449709078442.

[72] EFSA, Scientific opinion on dietary reference values for chromium, Eur. Food Saf. Auth. 12 (2014) 3845. https://efsa.onlinelibrary.wiley.com/doi/epdf/10.2903/j.efsa.2014.3845.

[73] A.M. Urbano, L.M.R. Ferreira, M.C. Alpoim, Molecular and cellular mechanisms of hexavalent chromium-induced lung cancer: an updated perspective, Curr. Drug Metab. 13 (2012) 284–305. https://doi.org/10.2174/138920012799320464.

[74] A. Zhitkovich, Chromium in drinking water: sources, metabolism, and cancer risks,

Chem. Res. Toxicol. 24 (2011) 1617–1629. https://doi.org/10.1021/tx200251t.

[75] R.M.J. Donaldson, R.F. Barreras, Intestinal absorption of trace quantities of chromium, J. Lab. Clin. Med. 68 (1966) 484–493.

[76] M. Gonçalves, A. Santos, C. Rodrigues, P. Coelho, A. Costa, A. Guiomar, M. Santos, M. Alpoim, A. Urbano, Changes in glucose uptake rate and in the energy status of PC-12 cells acutely exposed to hexavalent chromium, an established human carcinogen, Toxicol. Environ. Chem. 93 (2011) 1202–1211. https://doi.org/10.1080/02772248.2011.581340.

[77] T. Norseth, The carcinogenicity of chromium, Environ. Health Perspect. 40 (1981) 121–130. https://doi.org/10.1289/ehp.8140121.

[78] C.M. Thompson, D.M. Proctor, M. Suh, L.C. Haws, C.R. Kirman, M.A. Harris, Assessment of the mode of action underlying development of rodent small intestinal tumors following oral exposure to hexavalent chromium and relevance to humans, Crit. Rev. Toxicol. 43 (2013) 244–274. https://doi.org/10.3109/10408444.2013.768596.

[79] R. Jobby, P. Jha, A.K. Yadav, N. Desai, Biosorption and biotransformation of hexavalent chromium [Cr(VI)]: A comprehensive review, Chemosphere. 207 (2018) 255–266. https://doi.org/10.1016/j.chemosphere.2018.05.050.

[80] Y. Wang, H. Su, Y. Gu, X. Song, J. Zhao, Carcinogenicity of chromium and chemoprevention: a brief update, Onco. Targets. Ther. 10 (2017) 4065–4079. https://doi.org/10.2147/OTT.S139262.

[81] K.A. Biedermann, J.R. Landolph, Induction of anchorage independence in human diploid foreskin fibroblasts by carcinogenic metal salts, Cancer Res. 47 (1987) 3815–3823.

[82] K.A. Biedermann, J.R. Landolph, Role of valence state and solubility of chromium compounds on induction of cytotoxicity, mutagenesis, and anchorage independence in diploid human fibroblasts, Cancer Res. 50 (1990) 7835–7842.

[83] S. De Flora, M. Bagnasco, D. Serra, P. Zanacchi, Genotoxicity of chromium compounds. A review, Mutat. Res. 238 (1990) 99–172. https://doi.org/10.1016/0165-1110(90)90007-x.

[84] R.S. Slesinski, J.J. Clarke, R.H.C. San, R. Gudi, Lack of mutagenicity of chromium picolinate in the hypoxanthine phosphoribosyltransferase gene mutation assay in Chinese hamster ovary cells, Mutat. Res. 585 (2005) 86–95. https://doi.org/10.1016/j.mrgentox.2005.04.001.

[85] S. De Flora, A. Camoirano, M. Bagnasco, C. Bennicelli, G.E. Corbett, B.D. Kerger, Estimates of the chromium(VI) reducing capacity in human body compartments as a mechanism for attenuating its potential toxicity and carcinogenicity, Carcinogenesis. 18 (1997) 531–537. https://doi.org/10.1093/carcin/18.3.531.

[86] K.B. Olson, G. Heggen, C.F. Edwards, L.W. Gorham, Trace element content of cancerous and noncancerous human liver tissue, Science (80-.). 119 (1954) 772 LP – 773. https://doi.org/10.1126/science.119.3100.772.

[87] L.M.R. Ferreira, T. Cunha-Oliveira, M.C. Sobral, P.L. Abreu, M.C. Alpoim, A.M. Urbano, Impact of carcinogenic chromium on the cellular response to proteotoxic stress, Int. J. Mol. Sci. 20 (2019) 4901. https://doi.org/10.3390/ijms20194901.

[88] Y. Ishikawa, K. Nakagawa, Y. Satoh, T. Kitagawa, H. Sugano, T. Hirano, E. Tsuchiya, Characteristics of chromate workers' cancers, chromium lung deposition and precancerous bronchial lesions: an autopsy study, Br. J. Cancer. 70 (1994) 160–166.

https://doi.org/10.1038/bjc.1994.268.

[89] Y. Ishikawa, K. Nakagawa, Y. Satoh, T. Kitagawa, H. Sugano, T. Hirano, E. Tsuchiya, "Hot Spots" of chromium accumulation at bifurcations of chromate workers' bronchi, Cancer Res. 54 (1994) 2342–2346.

[90] S. Langård, T. Norseth, A cohort study of bronchial carcinomas in workers producing chromate pigments, Br. J. Ind. Med. 32 (1975) 62–65. https://doi.org/10.1136/oem.32.1.62.

[91] NTP, Chromium hexavalent compounds, Rep. Carcinog. Fourteenth Ed. (2014). https://ntp.niehs.nih.gov/ntp/roc/content/profiles/chromiumhexavalentcompounds.pdf (accessed May 13, 2020).

[92] IARC, Chromium, nickel and welding, in: IARC Monogr. Eval. Carcinog. Risks to Humans, Vol. 49, IARC Scientific Publications, Lyon, 1990. https://publications.iarc.fr/67.

[93] USEPA, Integrated risk information system (IRIS), in: US Environ. Prot. Agency, Environmental Criteria and Assessment Office, Cincinnati, 1992.

[94] K. Straif, L. Benbrahim-Tallaa, R. Baan, Y. Grosse, B. Secretan, F. El Ghissassi, V. Bouvard, N. Guha, C. Freeman, L. Galichet, V. Cogliano, A review of human carcinogens--Part C: metals, arsenic, dusts, and fibres, Lancet. Oncol. 10 (2009) 453–454. https://doi.org/10.1016/s1470-2045(09)70134-2.

[95] S. Langård, A. Andersen, J. Ravnestad, Incidence of cancer among ferrochromium and ferrosilicon workers: an extended observation period, Br. J. Ind. Med. 47 (1990) 14–19. https://doi.org/10.1136/oem.47.1.14.

[96] H.J. Gibb, P.S. Lees, P.F. Pinsky, B.C. Rooney, Clinical findings of irritation among chromium chemical production workers, Am. J. Ind. Med. 38 (2000) 127–131. https://doi.org/10.1002/1097-0274(200008)38:2<127::aid-ajim2>3.0.co;2-q.

[97] H.J. Gibb, P.S. Lees, P.F. Pinsky, B.C. Rooney, Lung cancer among workers in chromium chemical production, Am. J. Ind. Med. 38 (2000) 115–126. https://doi.org/10.1002/1097-0274(200008)38:2<115::aid-ajim1>3.0.co;2-y.

[98] R.S. Luippold, K.A. Mundt, R.P. Austin, E. Liebig, J. Panko, C. Crump, K. Crump, D. Proctor, Lung cancer mortality among chromate production workers, Occup. Environ. Med. 60 (2003) 451–457. https://doi.org/10.1136/oem.60.6.451.

[99] D.M. Proctor, J.P. Panko, E.W. Liebig, P.K. Scott, K.A. Mundt, M.A. Buczynski, R.J. Barnhart, M.A. Harris, R.J. Morgan, D.J. Paustenbach, Workplace airborne hexavalent chromium concentrations for the Painesville, Ohio, chromate production plant (1943-1971), Appl. Occup. Environ. Hyg. 18 (2003) 430–449. https://doi.org/10.1080/10473220301421.

[100] D.M. Proctor, J.P. Panko, E.W. Liebig, D.J. Paustenbach, Estimating historical occupational exposure to airborne hexavalent chromium in a chromate production plant: 1940-1972, J. Occup. Environ. Hyg. 1 (2004) 752–767. https://doi.org/10.1080/15459620490523294.

[101] T. Birk, K.A. Mundt, L.D. Dell, R.S. Luippold, L. Miksche, W. Steinmann-Steiner-Haldenstaett, D.J. Mundt, Lung cancer mortality in the German chromate industry, 1958 to 1998, J. Occup. Environ. Med. 48 (2006).

[102] T. Sorahan, D.C. Burges, J.A. Waterhouse, A mortality study of nickel/chromium platers, Br. J. Ind. Med. 44 (1987) 250–258. https://doi.org/10.1136/oem.44.4.250.

[103] S. Langård, T. Vigander, Occurrence of lung cancer in workers producing chromium pigments, Br. J. Ind. Med. 40 (1983) 71–74. https://doi.org/10.1136/oem.40.1.71.

[104] J.D. Boice Jr, D.E. Marano, J.P. Fryzek, C.J. Sadler, J.K. McLaughlin, Mortality among aircraft manufacturing workers, Occup. Environ. Med. 56 (1999) 581–597. https://doi.org/10.1136/oem.56.9.581.

[105] D.E. Marano, J.D.J. Boice, J.P. Fryzek, J.A. Morrison, C.J. Sadler, J.K. McLaughlin, Exposure assessment for a large epidemiological study of aircraft manufacturing workers, Appl. Occup. Environ. Hyg. 15 (2000) 644–656. https://doi.org/10.1080/10473220050075653.

[106] M. Gérin, A.C. Fletcher, C. Gray, R. Winkelmann, P. Boffetta, L. Simonato, Development and use of a welding process exposure matrix in a historical prospective study of lung cancer risk in european welders, Int. J. Epidemiol. 22 (1993) S22–S28. https://doi.org/10.1093/ije/22.Supplement_2.S22.

[107] S. Langård, A. a Andersen, B. Gylseth, Incidence of cancer among ferrochromium and ferrosilicon workers, Br. J. Ind. Med. 37 (1980) 114–120. https://doi.org/10.1136/oem.37.2.114.

[108] G. Axelsson, R. Rylander, A. Schmidt, Mortality and incidence of tumours among ferrochromium workers, Br. J. Ind. Med. 37 (1980) 121–127. https://doi.org/10.1136/oem.37.2.121.

[109] L.S. Levy, P.A. Martin, P.L. Bidstrup, Investigation of the potential carcinogenicity of a range of chromium containing materials on rat lung, Br. J. Ind. Med. 43 (1986) 243–256. https://doi.org/10.1136/oem.43.4.243.

[110] T.E. Iaia, D. Bartoli, P. Calzoni, P. Comba, M. De Santis, F. Dini, G.A. Farina, M. Valiani, R. Pirastu, A cohort mortality study of leather tanners in Tuscany, Italy, Am. J. Ind. Med. 49 (2006) 452–459. https://doi.org/10.1002/ajim.20309.

[111] T. Hara, T. Hoshuyama, K. Takahashi, V. Delgermaa, T. Sorahan, Cancer risk among Japanese chromium platers, 1976-2003, Scand. J. Work. Environ. Health. 36 (2010) 216–221. https://doi.org/10.5271/sjweh.2889.

[112] R. Welling, J.J. Beaumont, S.J. Petersen, G. V Alexeeff, C. Steinmaus, Chromium VI and stomach cancer: a meta-analysis of the current epidemiological evidence, Occup. Environ. Med. 72 (2015) 151–159. https://doi.org/10.1136/oemed-2014-102178.

[113] Y. Deng, M. Wang, T. Tian, S. Lin, P. Xu, L. Zhou, C. Dai, Q. Hao, Y. Wu, Z. Zhai, Y. Zhu, G. Zhuang, Z. Dai, The effect of hexavalent chromium on the incidence and mortality of human cancers: a meta-analysis based on published epidemiological cohort studies, Front. Oncol. 9 (2019) 24. https://doi.org/10.3389/fonc.2019.00024.

[114] A.D. Dayan, A.J. Paine, Mechanisms of chromium toxicity, carcinogenicity and allergenicity: review of the literature from 1985 to 2000, Hum. Exp. Toxicol. 20 (2001) 439–451. https://doi.org/10.1191/096032701682693062.

[115] L.A. Saryan, M. Reedy, Chromium determinations in a case of chromic acid ingestion, J. Anal. Toxicol. 12 (1988) 162–164. https://doi.org/10.1093/jat/12.3.162.

[116] P.P. Varma, V. Jha, A.K. Ghosh, K. Joshi, V. Sakhuja, Acute renal failure in a case of fatal chromic acid poisoning, Ren. Fail. 16 (1994) 653–657. https://doi.org/10.3109/08860229409044893.

[117] P.H. Connett, K.E. Wetterhahn, Metabolism of the carcinogen chromate by cellular constituents, Inorg. Elem. Biochem. (1983) 93–124.

[118] A. Kortenkamp, Z. Ozolins, D. Beyersmann, P. O'Brien, Generation of PM2 DNA breaks in the course of reduction of chromium(VI) by glutathione, Mutat. Res. Mutagen. Relat. Subj. 216 (1989) 19–26. https://doi.org/https://doi.org/10.1016/0165-1161(89)90019-8.

[119] R.R. Ray, Adverse hematological effects of hexavalent chromium: an overview, Interdiscip. Toxicol. 9 (2016) 55–65. https://doi.org/10.1515/intox-2016-0007.

[120] D.M. Proctor, M. Suh, S.L. Campleman, C.M. Thompson, Assessment of the mode of action for hexavalent chromium-induced lung cancer following inhalation exposures, Toxicology. 325 (2014) 160–179. https://doi.org/10.1016/j.tox.2014.08.009.

[121] T.J. O'Brien, S. Ceryak, S.R. Patierno, Complexities of chromium carcinogenesis: role of cellular response, repair and recovery mechanisms, Mutat. Res. 533 (2003) 3–36. https://doi.org/10.1016/j.mrfmmm.2003.09.006.

[122] G. Quievryn, E. Peterson, J. Messer, A. Zhitkovich, Genotoxicity and mutagenicity of chromium(VI)/ascorbate-generated DNA adducts in human and bacterial cells, Biochemistry. 42 (2003) 1062–1070. https://doi.org/10.1021/bi0271547.

[123] G. Quievryn, M. Goulart, J. Messer, A. Zhitkovich, Reduction of Cr(VI) by cysteine: significance in human lymphocytes and formation of DNA damage in reactions with variable reduction rates, Mol. Cell. Biochem. 222 (2001) 107–118. https://doi.org/10.1023/A:1017923609175.

[124] A. Zhitkovich, G. Quievryn, J. Messer, Z. Motylevich, Reductive activation with cysteine represents a chromium(III)-dependent pathway in the induction of genotoxicity by carcinogenic chromium(VI), Environ. Health Perspect. 110 Suppl (2002) 729–731. https://doi.org/10.1289/ehp.02110s5729.

[125] A. Nigam, S. Priya, P. Bajpai, S. Kumar, Cytogenomics of hexavalent chromium (Cr6+) exposed cells: a comprehensive review, Indian J. Med. Res. 139 (2014) 349–370.

[126] L. Diebold, N.S. Chandel, Mitochondrial ROS regulation of proliferating cells, Free Radic. Biol. Med. 100 (2016) 86–93. https://doi.org/10.1016/j.freeradbiomed.2016.04.198.

[127] X.L. Shi, N.S. Dalal, Chromium (V) and hydroxyl radical formation during the glutathione reductase-catalyzed reduction of chromium (VI), Biochem. Biophys. Res. Commun. 163 (1989) 627–634. https://doi.org/10.1016/0006-291x(89)92183-9.

[128] X. Shi, Y. Mao, A.D. Knapton, M. Ding, Y. Rojanasakul, P.M. Gannett, N. Dalal, K. Liu, Reaction of Cr(VI) with ascorbate and hydrogen peroxide generates hydroxyl radicals and causes DNA damage: role of a Cr(IV)-mediated Fenton-like reaction, Carcinogenesis. 15 (1994) 2475–2478. https://doi.org/10.1093/carcin/15.11.2475.

[129] X.G. Shi, N.S. Dalal, On the hydroxyl radical formation in the reaction between hydrogen peroxide and biologically generated chromium(V) species, Arch. Biochem. Biophys. 277 (1990) 342–350. https://doi.org/10.1016/0003-9861(90)90589-q.

[130] X. Shi, N.S. Dalal, Generation of hydroxyl radical by chromate in biologically relevant systems: role of Cr(V) complexes versus tetraperoxochromate(V), Environ. Health Perspect. 102 Suppl (1994) 231–236. https://doi.org/10.1289/ehp.94102s3231.

[131] X. Shi, Z. Dong, N.S. Dalal, P.M. Gannett, Chromate-mediated free radical generation from cysteine, penicillamine, hydrogen peroxide, and lipid hydroperoxides, Biochim. Biophys. Acta. 1226 (1994) 65–72. https://doi.org/10.1016/0925-4439(94)90060-4.

[132] S. Kawanishi, S. Inoue, S. Sano, Mechanism of DNA cleavage induced by sodium chromate(VI) in the presence of hydrogen peroxide, J. Biol. Chem. 261 (1986) 5952–5958.

[133] D. Bagchi, P.J. Vuchetich, M. Bagchi, E.A. Hassoun, M.X. Tran, L. Tang, S.J. Stohs, Induction of oxidative stress by chronic administration of sodium dichromate [chromium VI] and cadmium chloride [cadmium II] to rats, Free Radic. Biol. Med. 22

(1997) 471–478. https://doi.org/10.1016/s0891-5849(96)00352-8.

[134] P.L. Abreu, L.M.R. Ferreira, M.C. Alpoim, A.M. Urbano, Impact of hexavalent chromium on mammalian cell bioenergetics: phenotypic changes, molecular basis and potential relevance to chromate-induced lung cancer, Biometals. 27 (2014) 409–443. https://doi.org/10.1007/s10534-014-9726-7.

[135] C.R. Myers, The effects of chromium(VI) on the thioredoxin system: implications for redox regulation, Free Radic. Biol. Med. 52 (2012) 2091–2107. https://doi.org/10.1016/j.freeradbiomed.2012.03.013.

[136] K.D. Sugden, C.K. Campo, B.D. Martin, Direct oxidation of guanine and 7,8-dihydro-8-oxoguanine in DNA by a high-valent chromium complex: a possible mechanism for chromate genotoxicity, Chem. Res. Toxicol. 14 (2001) 1315–1322. https://doi.org/10.1021/tx010088+.

[137] A.M. Urbano, L.M.R. Ferreira, J.F. Cerveira, C.F. Rodrigues, M.C. Alpoim, DNA damage, repair and misrepair in cancer and in cancer therapy, in: S. Vengrova (Ed.), DNA Repair Hum. Heal., IntechOpen, 2011: pp. 178–238.

[138] H. Kim, S. Lee, B. Jang, Subchronic inhalation toxicity of soluble hexavalent chromium trioxide in rats, Arch. Toxicol. 78 (2004) 363–368. https://doi.org/10.1007/s00204-004-0553-4.

[139] L.M. Beaver, E.J. Stemmy, A.M. Schwartz, J.M. Damsker, S.L. Constant, S.M. Ceryak, S.R. Patierno, Lung inflammation, injury, and proliferative response after repetitive particulate hexavalent chromium exposure, Environ. Health Perspect. 117 (2009) 1896–1902. https://doi.org/10.1289/ehp.0900715.

[140] K. Salnikow, A. Zhitkovich, Genetic and epigenetic mechanisms in metal carcinogenesis and cocarcinogenesis: nickel, arsenic, and chromium, Chem. Res. Toxicol. 21 (2008) 28–44. https://doi.org/10.1021/tx700198a.

[141] A. Zhitkovich, V. Voitkun, M. Costa, Glutathione and free amino acids form stable complexes with DNA following exposure of intact mammalian cells to chromate, Carcinogenesis. 16 (1995) 907–913. https://doi.org/10.1093/carcin/16.4.907.

[142] A. Zhitkovich, Importance of chromium-DNA adducts in mutagenicity and toxicity of chromium(VI), Chem. Res. Toxicol. 18 (2005) 3–11. https://doi.org/10.1021/tx049774+.

[143] D. Lopez-Martinez, C.-C. Liang, M.A. Cohn, Cellular response to DNA interstrand crosslinks: the Fanconi anemia pathway, Cell. Mol. Life Sci. 73 (2016) 3097–3114. https://doi.org/10.1007/s00018-016-2218-x.

[144] W.J. Cannan, D.S. Pederson, Mechanisms and consequences of double-strand DNA break formation in chromatin, J. Cell. Physiol. 231 (2016) 3–14. https://doi.org/10.1002/jcp.25048.

[145] F. Bray, J. Ferlay, I. Soerjomataram, R.L. Siegel, L.A. Torre, A. Jemal, Global cancer statistics 2018: GLOBOCAN estimates of incidence and mortality worldwide for 36 cancers in 185 countries, CA. Cancer J. Clin. 68 (2018) 394–424. https://doi.org/10.3322/caac.21492.

[146] D. Hanahan, R.A. Weinberg, The hallmarks of cancer, Cell. 100 (2000) 57–70. https://doi.org/10.1016/s0092-8674(00)81683-9.

[147] D. Hanahan, R.A. Weinberg, Hallmarks of cancer: the next generation, Cell. 144 (2011) 646–674. https://doi.org/10.1016/j.cell.2011.02.013.

[148] J. Luo, N.L. Solimini, S.J. Elledge, Principles of cancer therapy: oncogene and non-oncogene addiction, Cell. 136 (2009) 823–837.

https://doi.org/10.1016/j.cell.2009.02.024.

[149] E.R. Fearon, B. Vogelstein, A genetic model for colorectal tumorigenesis, Cell. 61 (1990) 759–767. https://doi.org/10.1016/0092-8674(90)90186-i.

[150] C. Lengauer, K.W. Kinzler, B. Vogelstein, Genetic instabilities in human cancers, Nature. 396 (1998) 643–649. https://doi.org/10.1038/25292.

[151] S. Negrini, V.G. Gorgoulis, T.D. Halazonetis, Genomic instability - an evolving hallmark of cancer, Nat. Rev. Mol. Cell Biol. 11 (2010) 220–228. https://doi.org/10.1038/nrm2858.

[152] T. Sjöblom, S. Jones, L.D. Wood, D.W. Parsons, J. Lin, T.D. Barber, D. Mandelker, R.J. Leary, J. Ptak, N. Silliman, S. Szabo, P. Buckhaults, C. Farrell, P. Meeh, S.D. Markowitz, J. Willis, D. Dawson, J.K. V Willson, A.F. Gazdar, J. Hartigan, L. Wu, C. Liu, G. Parmigiani, B.H. Park, K.E. Bachman, N. Papadopoulos, B. Vogelstein, K.W. Kinzler, V.E. Velculescu, The consensus coding sequences of human breast and colorectal cancers, Science. 314 (2006) 268–274. https://doi.org/10.1126/science.1133427.

[153] L.D. Wood, D.W. Parsons, S. Jones, J. Lin, T. Sjöblom, R.J. Leary, D. Shen, S.M. Boca, T. Barber, J. Ptak, N. Silliman, S. Szabo, Z. Dezso, V. Ustyanksky, T. Nikolskaya, Y. Nikolsky, R. Karchin, P.A. Wilson, J.S. Kaminker, Z. Zhang, R. Croshaw, J. Willis, D. Dawson, M. Shipitsin, J.K. V Willson, S. Sukumar, K. Polyak, B.H. Park, C.L. Pethiyagoda, P.V.K. Pant, D.G. Ballinger, A.B. Sparks, J. Hartigan, D.R. Smith, E. Suh, N. Papadopoulos, P. Buckhaults, S.D. Markowitz, G. Parmigiani, K.W. Kinzler, V.E. Velculescu, B. Vogelstein, The genomic landscapes of human breast and colorectal cancers, Science. 318 (2007) 1108–1113. https://doi.org/10.1126/science.1145720.

[154] S. Jones, X. Zhang, D.W. Parsons, J.C.-H. Lin, R.J. Leary, P. Angenendt, P. Mankoo, H. Carter, H. Kamiyama, A. Jimeno, S.-M. Hong, B. Fu, M.-T. Lin, E.S. Calhoun, M. Kamiyama, K. Walter, T. Nikolskaya, Y. Nikolsky, J. Hartigan, D.R. Smith, M. Hidalgo, S.D. Leach, A.P. Klein, E.M. Jaffee, M. Goggins, A. Maitra, C. Iacobuzio-Donahue, J.R. Eshleman, S.E. Kern, R.H. Hruban, R. Karchin, N. Papadopoulos, G. Parmigiani, B. Vogelstein, V.E. Velculescu, K.W. Kinzler, Core signaling pathways in human pancreatic cancers revealed by global genomic analyses, Science. 321 (2008) 1801–1806. https://doi.org/10.1126/science.1164368.

[155] T.D. Halazonetis, V.G. Gorgoulis, J. Bartek, An oncogene-induced DNA damage model for cancer development, Science. 319 (2008) 1352–1355. https://doi.org/10.1126/science.1140735.

[156] K.K. Khanna, S.P. Jackson, DNA double-strand breaks: signaling, repair and the cancer connection, Nat. Genet. 27 (2001) 247–254. https://doi.org/10.1038/85798.

[157] J. Falck, J. Coates, S.P. Jackson, Conserved modes of recruitment of ATM, ATR and DNA-PKcs to sites of DNA damage, Nature. 434 (2005) 605–611. https://doi.org/10.1038/nature03442.

[158] Z. DeLoughery, M.W. Luczak, S. Ortega-Atienza, A. Zhitkovich, DNA double-strand breaks by Cr(VI) are targeted to euchromatin and cause ATR-dependent phosphorylation of histone H2AX and its ubiquitination, Toxicol. Sci. 143 (2015) 54–63. https://doi.org/10.1093/toxsci/kfu207.

[159] S. Vamvakas, E.H. Vock, W.K. Lutz, On the role of DNA double-strand breaks in toxicity and carcinogenesis, Crit. Rev. Toxicol. 27 (1997) 155–174. https://doi.org/10.3109/10408449709021617.

[160] D.E. Pritchard, S. Ceryak, K.E. Ramsey, T.J. O'Brien, L. Ha, J.L. Fornsaglio, D.A. Stephan, S.R. Patierno, Resistance to apoptosis, increased growth potential, and altered gene expression in cells that survived genotoxic hexavalent chromium [Cr(VI)] exposure, Mol. Cell. Biochem. 279 (2005) 169–181. https://doi.org/10.1007/s11010-005-8292-2.

[161] Y.-O. Son, P. Pratheeshkumar, L. Wang, X. Wang, J. Fan, D.-H. Kim, J.-Y. Lee, Z. Zhang, J.-C. Lee, X. Shi, Reactive oxygen species mediate Cr(VI)-induced carcinogenesis through PI3K/AKT-dependent activation of GSK-3beta/beta-catenin signaling, Toxicol. Appl. Pharmacol. 271 (2013) 239–248. https://doi.org/10.1016/j.taap.2013.04.036.

[162] B.-J. Wang, H.-M. Sheu, Y.-L. Guo, Y.-H. Lee, C.-S. Lai, M.-H. Pan, Y.-J. Wang, Hexavalent chromium induced ROS formation, Akt, NF-kappaB, and MAPK activation, and TNF-alpha and IL-1alpha production in keratinocytes, Toxicol. Lett. 198 (2010) 216–224. https://doi.org/10.1016/j.toxlet.2010.06.024.

[163] A.L. Holmes, S.S. Wise, J.P. Wise, Carcinogenicity of hexavalent chromium, Indian J. Med. Res. 128 (2008) 353–372. https://pubmed.ncbi.nlm.nih.gov/19106434/.

[164] T. Hirose, K. Kondo, Y. Takahashi, H. Ishikura, H. Fujino, M. Tsuyuguchi, M. Hashimoto, T. Yokose, K. Mukai, T. Kodama, Y. Monden, Frequent microsatellite instability in lung cancer from chromate-exposed workers, Mol. Carcinog. 33 (2002) 172–180. https://doi.org/10.1002/mc.10035.

[165] S.S. Wise, J.P. Wise, Aneuploidy as an early mechanistic event in metal carcinogenesis, Biochem. Soc. Trans. 38 (2010) 1650–1654. https://doi.org/10.1042/BST0381650.

[166] A.L. Holmes, S.S. Wise, S.J. Sandwick, W.L. Lingle, V.C. Negron, W.D. Thompson, J.P.S. Wise, Chronic exposure to lead chromate causes centrosome abnormalities and aneuploidy in human lung cells, Cancer Res. 66 (2006) 4041–4048. https://doi.org/10.1158/0008-5472.CAN-05-3312.

[167] A.L. Holmes, S.S. Wise, S.C. Pelsue, A.-M. Aboueissa, W. Lingle, J. Salisbury, J. Gallagher, J.P. Wise Sr, Chronic exposure to zinc chromate induces centrosome amplification and spindle assembly checkpoint bypass in human lung fibroblasts, Chem. Res. Toxicol. 23 (2010) 386–395. https://doi.org/10.1021/tx900360w.

[168] H. Xie, A.L. Holmes, S.S. Wise, S. Huang, C. Peng, J.P.S. Wise, Neoplastic transformation of human bronchial cells by lead chromate particles, Am. J. Respir. Cell Mol. Biol. 37 (2007) 544–552. https://doi.org/10.1165/rcmb.2007-0058OC.

[169] C.L. Browning, Q. Qin, D.F. Kelly, R. Prakash, F. Vanoli, M. Jasin, J.P.S. Wise, Prolonged particulate hexavalent chromium exposure suppresses homologous recombination repair in human lung cells, Toxicol. Sci. 153 (2016) 70–78. https://doi.org/10.1093/toxsci/kfw103.

[170] J. Chen, D.P. Silver, D. Walpita, S.B. Cantor, A.F. Gazdar, G. Tomlinson, F.J. Couch, B.L. Weber, T. Ashley, D.M. Livingston, R. Scully, Stable interaction between the products of the BRCA1 and BRCA2 tumor suppressor genes in mitotic and meiotic cells, Mol. Cell. 2 (1998) 317–328. https://doi.org/10.1016/s1097-2765(00)80276-2.

[171] M.E. Moynahan, J.W. Chiu, B.H. Koller, M. Jasin, Brca1 controls homology-directed DNA repair, Mol. Cell. 4 (1999) 511–518. https://doi.org/10.1016/s1097-2765(00)80202-6.

[172] C.L. Browning, J.P. Wise Sr, Prolonged exposure to particulate chromate inhibits RAD51 nuclear import mediator proteins, Toxicol. Appl. Pharmacol. 331 (2017) 101–

107. https://doi.org/10.1016/j.taap.2017.05.030.

[173] H. Itoh, Y. Tashima, The stress (heat shock) proteins, Int. J. Biochem. 23 (1991) 1185–1191.

[174] A.A.A. Asea, P. Kaur, Heat shock proteins and stress, 15th ed., Springer International Publishing, Toledo, 2018. https://doi.org/10.1007/978-3-319-90725-3.

[175] F. Ritossa, A new puffing pattern induced by temperature shock and DNP in drosophila, Experientia. 18 (1962) 571–573. https://doi.org/10.1007/BF02172188.

[176] A. Tissières, H.K. Mitchell, U.M. Tracy, Protein synthesis in salivary glands of Drosophila melanogaster: relation to chromosome puffs, J. Mol. Biol. 84 (1974) 389–398. https://doi.org/10.1016/0022-2836(74)90447-1.

[177] K.T. Riabowol, L.A. Mizzen, W.J. Welch, Heat shock is lethal to fibroblasts microinjected with antibodies against hsp70, Science. 242 (1988) 433–436. https://doi.org/10.1126/science.3175665.

[178] S.K. Calderwood, Heat shock proteins and cancer: intracellular chaperones or extracellular signalling ligands?, Philos. Trans. R. Soc. Lond. B. Biol. Sci. 373 (2018). https://doi.org/10.1098/rstb.2016.0524.

[179] J.Á. Fernández-Higuero, I. Betancor-Fernández, N. Mesa-Torres, A. Muga, E. Salido, A.L. Pey, Structural and functional insights on the roles of molecular chaperones in the mistargeting and aggregation phenotypes associated with primary hyperoxaluria type I, Adv. Protein Chem. Struct. Biol. 114 (2019) 119–152. https://doi.org/10.1016/bs.apcsb.2018.09.003.

[180] L. Boyd, K. Sampuda, Molecular chaperones and the nuclear response to stress, in: Heat Shock Proteins Stress, Springer International Publishing, 2018: pp. 3–11. https://doi.org/10.1007/978-3-319-90725-3_1.

[181] J. Wu, T. Liu, Z. Rios, Q. Mei, X. Lin, S. Cao, Heat shock proteins and cancer, Trends Pharmacol. Sci. 38 (2017) 226–256. https://doi.org/10.1016/j.tips.2016.11.009.

[182] S.K. Calderwood, J. Gong, Heat shock proteins promote cancer: it's a protection racket, Trends Biochem. Sci. 41 (2016) 311–323. https://doi.org/https://doi.org/10.1016/j.tibs.2016.01.003.

[183] R.I. Morimoto, Cells in stress: transcriptional activation of heat shock genes, Science. 259 (1993) 1409–1410. https://doi.org/10.1126/science.8451637.

[184] S. Chatterjee, T.F. Burns, Targeting heat shock proteins in cancer: a promising therapeutic approach, Int. J. Mol. Sci. 18 (2017). https://doi.org/10.3390/ijms18091978.

[185] C. V Dang, L.M. Resar, E. Emison, S. Kim, Q. Li, J.E. Prescott, D. Wonsey, K. Zeller, Function of the c-Myc oncogenic transcription factor, Exp. Cell Res. 253 (1999) 63–77. https://doi.org/10.1006/excr.1999.4686.

[186] P. Abreu, L. Ferreira, T. Cunha-Oliveira, M. Alpoim, A. Urbano, HSP90: a key player in metal-induced carcinogenesis?, in: Heat Shock Protein 90 Hum. Dis. Disord., Springer Nature Switzerland, 2019: pp. 217–247. https://doi.org/10.1007/978-3-030-23158-3_11.

[187] M.M. Biebl, J. Buchner, Structure, function, and regulation of the Hsp90 machinery, Cold Spring Harb. Perspect. Biol. 11 (2019). https://doi.org/10.1101/cshperspect.a034017.

[188] S.K. Calderwood, L. Neckers, Hsp90 in cancer: transcriptional roles in the nucleus, Adv. Cancer Res. 129 (2016) 89–106. https://doi.org/10.1016/bs.acr.2015.08.002.

[189] O. Genest, S. Wickner, S.M. Doyle, Hsp90 and Hsp70 chaperones: collaborators in

protein remodeling, J. Biol. Chem. 294 (2019) 2109–2120. https://doi.org/10.1074/jbc.REV118.002806.

[190] P. Csermely, T. Schnaider, C. So″ti, Z. Prohászka, G. Nardai, The 90-kDa molecular chaperone family: structure, function, and clinical applications. A comprehensive review., Pharmacol. Ther. 79 (1998) 129–168. https://doi.org/https://doi.org/10.1016/S0163-7258(98)00013-8.

[191] S.E. Jackson, Hsp90: structure and function, Top. Curr. Chem. 328 (2013) 155–240. https://doi.org/10.1007/128_2012_356.

[192] D. Jarosz, Hsp90: A global regulator of the genotype to phenotype map in cancers, Adv. Cancer Res. 129 (2016) 225–247. https://doi.org/10.1016/bs.acr.2015.11.001.

[193] B.K. Eustace, T. Sakurai, J.K. Stewart, D. Yimlamai, C. Unger, C. Zehetmeier, B. Lain, C. Torella, S.W. Henning, G. Beste, B.T. Scroggins, L. Neckers, L.L. Ilag, D.G. Jay, Functional proteomic screens reveal an essential extracellular role for hsp90α in cancer cell invasiveness., Nat. Cell Biol. 6 (2004) 507–514. https://doi.org/10.1038/ncb1131.

[194] K. Sidera, M. Gaitanou, D. Stellas, R. Matsas, E. Patsavoudi, A critical role for HSP90 in cancer cell invasion involves interaction with the extracellular domain of HER-2., J. Biol. Chem. 283 (2008) 2031–2041. https://doi.org/10.1074/jbc.M701803200.

[195] L.M.R. Ferreira, M.S. Santos, M.C. Alpoim, A.M. Urbano, Metabolic changes in human bronchial epithelial cells upon chronic exposure to hexavalent chromium, BMC Proc. 4 (2010) P16. https://doi.org/10.1186/1753-6561-4-S2-P16.

[196] E.T. Snow, L.S. Xu, Chromium(III) bound to DNA templates promotes increased polymerase processivity and decreased fidelity during replication in vitro, Biochemistry. 30 (1991) 11238–11245. https://doi.org/10.1021/bi00111a007.

[197] Improve the consistency of bronchial epithelial cell cultures, ThermoFisher Sci. (n.d.) 2. https://www.thermofisher.com/document-connect/document-connect.html?url=https%3A%2F%2Fassets.thermofisher.com%2FTFS-Assets%2FLSG%2Fbrochures%2FF-067155LHCrelaunchflyer_FLR.pdf&title=SW1wcm92ZSB0aGUgY29uc2lzdGVuY3kgb2YgYnJvbmNoaWFsIGVwaXRoZWxpYWwgY2VsbCBjd (accessed April 20, 2020).

[198] M.A. Harrison, Cryopreservation of cells, ELS. (2001). https://doi.org/doi:10.1038/npg.els.0002561.

[199] W. Strober, Trypan blue exclusion test of cell viability, Curr. Protoc. Immunol. Appendix 3 (2001) Appendix 3B. https://doi.org/10.1002/0471142735.ima03bs21.

[200] J.A. Molina-Bolívar, J. Aguiar, C.C. Ruiz, Growth and hydration of Triton X-100 micelles in monovalent alkali salts: a light scattering study, J. Phys. Chem. B. 106 (2002) 870–877. https://doi.org/10.1021/jp0119936.

[201] C. De Duve, R. Wattiaux, Tissue fractionation studies. VII. Release of bound hydrolases by means of triton X-100, Biochem. J. 63 (1956) 606–608. https://doi.org/10.1042/bj0630606.

[202] S.J. Compton, C.G. Jones, Mechanism of dye response and interference in the Bradford protein assay, Anal. Biochem. 151 (1985) 369–374. https://doi.org/10.1016/0003-2697(85)90190-3.

[203] G.L. Peterson, Determination of total protein, Methods Enzymol. 91 (1983) 95–119. https://doi.org/10.1016/s0076-6879(83)91014-5.

[204] N.J. Kruger, The Bradford method for protein quantitation, in: J.M. Walker (Ed.),

Protein Protoc. Handb., second edi, Humana Press Inc., Hatfield, 2002: pp. 15–21.

[205] M.M. Bradford, A rapid and sensitive method for the quantitation of microgram quantities of protein utilizing the principle of protein-dye binding, Anal. Biochem. 72 (1976) 248–254. https://doi.org/10.1006/abio.1976.9999.

[206] E. Chacon, D. Acosta, J.J. Lemasters, Primary cultures of cardiac myocytes as in vitro models for pharmacological and toxicological assessments, in: J. V Castell, M.J.B.T.-I.V.M. in P.R. Gómez-Lechón (Eds.), Vitr. Methods Pharm. Res., 1st ed., Academic Press, San Diego, 1997: pp. 209–223. https://doi.org/10.1016/B978-012163390-5.50010-7.

[207] ATCC®, Animal cell culture guide - tips and techniques for continuous cell lines, (2014) 39. https://www.atcc.org/~/media/PDFs/Culture Guides/AnimCellCulture_Guide.ashx (accessed April 21, 2020).

[208] N.A.P. Franken, H.M. Rodermond, J. Stap, J. Haveman, C. van Bree, Clonogenic assay of cells in vitro, Nat. Protoc. 1 (2006) 2315–2319. https://doi.org/10.1038/nprot.2006.339.

[209] J.F. Cerveira, M. Sánchez-Aragó, A.M. Urbano, J.M. Cuezva, Short-term exposure of nontumorigenic human bronchial epithelial cells to carcinogenic chromium(VI) compromises their respiratory capacity and alters their bioenergetic signature, FEBS Open Bio. 4 (2014) 594–601. https://doi.org/10.1016/j.fob.2014.06.006.

[210] P.L. Abreu, T. Cunha-Oliveira, L.M.R. Ferreira, A.M. Urbano, Hexavalent chromium, a lung carcinogen, confers resistance to thermal stress and interferes with heat shock protein expression in human bronchial epithelial cells, Biometals. 31 (2018) 477–487. https://doi.org/10.1007/s10534-018-0093-7.

[211] L.B. Gladden, A lactatic perspective on metabolism, Med. Sci. Sports Exerc. 40 (2008) 477–485. https://doi.org/10.1249/MSS.0b013e31815fa580.

[212] M.J. Rogatzki, B.S. Ferguson, M.L. Goodwin, L.B. Gladden, Lactate is always the end product of glycolysis, Front. Neurosci. 9 (2015) 22. https://doi.org/10.3389/fnins.2015.00022.

[213] B.F. Miller, J.A. Fattor, K.A. Jacobs, M.A. Horning, F. Navazio, M.I. Lindinger, G.A. Brooks, Lactate and glucose interactions during rest and exercise in men: effect of exogenous lactate infusion, J. Physiol. 544 (2002) 963–975. https://doi.org/10.1113/jphysiol.2002.027128.

[214] L.M.R. Ferreira, A.M. Li, T.L. Serafim, M.C. Sobral, M.C. Alpoim, A.M. Urbano, Intermediary metabolism: an intricate network at the crossroads of cell fate and function, Biochim. Biophys. Acta - Mol. Basis Dis. 10 (2020) 165887.

[215] A.M. Urbano, Otto Warburg: the journey towards the seminal discovery of tumor cell bioenergetic reprogramming, Biochim. Biophys. Acta. Mol. Basis Dis. 1867 (2020) 165965. https://doi.org/10.1016/j.bbadis.2020.165965.

[216] P.L. Abreu, A.M. Urbano, Targeting the Warburg effect for cancer therapy: a long and winding road, in: Front. Clin. Drug Res. - Anti-Cancer Agents, Volume 3, Bentham Science Publishers, 2016: pp. 271–324. https://doi.org/10.2174/9781681082899116030006.

[217] G. Bozzuto, P. Ruggieri, A. Molinari, Molecular aspects of tumor cell migration and invasion, Ann. Ist. Super. Sanita. 46 (2010) 66–80. https://doi.org/10.4415/ANN_10_01_09.

[218] R.O. Hynes, J.M. Bye, Density and cell cycle dependence of cell surface proteins in hamster fibroblasts, Cell. 3 (1974) 113–120.

https://doi.org/https://doi.org/10.1016/0092-8674(74)90114-7.

[219] R.I. Freshney, Transformation and immortalization, in: Cult. Anim. Cells A Man. Basic Tech., 5th ed., John Wiley & Sons, Inc., 2005. https://doi.org/doi:10.1002/0471747599.cac018.

[220] K. Usuda, Y. Saito, M. Sagawa, M. Sato, K. Kanma, S. Takahashi, C. Endo, Y. Chen, A. Sakurada, S. Fujimura, Tumor doubling time and prognostic assessment of patients with primary lung cancer, Cancer. 74 (1994) 2239–2244. https://doi.org/10.1002/1097-0142(19941015)74:8<2239::AID-CNCR2820740806>3.0.CO;2-P.

[221] D.M. Xu, H. Gietema, H. de Koning, R. Vernhout, K. Nackaerts, M. Prokop, C. Weenink, J.-W. Lammers, H. Groen, M. Oudkerk, R. van Klaveren, Nodule management protocol of the NELSON randomised lung cancer screening trial, Lung Cancer. 54 (2006) 177–184. https://doi.org/10.1016/j.lungcan.2006.08.006.

[222] E.B. Ryu, J.M. Chang, M. Seo, S.A. Kim, J.H. Lim, W.K. Moon, Tumour volume doubling time of molecular breast cancer subtypes assessed by serial breast ultrasound, Eur. Radiol. 24 (2014) 2227–2235. https://doi.org/10.1007/s00330-014-3256-0.

[223] J.K. Kim, H.-D. Kim, M.-J. Jun, S.-C. Yun, J.H. Shim, H.C. Lee, D. Lee, J. An, Y.-S. Lim, Y.-H. Chung, Y.S. Lee, K.M. Kim, Tumor volume doubling time as a dynamic prognostic marker for patients with hepatocellular carcinoma, Dig. Dis. Sci. 62 (2017) 2923–2931. https://doi.org/10.1007/s10620-017-4708-6.

[224] C. GM., The development and causes of cancer, in: Cell A Mol. Approach, 2nd ed., Sinauer Associates, Sunderland, 2000.